

https://dspace.org/

The transport of the Rooibos tea flavonoid aspalathin across the skin and the intestinal epithelium

Huang, Miao-Juei

2008-03-18T08:05:03Z
http://hdl.handle.net/10539/4673

Downloaded from a DSpace repository. https://dspace.org/

The transport of the Rooibos tea flavonoid aspalathin across the skin and the intestinal epithelium

Miao-Juei Huang

A dissertation submitted to the Faculty of Health Sciences, University of the Witwatersrand, Johannesburg, in fulfilment of the requirements for the degree of Master in Pharmacy.

Johannesburg, South Africa, 2006

DECLARATION

I, Miao-Juei Huang, declare that this dissertation is my own work. It is being submitted in fulfilment for the degree, Master of Pharmacy, University of the Witwatersrand, Johannesburg. It has not been submitted before for any degree or examination at this or any other University.

Signature_____

_____day of_____, 2006.

DEDICATION

I dedicate this dissertation to my parents

Hsiu-Lin Huang and Yi-Sheng Huang,

For their love and support,

guidance and encouragement in life.

ACKNOWLEDGEMENTS

I would like to express my sincere gratitude to my supervisor, Professor Alvaro M. Viljoen for the knowledge impacted on me, the support, encouragement and guidance provided throughout the duration of the research, and for his motivation towards the completion of this project.

I am also indebted to my co-supervisors, Professors Jeanetta du Plesssis and Josias Hamman. I am very appreciative of the knowledge I gained from them. Without their guidance and assistance this project would not have been taken to completion.

Acknowledgements to Professor Jan du Preez, I appreciate his technical assistance in the HPLC analysis. I am very grateful for the interest he showed and for his willingness to always help.

I am sincerely grateful to Miss Anja Judeinfield and Mr Ruaan Louw for their assistance in teaching me the percutaneous permeation experiment and their generosity in sharing their knowledge and information with me.

A sincere thank you to Mr Jason Lu for his assistance in culturing Caco-2 cells and assiting me during the Caco-2 transport experiment.

Thank you to my friends Carli, Madeli and Linda for their help, encouragement and hospitality during my visit at the North-West University (Potchefstroom campus).

I also would like to thank my friends, Maria, Jacqui, Ayesha, and Aneesa. I appreciate all the encouragement and advice they gave me.

I would like to thank the National Research Foundation (Indigenous Knowledge Systems) for the financial assistance.

A special word of thanks to Po-Chieh Cheng for your patience, understanding and your moral support. Thank you for always being on my side.

Thank you to my brother Cheng-Che for your inspiration and always taking care of me.

Finally, thank you to my parents for loving and supporting me. I am sincerely grateful for your guidance and all that you have given to me. Without your encouragement I could have not come this far in life.

ABSTRACT

The aqueous extract of rooibos has been used for more than three hundred years since its discovery by the indigenous people. Currently, rooibos is gaining popularity in the cosmetic industry and incorporation of rooibos extracts in topical cosmetic formulations has become a fashionable trend. Both topical and intestinal absorption of rooibos tea were investigated. The transport of aspalathin in the unfermented (green) rooibos aqueous extracts and aqueous solution of pure aspalathin were studied.

The percutaneous permeation experiments were conducted with vertical Franz diffusion cells using human female abdominal skin obtained from patients who underwent cosmetic surgery. The green rooibos extract and pure aspalathin solution buffered in phosphate buffer system (pH 5.5) were applied to the skin for 12 hours. Samples of the permeants were obtained from the receptor fluid phase and from the stratified layers of the skin by using the tape-stripping technique and analysed by HPLC.

In vitro intestinal epithelial transport experiments were carried out by using Caco-2 cell monolayers, isolated and cultured from human colonic adenocarcinoma cells, in a six-well transwell system. The green rooibos extract and pure aspalathin solution buffered in phosphate buffer (pH 7.4) were applied on to the cell monolayers and incubated for 2 hours. Samples were obtained from the basolateral phase at predetermined time intervals and analysed by HPLC.

Less than 0.1 % of the applied dose of aspalathin permeated the skin. Most of the permeated aspalathin accumulated in the stratum corneum. Close to 100 % of aspalathin was transported across the Caco-2 cell monolayers at a concentration dependent manner. Better absorption of aspalathin was observed using the green rooibos extract than with

the pure aspalathin solution across the Caco-2 cell monolayers.

TABLE OF CONTENTS

DECLARATION ii

DEDICATION iii

ACKNOWLEDGEMENTS iv

ABSTRACT vi

TABLE OF CONTENTS viii

LIST OF FIGURES xiii

LIST OF TABLES xviii

CHAPTER 1

GENERAL INTRODUCTION

1.1 Taxonomy of *Aspalathus linearis* 1

1.2 Botanical description 1

1.3 Variation in the *Aspalathus linearis* species complex 3

1.4 The history of rooibos tea 4

1.5 Uses and benefits of rooibos 6

1.6 Rooibos polyphenolic compounds 8

1.6.1 Free radical attack 8

1.6.2 Rooibos antioxidants 9

1.6.3 Total polyphenolic content 14

1.6.4 Total antioxidant capacity 15

1.7 Biological activities of rooibos tea 16

1.8 Aims of the study 17

CHAPTER 2

***IN VITRO* PERCUTANEOUS PERMEATION OF ASPALATHIN**

2.1 Overview of the human skin 19

2.1.1 Structure of the skin 20

2.1.1.1 Epidermis **21**

2.1.1.2 Dermis and hypodermis **23**

2.1.2 Routes of penetration through the skin 24

2.1.3 Physicochemical parameters influencing transdermal drug delivery 26

2.2 Materials and methods 28

2.2.1 Materials 28

2.2.2 High performance liquid chromatography (HPLC) method for the analysis of aspalathin 29

2.2.2.1 Apparatus **29**

2.2.2.2 Chromatographic conditions **29**

2.2.2.3 Preparation of stock solution **30**

2.2.2.4 Validation of HPLC procedure **30**

2.2.2.4.1 Linearity **30**

2.2.2.4.2 Accuracy and precision **31**

2.2.2.4.3 Sensitivity **32**

2.2.2.4.4 Selectivity **32**

2.2.3 Determination of stability of aspalathin in transport medium 36

2.2.4 Determination of octanol/water partition coefficient (K_{ow}) 36

2.2.5 Determination of aspalathin in commercial products 38

2.2.6 Aspalathin permeation study 38

2.2.6.1 Preparation of test formulations **38**

2.2.6.2 Preparation of skin **38**

2.2.6.3 Transport of aspalathin across the skin 39

2.2.6.4 Tape stripping the stratum corneum and epidermis 41

2.2.6.5 Sample analysis 42

2.2.6.6 Statistical analysis 42

2.3 Results and discussion 42

2.3.1 Stability in transport medium 42

2.3.2 Octanol/water partition coefficient (K_{ow}) 44

2.3.3 Determination of aspalathin in commercial products 45

2.3.4 Aspalathin permeation study 46

2.4 Conclusion 51

CHAPTER 3

***IN VITRO* INTESTINAL EPITHELIAL TRANSPORT OF ASPALATHIN ACROSS CACO-2 CELL MONOLAYERS**

3.1 Introduction 52

3.2 Comparison of *in vivo* and *in vitro* human intestinal epithelia 52

3.2.1 Anatomy and physiology of the small intestine 52

3.2.2 Pathways of intestinal absorption 55

3.2.3 The *in vitro* Caco-2 cell model for transport study 57

3.2.4 *In vitro*/*in vivo* correlations 58

3.3 *In vitro* Caco-2 cell monolayer transport study 60

3.3.1 Caco-2 cell culture and setup for transport studies 60

3.3.2 Determination of the apparent permeability coefficient (P_{app}) 61

3.3.3 Measurement of transepithelial electrical resistance (TEER) 62

3.4 Pheroid technology 62

3.5 Materials and methods 64

3.5.1 Materials 64

3.5.2 High performance liquid chromatography (HPLC) method for the analysis of aspalathin 64

3.5.3 Determination of stability of aspalathin 65

3.5.3.1 Stability in the transport medium 65

3.5.4 *In vitro* transport study 66

3.5.4.1 Preparation of test formulations for the transport study 66

3.5.4.2 Preparation of Caco-2 cell monolayers 66

3.5.4.2.1 Culturing of Caco-2 cells 66

3.5.4.2.2 Trypsination of the Caco-2 cells 66

3.5.4.2.3 Seeding and culturing of Caco-2 cell monolayers on 6-well filter plates 67

3.5.4.2.4 Measurement of TEER 68

3.5.4.3 Transport of aspalathin across Caco-2 cell monolayers 68

3.5.4.4 Sample analysis 69

3.5.4.5 Statistical analysis 69

3.6 Results and discussion 70

3.6.1 Stability of aspalathin in transport medium 70

3.6.2 Transport of aspalathin in green rooibos extracts 71

3.6.3 Transport of aspalathin in pure aspalathin solution 73

3.6.4 Transport of aspalathin in Pheroids 75

3.6.5 Comparison of apparent permeability coefficient (P_{app}) 77

3.7 Conclusions 79

CHAPTER 4

CONCLUSION AND FUTURE PROSPECTIVE

4.1 Summary and conclusion **81**

4.2 Future prospective **82**

REFERENCES **83**

ANNEXURE 1 **97**

LIST OF FIGURES

Figure 1.1 The natural habitat of *Aspalathus linearis* in the Cederberg Mountain regions (marked in red) north-west of Cape Town in South Africa (picture provided by A.M. Viljoen). **2**

Figure 1.2 Rooibos plantation (Erickson, 2003). **3**

Figure 1.3 The rooibos plant bearing needle-like leaves and pea-shaped flowers on ferruginous young branches. **3**

Figure 1.4 The chemical structures of quercetin (I) and luteolin (II). **11**

Figure 1.5 The isomeric forms of orientin (Koeppen and Roux, 1965a). **12**

Figure 1.6 The chemical structure of rutin. **12**

Figure 1.7 The isomeric forms of aspalathin (Koeppen and Roux, 1965b). **14**

Figure 2.1 Schematic diagram of cross-section of human skin (http://rds.yahoo.com/_ylt=A9G_RtvPXEdE8BcB6pujzbkF;_ylu=X3oDMTA4NDgyNWN0BHNlYwNwcm9m/SIG=12ve841bm/EXP=1145613903/**http://www.anti-aging-skin-care.com/forever-young-how-it-works-diagram.html). **21**

Figure 2.2 Skin permeation routes: (1) intercellular diffusion through the lipid

lamellae; (2) transcellular diffusion through both the corneocytes and the lipid lamellae; and (3) diffusion through skin appendages (hair follicles and sweat ducts) (Ho, 2004). **24**

Figure 2.3 Schematic diagram showing principal steps of permeation (modified from Zatz, 1993). **25**

Figure 2.4a HPLC chromatogram and UV spectrum of aspalathin (7.05 µg/ml), Rt = 7.658 min. **33**

Figure 2.4b HPLC chromatogram and UV spectrum of green rooibos extracts (5 µg/ml) aspalathin Rt = 7.823. **34**

Figure 2.4c HPLC chromatogram of skin tissue. **35**

Figure 2.4d HPLC chromatogram of skin surface sample. **35**

Figure 2.5 Skin dermatome obtaining split-thickness skin using a electric dermatome (http://www.zimmergermany.de and http://www.residentnet.com). **39**

Figure 2.6 Vertical Franz diffusion cell consisting of an upper donor compartment (chamber) and bottom receptor compartment (re-drawn from http://www.permegear.com/franz.htm). **41**

Figure 2.7a Amount of aspalathin (% of initial concentration) in 1.4 µg/ml of aspalathin solution, buffered at pH 5.0, 6.0, and 7.0, stored for 14 hours at

room temperature (25 °C). **43**

Figure 2.7b Amount of aspalathin (% of initial concentration) in 1.4 µg/ml aspalathin solution, buffered at pH 5.0 and 5.5, at room temperature (25 °C) for 9 hours. **43**

Figure 2.8 Chromatogram of a water/methanol extract of cream A depicting aspalathin at 7.48 min and other flavonoid compounds. **46**

Figure 2.9 The average percentage (%) of aspalathin that permeated the skin in green rooibos extract and aspalathin solution applied. (The outlier has been excluded). **48**

Figure 2.10 Comparison of the absolute amount of aspalathin permeated in green rooibos extracts and aspalathin solutions. (The outlier has been excluded). **48**

Figure 3.1 Villi and microvilli increase the absorptive surface area of the small intestine (re-drawn from http://www.emc.maricopa.edu/faculty/farabee/BIOBK/BioBookDIGEST.html). **54**

Figure 3.2 Routes of drug transport. (A) Passive transcellular absorption across intestinal epithelium. (B) Paracellualr absorption mediated by tight junctions. (C) Carrier-mediated transcellular transport at the apical and/or basolateral membranes. (D) Efflux transporter at the apical membrane may

actively drive compounds back into the intestinal lumen thus restricting their absorption into the blood. (E) Apical efflux transporters that facilitate intestinal clearance of compounds that are already present in blood. (F) Intracellular metabolising enzymes may modify compounds before they enter the blood. (G) Apical efflux transporters and intracellular metabolising enzymes may co-ordinately metabolise and excrete compounds, forming an effective barrier against intestinal absorption. (H) Transcellular vesicular transport (modified from Chan *et al*., 2004; Hunter and Hirst, 1997). **56**

Figure 3.3 A comparison of *in vivo* extensively folded intestinal epithelia and *in vitro* flat Caco-2 cell monolayer, and barriers across which drugs must pass to reach the basolateral phase (Youdim *et al.*, 2003). **60**

Figure 3.4 The *in vitro* cell culture model (modified from Youdim *et al.*, 2003; During and Harrison, 2005). **61**

Figure 3.5 Procedures of *in vitro* transport across Caco-2 cell monolayers (A) Seeding of Caco-2 cells. (B) Measurement of TEER. (C) Removal of growth medium. (D) Loading of test formulation onto Caco-2 cell monolayers. (E) Sampling from the basolateral phase at predetermined time intervals (photos provided by A.M. Viljoen). **69**

Figure 3.6 Loss of aspalathin over time in vehicles of (i) double distilled water, (ii) phosphate buffer solution (PBS) (pH 7.4), and (iii) Dulbecco's Modified Eagle's Medium (DMEM). **70**

Figure 3.7 Plot of the cumulative transport of aspalathin in green rooibos extracts over time. **72**

Figure 3.8 Plot of the cumulative transport of aspalathin in pure aspalathin solution over time. **74**

Figure 3.9 Plot of the cumulative transport of aspalathin in Pheroids over time. **76**

Figure 3.10 Comparison of the apparent permeability coefficient (P_{app}) of: (i) GRE, (ii) aspalathin solution, and (iii) Pheroids at three different concentrations. **78**

LIST OF TABLES

Table 1.1 Nutritional content of Rooibos tea (Morton, 1983). **7**

Table 2.1 Gradient elution employed for reverse-phase HPLC separation of aspalathin. **30**

Table 2.2 Quantification of accuracy and precision of aspalathin recovery from three concentration levels. **31**

Table 2.3 Octanol-water partition coefficient (K_{ow}) of aspalathin and log P value. **45**

Table 2.4 Amount of aspalathin extracted per gram of cream using (i) water/methanol (1:1) and (ii) tetrahydrofuran extraction methods (n = 2). **46**

Table 2.5 Distribution data of aspalathin in green rooibos extract (GRE) and standard aspalathin (As) solution both with a concentration of approximately 1 mg/ml aspalathin. **49**

Table 3.1 Biological and physiological characteristics of the human gastrointestinal tract (Balimane and Chong, 2005). **53**

Table 3.2 The cumulative (% of initial dose) transport ± SD of aspalathin in green rooibos extract across Caco-2 cell monolayers. **72**

Table 3.3 The cumulative (% of initial dose) transport ± SD of aspalathin in pure

aspalathin solution across Caco-2 cell monolayers. **74**

Table 3.4 The cumulative (% of initial dose) transport ± SD of aspalathin in Pheroids across Caco-2 cell monolayers. **76**

Table 3.5 The apparent permeability coefficient of (i) GRE, (ii) aspalathin solution, and (iii) Pheroids at three different concentrations. **78**

The transport of the Rooibos tea flavonoid aspalathin across the skin and the intestinal epithelium

Miao-Juei Huang

A dissertation submitted to the Faculty of Health Sciences, University of the Witwatersrand, Johannesburg, in fulfilment of the requirements for the degree of Master in Pharmacy.

Johannesburg, South Africa, 2006

DECLARATION

I, Miao-Juei Huang, declare that this dissertation is my own work. It is being submitted in fulfilment for the degree, Master of Pharmacy, University of the Witwatersrand, Johannesburg. It has not been submitted before for any degree or examination at this or any other University.

Signature_____

_____day of_____, 2006.

DEDICATION

I dedicate this dissertation to my parents

Hsiu-Lin Huang and Yi-Sheng Huang,

For their love and support,

guidance and encouragement in life.

ACKNOWLEDGEMENTS

I would like to express my sincere gratitude to my supervisor, Professor Alvaro M. Viljoen for the knowledge impacted on me, the support, encouragement and guidance provided throughout the duration of the research, and for his motivation towards the completion of this project.

I am also indebted to my co-supervisors, Professors Jeanetta du Plesssis and Josias Hamman. I am very appreciative of the knowledge I gained from them. Without their guidance and assistance this project would not have been taken to completion.

Acknowledgements to Professor Jan du Preez, I appreciate his technical assistance in the HPLC analysis. I am very grateful for the interest he showed and for his willingness to always help.

I am sincerely grateful to Miss Anja Judeinfield and Mr Ruaan Louw for their assistance in teaching me the percutaneous permeation experiment and their generosity in sharing their knowledge and information with me.

A sincere thank you to Mr Jason Lu for his assistance in culturing Caco-2 cells and assiting me during the Caco-2 transport experiment.

Thank you to my friends Carli, Madeli and Linda for their help, encouragement and hospitality during my visit at the North-West University (Potchefstroom campus).

I also would like to thank my friends, Maria, Jacqui, Ayesha, and Aneesa. I appreciate all the encouragement and advice they gave me.

I would like to thank the National Research Foundation (Indigenous Knowledge Systems) for the financial assistance.

A special word of thanks to Po-Chieh Cheng for your patience, understanding and your moral support. Thank you for always being on my side.

Thank you to my brother Cheng-Che for your inspiration and always taking care of me.

Finally, thank you to my parents for loving and supporting me. I am sincerely grateful for your guidance and all that you have given to me. Without your encouragement I could have not come this far in life.

ABSTRACT

The aqueous extract of rooibos has been used for more than three hundred years since its discovery by the indigenous people. Currently, rooibos is gaining popularity in the cosmetic industry and incorporation of rooibos extracts in topical cosmetic formulations has become a fashionable trend. Both topical and intestinal absorption of rooibos tea were investigated. The transport of aspalathin in the unfermented (green) rooibos aqueous extracts and aqueous solution of pure aspalathin were studied.

The percutaneous permeation experiments were conducted with vertical Franz diffusion cells using human female abdominal skin obtained from patients who underwent cosmetic surgery. The green rooibos extract and pure aspalathin solution buffered in phosphate buffer system (pH 5.5) were applied to the skin for 12 hours. Samples of the permeants were obtained from the receptor fluid phase and from the stratified layers of the skin by using the tape-stripping technique and analysed by HPLC.

In vitro intestinal epithelial transport experiments were carried out by using Caco-2 cell monolayers, isolated and cultured from human colonic adenocarcinoma cells, in a six-well transwell system. The green rooibos extract and pure aspalathin solution buffered in phosphate buffer (pH 7.4) were applied on to the cell monolayers and incubated for 2 hours. Samples were obtained from the basolateral phase at predetermined time intervals and analysed by HPLC.

Less than 0.1 % of the applied dose of aspalathin permeated the skin. Most of the permeated aspalathin accumulated in the stratum corneum. Close to 100 % of aspalathin was transported across the Caco-2 cell monolayers at a concentration dependent manner. Better absorption of aspalathin was observed using the green rooibos extract than with

the pure aspalathin solution across the Caco-2 cell monolayers.

TABLE OF CONTENTS

DECLARATION ii

DEDICATION iii

ACKNOWLEDGEMENTS iv

ABSTRACT vi

TABLE OF CONTENTS viii

LIST OF FIGURES xiii

LIST OF TABLES xviii

CHAPTER 1

GENERAL INTRODUCTION

1.1 Taxonomy of *Aspalathus linearis* 1

1.2 Botanical description 1

1.3 Variation in the *Aspalathus linearis* species complex 3

1.4 The history of rooibos tea 4

1.5 Uses and benefits of rooibos 6

1.6 Rooibos polyphenolic compounds 8

1.6.1 Free radical attack 8

1.6.2 Rooibos antioxidants 9

1.6.3 Total polyphenolic content 14

1.6.4 Total antioxidant capacity 15

1.7 Biological activities of rooibos tea 16

1.8 Aims of the study 17

CHAPTER 2

***IN VITRO* PERCUTANEOUS PERMEATION OF ASPALATHIN**

2.1 Overview of the human skin 19

2.1.1 Structure of the skin 20

2.1.1.1 Epidermis **21**

2.1.1.2 Dermis and hypodermis **23**

2.1.2 Routes of penetration through the skin 24

2.1.3 Physicochemical parameters influencing transdermal drug delivery 26

2.2 Materials and methods 28

2.2.1 Materials 28

2.2.2 High performance liquid chromatography (HPLC) method for the analysis of aspalathin 29

2.2.2.1 Apparatus **29**

2.2.2.2 Chromatographic conditions **29**

2.2.2.3 Preparation of stock solution **30**

2.2.2.4 Validation of HPLC procedure **30**

2.2.2.4.1 Linearity **30**

2.2.2.4.2 Accuracy and precision **31**

2.2.2.4.3 Sensitivity **32**

2.2.2.4.4 Selectivity **32**

2.2.3 Determination of stability of aspalathin in transport medium 36

2.2.4 Determination of octanol/water partition coefficient (K_{ow}) 36

2.2.5 Determination of aspalathin in commercial products 38

2.2.6 Aspalathin permeation study 38

2.2.6.1 Preparation of test formulations **38**

2.2.6.2 Preparation of skin **38**

2.2.6.3 Transport of aspalathin across the skin 39

2.2.6.4 Tape stripping the stratum corneum and epidermis 41

2.2.6.5 Sample analysis 42

2.2.6.6 Statistical analysis 42

2.3 Results and discussion 42

2.3.1 Stability in transport medium 42

2.3.2 Octanol/water partition coefficient (K_{ow}) 44

2.3.3 Determination of aspalathin in commercial products 45

2.3.4 Aspalathin permeation study 46

2.4 Conclusion 51

CHAPTER 3

***IN VITRO* INTESTINAL EPITHELIAL TRANSPORT OF ASPALATHIN ACROSS CACO-2 CELL MONOLAYERS**

3.1 Introduction 52

3.2 Comparison of *in vivo* and *in vitro* human intestinal epithelia 52

3.2.1 Anatomy and physiology of the small intestine 52

3.2.2 Pathways of intestinal absorption 55

3.2.3 The *in vitro* Caco-2 cell model for transport study 57

3.2.4 *In vitro*/*in vivo* correlations 58

3.3 *In vitro* Caco-2 cell monolayer transport study 60

3.3.1 Caco-2 cell culture and setup for transport studies 60

3.3.2 Determination of the apparent permeability coefficient (P_{app}) 61

3.3.3 Measurement of transepithelial electrical resistance (TEER) 62

3.4 Pheroid technology 62

3.5 Materials and methods 64

3.5.1 Materials 64

3.5.2 High performance liquid chromatography (HPLC) method for the analysis of aspalathin 64

3.5.3 Determination of stability of aspalathin 65

3.5.3.1 Stability in the transport medium 65

3.5.4 *In vitro* transport study 66

3.5.4.1 Preparation of test formulations for the transport study 66

3.5.4.2 Preparation of Caco-2 cell monolayers 66

3.5.4.2.1 Culturing of Caco-2 cells 66

3.5.4.2.2 Trypsination of the Caco-2 cells 66

3.5.4.2.3 Seeding and culturing of Caco-2 cell monolayers on 6-well filter plates 67

3.5.4.2.4 Measurement of TEER 68

3.5.4.3 Transport of aspalathin across Caco-2 cell monolayers 68

3.5.4.4 Sample analysis 69

3.5.4.5 Statistical analysis 69

3.6 Results and discussion 70

3.6.1 Stability of aspalathin in transport medium 70

3.6.2 Transport of aspalathin in green rooibos extracts 71

3.6.3 Transport of aspalathin in pure aspalathin solution 73

3.6.4 Transport of aspalathin in Pheroids 75

3.6.5 Comparison of apparent permeability coefficient (P_{app}) 77

3.7 Conclusions 79

CHAPTER 4

CONCLUSION AND FUTURE PROSPECTIVE

4.1 Summary and conclusion **81**

4.2 Future prospective **82**

REFERENCES **83**

ANNEXURE 1 **97**

LIST OF FIGURES

Figure 1.1 The natural habitat of *Aspalathus linearis* in the Cederberg Mountain regions (marked in red) north-west of Cape Town in South Africa (picture provided by A.M. Viljoen). **2**

Figure 1.2 Rooibos plantation (Erickson, 2003). **3**

Figure 1.3 The rooibos plant bearing needle-like leaves and pea-shaped flowers on ferruginous young branches. **3**

Figure 1.4 The chemical structures of quercetin (I) and luteolin (II). **11**

Figure 1.5 The isomeric forms of orientin (Koeppen and Roux, 1965a). **12**

Figure 1.6 The chemical structure of rutin. **12**

Figure 1.7 The isomeric forms of aspalathin (Koeppen and Roux, 1965b). **14**

Figure 2.1 Schematic diagram of cross-section of human skin (http://rds.yahoo.com/_ylt=A9G_RtvPXEdE8BcB6pujzbkF;_ylu=X3oDMTA4NDgyNWN0BHNlYwNwcm9m/SIG=12ve841bm/EXP=1145613903/**http://www.anti-aging-skin-care.com/forever-young-how-it-works-diagram.html). **21**

Figure 2.2 Skin permeation routes: (1) intercellular diffusion through the lipid

lamellae; (2) transcellular diffusion through both the corneocytes and the lipid lamellae; and (3) diffusion through skin appendages (hair follicles and sweat ducts) (Ho, 2004). **24**

Figure 2.3 Schematic diagram showing principal steps of permeation (modified from Zatz, 1993). **25**

Figure 2.4a HPLC chromatogram and UV spectrum of aspalathin (7.05 µg/ml), Rt = 7.658 min. **33**

Figure 2.4b HPLC chromatogram and UV spectrum of green rooibos extracts (5 µg/ml) aspalathin Rt = 7.823. **34**

Figure 2.4c HPLC chromatogram of skin tissue. **35**

Figure 2.4d HPLC chromatogram of skin surface sample. **35**

Figure 2.5 Skin dermatome obtaining split-thickness skin using a electric dermatome (http://www.zimmergermany.de and http://www.residentnet.com). **39**

Figure 2.6 Vertical Franz diffusion cell consisting of an upper donor compartment (chamber) and bottom receptor compartment (re-drawn from http://www.permegear.com/franz.htm). **41**

Figure 2.7a Amount of aspalathin (% of initial concentration) in 1.4 µg/ml of aspalathin solution, buffered at pH 5.0, 6.0, and 7.0, stored for 14 hours at

room temperature (25 °C). **43**

Figure 2.7b Amount of aspalathin (% of initial concentration) in 1.4 µg/ml aspalathin solution, buffered at pH 5.0 and 5.5, at room temperature (25 °C) for 9 hours. **43**

Figure 2.8 Chromatogram of a water/methanol extract of cream A depicting aspalathin at 7.48 min and other flavonoid compounds. **46**

Figure 2.9 The average percentage (%) of aspalathin that permeated the skin in green rooibos extract and aspalathin solution applied. (The outlier has been excluded). **48**

Figure 2.10 Comparison of the absolute amount of aspalathin permeated in green rooibos extracts and aspalathin solutions. (The outlier has been excluded). **48**

Figure 3.1 Villi and microvilli increase the absorptive surface area of the small intestine (re-drawn from http://www.emc.maricopa.edu/faculty/farabee/BIOBK/BioBookDIGEST.html). **54**

Figure 3.2 Routes of drug transport. (A) Passive transcellular absorption across intestinal epithelium. (B) Paracellualr absorption mediated by tight junctions. (C) Carrier-mediated transcellular transport at the apical and/or basolateral membranes. (D) Efflux transporter at the apical membrane may

actively drive compounds back into the intestinal lumen thus restricting their absorption into the blood. (E) Apical efflux transporters that facilitate intestinal clearance of compounds that are already present in blood. (F) Intracellular metabolising enzymes may modify compounds before they enter the blood. (G) Apical efflux transporters and intracellular metabolising enzymes may co-ordinately metabolise and excrete compounds, forming an effective barrier against intestinal absorption. (H) Transcellular vesicular transport (modified from Chan *et al*., 2004; Hunter and Hirst, 1997). **56**

Figure 3.3 A comparison of *in vivo* extensively folded intestinal epithelia and *in vitro* flat Caco-2 cell monolayer, and barriers across which drugs must pass to reach the basolateral phase (Youdim *et al.*, 2003). **60**

Figure 3.4 The *in vitro* cell culture model (modified from Youdim *et al.*, 2003; During and Harrison, 2005). **61**

Figure 3.5 Procedures of *in vitro* transport across Caco-2 cell monolayers (A) Seeding of Caco-2 cells. (B) Measurement of TEER. (C) Removal of growth medium. (D) Loading of test formulation onto Caco-2 cell monolayers. (E) Sampling from the basolateral phase at predetermined time intervals (photos provided by A.M. Viljoen). **69**

Figure 3.6 Loss of aspalathin over time in vehicles of (i) double distilled water, (ii) phosphate buffer solution (PBS) (pH 7.4), and (iii) Dulbecco's Modified Eagle's Medium (DMEM). **70**

Figure 3.7 Plot of the cumulative transport of aspalathin in green rooibos extracts over time. **72**

Figure 3.8 Plot of the cumulative transport of aspalathin in pure aspalathin solution over time. **74**

Figure 3.9 Plot of the cumulative transport of aspalathin in Pheroids over time. **76**

Figure 3.10 Comparison of the apparent permeability coefficient (P_{app}) of: (i) GRE, (ii) aspalathin solution, and (iii) Pheroids at three different concentrations. **78**

LIST OF TABLES

Table 1.1 Nutritional content of Rooibos tea (Morton, 1983). **7**

Table 2.1 Gradient elution employed for reverse-phase HPLC separation of aspalathin. **30**

Table 2.2 Quantification of accuracy and precision of aspalathin recovery from three concentration levels. **31**

Table 2.3 Octanol-water partition coefficient (K_{ow}) of aspalathin and log P value. **45**

Table 2.4 Amount of aspalathin extracted per gram of cream using (i) water/methanol (1:1) and (ii) tetrahydrofuran extraction methods (n = 2). **46**

Table 2.5 Distribution data of aspalathin in green rooibos extract (GRE) and standard aspalathin (As) solution both with a concentration of approximately 1 mg/ml aspalathin. **49**

Table 3.1 Biological and physiological characteristics of the human gastrointestinal tract (Balimane and Chong, 2005). **53**

Table 3.2 The cumulative (% of initial dose) transport ± SD of aspalathin in green rooibos extract across Caco-2 cell monolayers. **72**

Table 3.3 The cumulative (% of initial dose) transport ± SD of aspalathin in pure

aspalathin solution across Caco-2 cell monolayers. **74**

Table 3.4 The cumulative (% of initial dose) transport ± SD of aspalathin in Pheroids across Caco-2 cell monolayers. **76**

Table 3.5 The apparent permeability coefficient of (i) GRE, (ii) aspalathin solution, and (iii) Pheroids at three different concentrations. **78**

CHAPTER 1: GENERAL INTRODUCTION

1.1 Taxonomy of *Aspalathus linearis*

As early as 1686, *Aspalathus linearis* (Burm. fil) R. Dahlgren was described by Ray in *Historia Plantarium* as "*Genista Africana frutescens, foliis Linearіae angustioribus glaucis, flore lutea* D. Sherard" (Dahlgren, 1968) and has also been validly known as "*Galega affinis Malabarica arborescens siliquis majoribus articulatus*" by Plukenet in 1700 (Dahlgren, 1968). Later on, numerous different names were given to *A. linearis* by several botanists and only in 1963, Dahlgren confirmed that the various descriptions were directed to the same plant. Together with N.L. Burman who described the plant in the name *Psoralea linearis* Burm. fil in 1768, Dahlgren (1968) made a combination resulting in the formally accepted description correctly known as "*Aspalathus* (subgen. *Nortieria*) *linearis* (Burm. fil. 1768) R. Dahlgren 1963" (Dahlgren, 1964).

1.2 Botanical description

Rooibos (*Aspalathus linearis*) is a shrub-like leguminous flowering plant that belongs to the Fabaceae (Leguminosae) family. It naturally inhabits the Cederberg Mountain regions, mountains of the Table Mountain series (Dahlgren, 1968), north-west of Cape Town in South Africa. The plant can grow up to 2 meters high, bearing slender branches that may be sparingly or closely distributed. The bark is ferruginous, dark red or purple on the younger branches, becoming grey upon ageing (more than 1½ years) (Dahlgren, 1963 and Dahlgren, 1968). Leaves are simple, long and narrow, ranging from 15 to 60 mm long and 0.4 to >1.0 mm broad. The leaves grow straight, may be slightly flattened and rigid, found singly or in bunches. Leaves may range from pale, bright or dull green, rarely light green, often becoming reddish-brown when dried (Dahlgren, 1968). Small short lateral teeth may occasionally be found at the base of the leaf (Dahlgren, 1963). Flowers are found on the

tips of the branches, one or up to seven together in terminal racemes or umbels, or in clusters on lateral short shoots (Dahlgren, 1968). The pea-shaped flowers are pale to bright yellow often with a touch of purple at the back and base of the petals (Dahlgren, 1963 and Dahlgren, 1968). The flowers are produced in spring through early summer (Erickson, 2003) and each flower generates one fruit referred to as a pod containing only one small, hard-shelled, dicotyledonous seed that becomes reddish-brown when ripe (Dahlgren, 1968 and http://members.tripod.com/~Meerkat_2/erooibos.html). The plant has a tap root system that can grow up to 2 m long to enable it to survive during periods of droughts in summer (Erickson, 2003). Nodules of nitrogen fixing bacteria, *Bradyrhizobium aspalti*, are found on the root systems that exist symbiotically with the plant (Boone *et al.*, 1999). These bacteria absorb atmospheric nitrogen dioxide converting it to biologically useful ammonia (Erickson, 2003 and Boone *et al.*, 1999), a process called nitrogen fixation, providing nutrients to the plant minimising the need for fertilising commercial crops for nitrogen, and in exchange the bacteria acquire their nutrients from the plant generated during photosynthesis (Erickson, 2003).

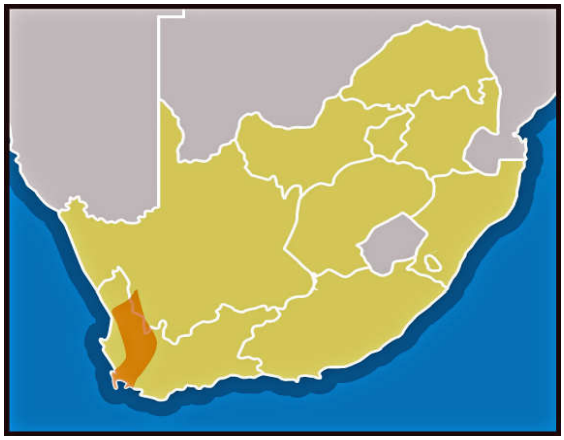


Figure 1.1: The natural habitat of *Aspalathus linearis* in the Cederberg Mountain regions (marked in red) north-west of Cape Town in South Africa (picture provided by A.M. Viljoen).



Figure 1.2: Rooibos plantation (Erickson, 2003).



Figure 1.3: The rooibos plant bearing needle-like leaves and pea-shaped flowers on ferruginous young branches (photo provided by A.M. Viljoen).

1.3 Variation in the *Aspalathus linearis* species complex

There are more than 200 species of *Aspalathus* indigenous to South Africa (Erickson, 2003) and the genus *Aspalathus* is a type of "sclerophyll bush" commonly called "fynbos" or "macchia" (Dahlgren, 1963). *A. linearis* together with *A. pendula* R. Dahlgren fall under the subgenus *Nortieria* (Dahlgren, 1968) of the genus *Aspalathus*. It is the leaf character that differentiates the subgenus *Nortieria* from the rest of the groups of *Aspalathus*

(Dahlgren, 1968). *A. linearis* is a polymorphic species that comprises three subspecies, namely, *Aspalathus linearis* (Burm. fil.) R. Dahlgren ssp. *linearis*; *Aspalathus linearis* (Burm. fil.) R. Dahlgr. ssp. *pinifolia* (Marl.) R. Dahlgren; and *Aspalathus linearis* (Burm. fil.) R. Dahlgren ssp. *latipetala* R. Dahlgren, each with characteristic morphology and geographical distribution. *A. linearis* ssp. *linearis* is the most common of the subspecies (Dahlgren, 1968), large variation in total size, length and coarseness of leaf, leaf colour etc. is present within this subspecies. Many of the commercially available rooibos tea plantations originate from wild forms of *A. linearis*, sometimes referred to as Rooi (Red), Rooi-Bruin (Red-Brown), Vaal (Grey), and Swart (Black) types, they are closely related and differ only in respect of slightly deviating in style of growth (habit), area of occurrence, the colour and aroma of tea they produce, and the quality of the processed product (Dahlgren, 1968 and http://members.tripod.com/~Meerkat_2/erooibos.html). Only the Red tea type is cultivated and commercialised (Dahlgren, 1968). Within the Red tea type it is further subdivided into two subtypes, namely, (i) Nortier-type, the cultivated and selected biotype that originated from the wild forms, has fresh green slender leaves and bright yellow flowers that produce reddish-coloured tea with a mild aroma (Dahlgren, 1968); (ii) Cederberg-type, which also originated from the same wild forms from which the Nortier-type was selected but occurs in slightly different regions to the Nortier-type. The tea produces the same colour and aroma but is said to be of inferior quality in comparison to the Nortier-type (Dahlgren, 1968).

1.4 The history of rooibos tea

By definition the word “tea” refers to infusions made from leaves of *Camellia sinensis* (L.) Kuntze (Theaceae), the evergreen shrub from which green tea or oolong tea is made. Infusions made from herbs like rooibos (*Aspalathus linearis*) are technically referred to as “tisanes”. It has now, however, become accepted to refer to herbal infusions as tea, and

rooibos makes a tea that is red-brown in colour hence the name “Rooibos” (meaning Redbush) (Erickson, 2003).

The use of rooibos dates back to more than 300 years ago when the indigenous mountain inhabitants of South Africa, the Khoisan, a tribe of South African Bushman, discovered that the rooibos could be brewed to make a sweet and tasty beverage (Erickson, 2003 and Cason, 2004). The use of this plant was then recorded by the botanist Carl Thunberg when the tea was introduced by the Khoisan in 1772 (Morton, 1983). Rooibos was collected by chopping the young branches of the wild shrubs in the mountains with axes, bruising the harvest with wooden hammers and leaving it in heaps to ferment (Dahlgren, 1968 and Erickson 2003). Today, the method of harvesting and processing is done in very much the same way but with more advanced technology, refined methods with systematic cultivation and strict quality control throughout (Erickson, 2003 and http://www.dr-nortier.com/history .htm)

Before 1925 the tea was exclusively collected from the wild in the mountains (Dahlgren, 1963). In 1904, a Russian immigrant Benjamin Ginsberg, whose family was involved in the tea industry in Europe for over a century realized the market potential and started to buy, pack and trade this “tea” collected in the mountains by the Khoisan. Cultivation of rooibos was attempted in about 1925 by Dr. P. le F. Nortier, who was a medical practitioner, and Mr. O. Berg who collected seeds in the Cederberg Mountains (Dahlgren, 1963). In the 1930’s, Dr. Nortier investigated how to collect the seeds effectively, how to improve germination, and how to handle the seedlings and grow the shrubs in plantations. Dr. Nortier shared his experience with some farmers resulting in rooibos being produced on a larger scale (Dahlgren, 1968). Ginsberg then bought the tea from the farmers and traded the product globally on a small scale. The demand for rooibos increased dramatically

during World War II when the availability of Oriental tea declined due to difficulties experienced with buying and shipping tea from war-ridden Asia. However, the rooibos tea market underwent a severe crisis in 1948 which resulted in establishing the Clanwilliam Tea Cooperative, in an attempt to save the interest of the tea producers. Over-production of rooibos tea led to another crisis in 1954, after which the Rooibos Tea Control Board was established and stabilised the market once again by improving, controlling and classifying the type of rooibos cultivated and marketed (Dahlgren, 1968).

In 1968, Annekie Theron discovered the ability of rooibos tea to calm her baby, relieving infant colic and insomnia. It was not until 1970 that rooibos tea became internationally recognized (Erickson, 2003 and Cason, 2004) with a book she wrote and published, titled *Allergies: An Amazing Discovery*. Since then she patented a rooibos extract that is now used in cosmetic products and started her own line of health and cosmetic products (Erickson, 2003).

1.5 Uses and benefits of rooibos

Rooibos is famous for being naturally caffeine-free (Morton, 1983) making it suitable for children, the elderly and people who are intolerant to the stimulative effects of caffeine, and its low tannin content (4.4%) minimises the risk of insufficient iron absorption, a condition frequently found in tea drinkers that result from iron-tannin complexation (Erickson, 2003 and Morton 1983). Rooibos tea also contains various amounts of minerals and nutrients (Table 1.1) making it a health beverage ideal to use as a fluid replacement for infants and athletes.

Table 1.1: Nutritional content of Rooibos tea (Morton, 1983).

Nutrient	Amount
Caffeine	0
Ascorbic acid	15.7mg/100g
Tannin (as gallic acid)	4.4%
Protein	6.9%
Ash	2.5%
Soluble ash	1.3%
Petroleum ether extract	1.7%
Iron	0.33%
Alumina	0.99%
Calcium	0.20%
Magnesium	0.33%
Potash	0.56%
Sulphate	0.11%
Manganese	0.012%
Phosphate	0.12%

Before Annekie Theron discovered the effects of rooibos tea on her baby, rooibos tea was purely a good-tasting beverage enjoyed by the people who discovered it (Erickson, 2003). After having found no documentation on the uses and benefits of rooibos tea she began her own experiments with local babies who had colic and allergies. A series of health claims for rooibos tea were then made and published including, among others, digestive disorders as in infant colic and stomach upsets, allergies such as hay fever, asthma, skin allergies, eczema and nappy rash, sleep disorders, headaches and migraine by calming the central nervous system (http://www.rooibosltd.co.za/ and http://www.redbushtea.com/). Although not enough research could substantiate these folk remedies, more scientists became intrigued by the unique properties of rooibos tea.

1.6 Rooibos polyphenolic compounds

1.6.1 Free radical attack

Superoxide radical ($\cdot O2^-$) is a common by-product generated from normal physiological functions in the body involving oxygen species, e.g. cellular respiration, activated polymorphonuclear lecocytes, endothelial cells, and mitochondrial electron flux (Muscoli *et al.*, 2003). These highly reactive oxygen species are characterised by the loss of an electronic spin resulting in a molecule with an unpaired electron. Superoxide radicals can react with hydrogen peroxide (H_2O_2) to generate hydroxyl radical ($\cdot OH^-$) and cause breakage in DNA strands, peroxidation of membrane lipids, and inactivation of cellular enzymes (Muscoli *et al.*, 2003; Chen and Pan, 1996). It is clear that superoxide radicals are associated with the pathogenesis of several diseases, such as endothelial cell damage and increased microvascular permeability, promoting the inflammatory process, autocatalytic destruction of neurotransmitters and adrenalin and noradrenalin hormones, inactivation of nitric oxide important to the capacity of blood vessels to vasodilate (Muscoli *et al*., 2003). By reaction with nitric oxide the superoxide radical becomes a potent cytotoxic and pro-inflammatory molecule, peroxynitrite. Some clinical manifestations of explicit production of superoxide radicals include ischemia and reperfusion, organ transplantation, shock and inflammation, neurodegeneration such as Alzheimer's disease.

Solar ultraviolet (UV) radiation exposure, for example, is one of the external contributing factors that also cause physiological increase in production of superoxide radicals. The superoxides result from the interaction of UV radiation with proteins, lipids, and DNA and results in physiological changes such as sunburn cell formation, basal and squamous cell carcinomas, melanomas, cataracts, photo-aging of the skin, and immune suppression. Free radical attack on nuclear and mitochondrial DNA is believed to be a major contributing

factor to aging (Juliet *et al.*, 2005)

The body contains several enzymatic and non-enzymatic superoxide detoxifying agents (e.g. superoxide dismutase, glutathione peroxidase, catalase, thioredoxin reductase, tocopherol, glutathione, and ascorbic acid) to combat the various physiological stressors (Afaq *et al*., 2005). However, these natural antioxidants may be depleted and the body is thus put under pro-oxidant/antioxidant disequilibrium called "oxidative stress". In order to restore homeostasis, antioxidants especially of botanical source have gained considerable attention as they are present in common foods and beverages.

1.6.2 Rooibos antioxidants

The full benefits of teas come from the combination of all the antioxidants rather than from just one substance (Erickson, 2003). Both flavonoids and phenolic acids in rooibos tea are powerful antioxidants. Flavonoids are a group of polyphenolic compounds with a flavan nucleus. More than 4000 flavonoids have been identified to date. In plants, they afford protection against UV radiation, pathogens, and herbivores. Most of the beneficial effects of flavonoids are attributed to their antioxidant and chelating abilities (Heim *et al.*, 2002 and Tammela *et al.*, 2004). These polyphenolic compounds competitively consume the reactive oxygen species thus sparing the target molecule, and quench the chain reaction propagating free radical oxidation (Afaq *et al*., 2005). They act by donating a hydrogen (H^+) atom from their hydroxyl functional groups to the reactive oxygen species. As the polyphenols are electron-rich compounds that contain several hydrolysable hydroxyl functional groups, the compound may stabilise itself when an electron is lost after hydrogen donation and thereby do not becoming radicals themselves.

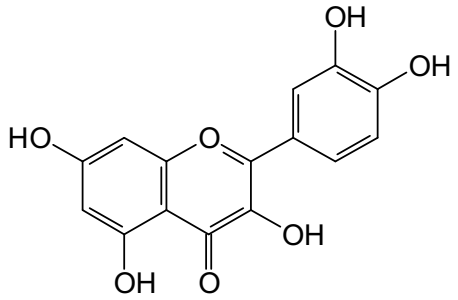
Flavonoids have been scientifically reviewed for their biological properties, apart from being potent antioxidants they also demonstrate to have, among others, hepatoprotective,

antithrombotic, antibacterial, antiviral, antitumourogenic, exhibit immunostimulant activities and can interact with protein phosphorylation (Bonina *et al*., 1996). Flavonoid antioxidants identified in rooibos include aspalathin, nothofagin, quercetin, isoquercetin, orientin, iso-orientin, rutin, luteolin, vitexin, and chrysoeriol (Bonina *et al*., 1996 and Joubert *et al.*, 2004). Of the flavonoids identified, aspalathin, rutin and orientin occur in the largest quantities followed by iso-orientin and isoquercetin (Erickson, 2003 and Bramati *et al*., 2002). Joubert *et al*. (2004) evaluated the radical scavenging capacity of rooibos flavonoids and tannins, as well as the aqueous extracts and crude phenolic fractions of unfermented and fermented rooibos. By using 2,2-diphenyl-1-picrylhydrazyl (DPPH·) and a superoxide radical (·O2-) they found that quercetin is a stronger antioxidant than orientin, followed by luteolin then aspalathin against the DPPH radical. Quercetin and aspalathin are equally powerful as antioxidant against the superoxide anion ($\cdot O2^-$).

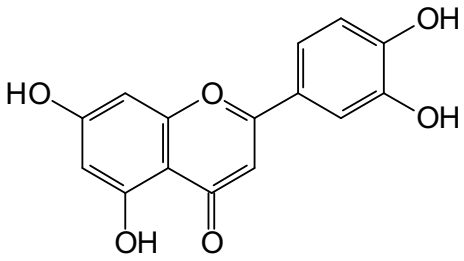
Phenolic acids found in rooibos also demonstrate antioxidant activity (Erickson, 2003). They are substances commonly found in fruit, vegetables and whole grains. The phenolic acids identified in decreasing order of activity against the DPPH radical include caffeic acid, protocatehuic acid, syringic acid, ferulic acid, vanillic acid, ρ-hydroxybenzoic acid, and ρ-coumaric acid. Caffeic acid has been found to be equally active against the DPPH radical compared to quercetin, aspalathin, and iso-quercetin (Joubert, 1996).

In relation to being a free radical scavenger the various flavonoids contained in rooibos have been intensively studied as they are common phenolic compounds found in a variety of fruits and vegetables. The various physiological activities may be associated with stabilizing the reactive oxygen species halting the series of alterations in various cellular, biochemical and molecular changes that ultimately lead to cancer formation.

Quercetin and luteolin have been shown to induce apoptosis in cancer cells (Lee *et al*., 2002) and may inhibit *in vitro* proliferation of thyroid and colon cancer cells. Quercetin may inhibit the effect on cyclooxygenase-2 (COX-2) expression in colonic cancer cells which may contribute to the prevention of colonic cancer. Both quercetin and luteolin (Figure 1.4) halt the formation of lipid peroxides. Quercetin also has antispasmodic properties that may help in infant colic (Erickson, 2003).



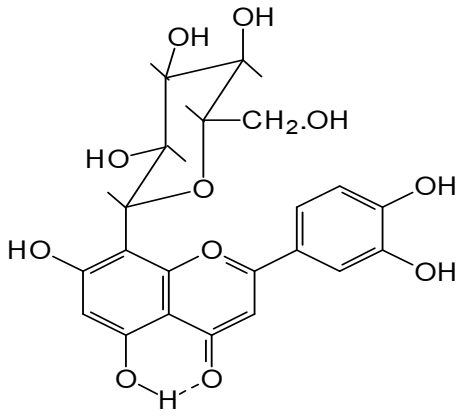
I



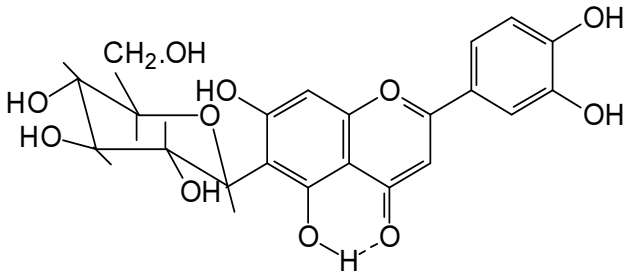
II

Figure 1.4: The chemical structures of quercetin (I) and luteolin (II).

Orientin (Figure 1.5) has been found to reduce the number of cancer-associated cellular changes in blood after exposure to radiation by arresting lipid peroxidation in the liver and reducing damage to the bone marrow and gastrointestinal tract (Erickson, 2003).



I



II

Figure 1.5: The isomeric forms of orientin (Koeppen and Roux, 1965a)

Rutin (Figure 1.6) maintains the strength and integrity of capillary walls and has been used to treat haemorhoids, varicose veins, and lower leg oedema associated with venous insufficiency and venous hypertension (Erickson, 2003).

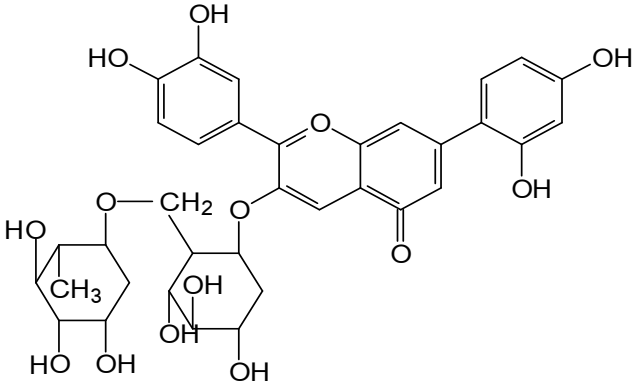
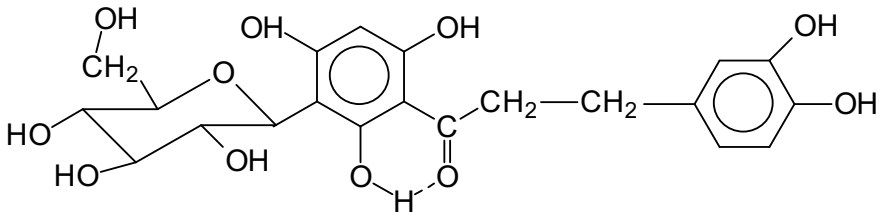
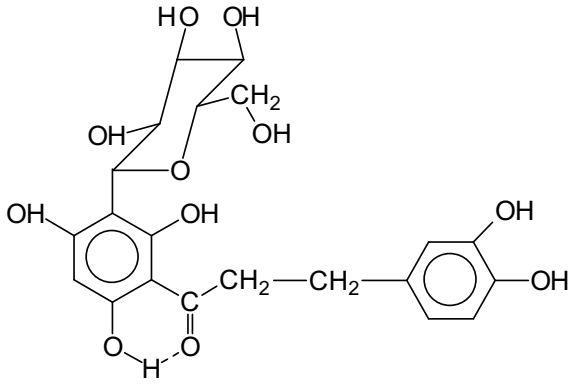


Figure 1.6: The chemical structure of rutin.

Aspalathin, $C_{21}H_{24}O_{11}$, is the major flavonoid constituent of rooibos and hence is the focus of this study. It is an amorphous compound and, like other rooibos constituents quercetin, orientin and vitexin, it is a C-glycosylflavonoid and has been characterised as 3'-C-β-D-glucopyranosyl-3,4,2',4',6'-pentahydroxydihydrochalcone (Koeppen and Roux, 1965b). The compound constitutes at least 20 % of the ethanol/acetone soluble material of the dried green leaves, thus considered as the major monomeric flavonoid present (Koeppen, 1963). This novel compound is the first known example of a naturally occurring C-glycosyldihydrochalcone and is found exclusively in *Aspalathus linearis* (Koeppen and Roux, 1965b and Koeppen, 1970). It can exist in two isomeric forms (Figure 1.7) which are readily interconvertable, and yields clusters of fine, colourless needles on crystallisation from acetone-ethyl acetate (Koeppen, 1970). Aspalathin is readily soluble in water and other polar solvents but is insoluble in non-polar media. Alkali fusion with dry potassium hydroxide (KOH) results in degradation of the compound to phloroglucinol and protocatechuic acid. However, it remains intact (no liberation of the sugar moiety) when refluxed with aqueous 2N hydrochloric acid (HCl) for 24 hours (Koeppen and Roux, 1966). This suggests that the compound may withstand gastric conditions after oral administration.



I



II

Figure 1.7: The isomeric forms of aspalathin (Koeppen and Roux, 1965b).

Under the normal process of rooibos tea manufacturing less than 7 % of the aspalathin originally present in the unfermented tea remains after the fermentation process (Von Gadow *et al.*, 1997). Koeppen and Roux (1966) found aspalathin undergoes cyclisation during oxidation to form the flavanones 2,3-dihydro-iso-orientin and 2,3-dihydro-orientin in the presence of oxygen and sunlight, and with prolonged exposure to sunlight the flavanones converted to unknown brown products. The dihydrochalcones are more effective as antioxidants than their corresponding flavanones, which may explain the decrease in hydrogen-donating ability of the rooibos tea after fermentation (Von Gadow *et al.*, 1997). Joubert (1996) discovered that sun-drying is not necessary for the degradation of aspalathin, other degradation mechanisms, such as enzymatic and chemical oxidation initiated with tea comminution at which time exposure to oxygen and cell damage occurs in the leaves may cause degradation of aspalathin in the absence of sunlight.

1.6.3 Total polyphenolic content

The traditional processing of rooibos tea entails fermentation of the harvested green leaves and stems producing tea that is reddish in colour with its characteristic sweet aroma.

During the process of fermentation, oxidation of the flavonoid contents takes place resulting in the loss of flavonoid antioxidants. A 150 to 200 ml serving of fermented rooibos tea can have up to 60 to 80 mg of total polyphenolics; a serving of 150 ml of fermented rooibos tea made with 2.5 g of tea leaves contain about 3 mg of aspalathin (Erickson, 2003). The phenolic composition of a tea extract is greatly influenced by fermentation, a reaction that takes place during the processing of the tea (Von Gadow *et al.*, 1997). Thus by eliminating the fermentation process of the tea after harvest may prevent loss of the flavonoids.

1.6.4 Total antioxidant capacity

The capacity of flavonoids, tannins, and phenolic fractions of fermented and unfermented rooibos aqueous extracts to scavenge the DPPH and superoxide anion (O_2^-) radicals were found, in decreasing order: (i) against the DPPH radical: quercetin ≥ proanthocyanidin B3 ≥ orientin ≥ luteolin ≥ aspalathin ≈ isoquercetrin > iso-orientin catechin > rutin >> vitexin ≥ chrysoeriol; and (ii) against O_2^-: quercetin ≈ aspalathin > orientin ≥ catechin ≥ rutin ≥ isoquercetrin > iso-orientin > luteolin > chrysoeriol > vitexin (Joubert *et al.*, 2004). Furthermore, Joubert *et al.* (2004) found that the ethyl/acetate solubles of the aqueous extract of unfermented rooibos and the crude aspalathin fraction exhibit the greatest anti-radical capacity. Marnewick *et al.* (2004) estimated that the total phenolic (TP) content of green tea as ethanol/acetone (E/A) soluble fractions was similar to that of unprocessed rooibos tea, and the flavonol/flavone content of the processed and unprocessed rooibos E/A fractions were significantly ($P < 0.001$) higher than that of the green tea and honeybush tea fractions investigated. Furthermore, when comparing green tea, unprocessed and processed rooibos and honeybush teas, and the green tea exhibited the greatest inhibition against lipid peroxidation (99%) followed by unprocessed rooibos tea (91%), processed rooibos tea (65%), unprocessed honeybush tea (63%), and processed honeybush tea had the least

protective effects (13%).

1.7 Biological activities of rooibos tea

Extracts of fermented and unfermented rooibos have been tested for various biological activities in the recent years. Sasaki *et al.* (1993) showed that fermented rooibos tea reduced cancer associated changes in animal cells induced by benzo(a)pyrene mutagen and mitomycin C mutagens both *in vitr*o and in *vivo* and exhibited greater activity than green tea. Marnewick *et al.* (2000) investigated the antimutagenic properties of rooibos tea using the *Salmonella typhimurium* antimutagenicity assay. Both aqueous extracts of fermented and unfermented rooibos teas exhibited antimutagenic activity against 2-acetylaminofluorene (2-AAF) and aflatoxin B_1 (AFB_1)-induced mutagenesis of tester strains TA 98 and TA 100 in the presence of metabolic activation. Oral administration of fermented and unfermented rooibos teas to male Fischer rats showed reduced activation of AFB_1 in the microsomal fractions of livers of the rats (Marnewick *et al*., 2004). Furthermore, topical application of ethanol/acetone (E/A) fractions of fermented and unfermented rooibos tea on IRC mouse skin prior to the tumour promoter, 12-*O*-tetra decanoylphorbol-13-acetate, also showed inhibition of skin tumour formation (Marnewick *et al*., 2004). Kunishiro *et al*. (2001) examined the immune response of female BALN/c rats and Wister/ST rats fed with aqueous extracts of rooibos tea and found that the tea facilitated (both *in vivo* and *in vitro*) the antigen-specific antibody production through selective augmentation of interleukin 2 generation, and suggests that the intake of rooibos tea may support in the prophylaxis of diseases involving severe defect in Th (helper T cell) 1 immune response, such as cancer, allergy, AIDS, and other infections (Kunishiro *et al*., 2001). Free radical production can be proportional to the amount of oxygen consumption. Neuronal cells may generate much higher free radicals than other cells (Juliet *et al*., 2005). Increases in lipid peroxides in the brain results in damage of neuronal cells and contribute

to age-related diseases (Inanami *et al*., 1995). By measuring the amount of thiobarbituric acid reactive substances (TBARS) Inanami *et al*. (1995) showed protection of rooibos tea against several regions of the brain against lipid peroxidation in rats fed with rooibos tea. Ulicna *et al.* (2003) investigated the hepatoprotective properties of rooibos tea. Using a rat model where liver injury is induced by carbon tetrachloride (CCl_4), rooibos tea showed histological regression of steatosis and cirrhosis in the liver tissue with a significant inhibition of the increase of liver tissue concentrations of malondialdehyde, triacylglycerols and cholesterol. The increase in plasma activities of aminotransferases (ALT, AST), alkaline phosphatase and bilirubin concentrations were also significantly suppressed.

1.8 Aims of the study

Over the past few years following the publication of A. Theron's discovery on the wonders of rooibos tea with emphasis on the antioxidant properties of rooibos, the global sales of rooibos tea has increased from 750 tons in 1993 to more than 3 500 tons in 2001 (Joubert *et al.*, 2004). Many studies, including animal studies, have proven that rooibos tea is biologically active and beneficial to the body. In relation to rooibos tea's powerful radical scavenging ability, anti-ageing and UV protective properties against photo-damage of the skin associated with skin cancer formation, have become the two additional selling points of rooibos. Rooibos is no longer used only as beverage, the traditional way of benefiting from rooibos. Since the skin is the largest, most accessible organ of the body that is the most exposed area to environmental oxidative stress (Mavon *et al*., 2004), incorporation of rooibos extracts in topical cosmetic formulations has become a trend in cosmaceuticals to directly target the site of action to fight UV radiation damage and photo-ageing.

Thus, the aim of this study was to investigate the absorption of aspalathin in rooibos tea via

the topical and oral routes of administration by conducting *in vitro* percutaneous and *in vitro* intestinal epithelial permeation experiments. Aqueous extracts of the unfermented (green) rooibos and pure aspalathin solution were used. Detection of aspalathin served as the marker of transport. The specific objectives of this study were to:

a. Assess the percutaneous permeation of aspalathin.
b. Quantify the amount of aspalathin permeable across the skin.
c. Evaluate the distribution of aspalathin across the stratified layers of the skin.
d. Assess the percutaneous permeation of skin care product containing rooibos extract.
e. Assess the permeation of aspalathin across intestinal epithelium.
f. Quantify the permeable aspalathin across the intestinal epithelium.
g. Evaluate the permeability of aspalathin in a Pheroid technology formulation across the intestinal epithelium.
h. Compare aspalathin permeation in the green rooibos aqueous extract and in the pure aspalathin solution.

In the *in vitro* percutaneous permeation study female human abdominal skin was used and the permeation experiments were conducted at the Department of Pharmaceutics, North-West University (Potchefstroom campus). The *in vitro* intestinal epithelial transport study involved Caco-2 cell monolayers and the transport experiments were performed at the School of Pharmacy, Tshwane University of Technology, Pretoria.

CHAPTER 2: *IN VITRO* PERCUTANEOUS PERMEATION OF ASPALATHIN

2.1 Overview of the human skin

Early records of Babylonian and Egyptian medicine indicate that topical delivery has been used as a route of medicinal delivery (Hadgraft and Lane, 2005) through ointments, salves and pomades (Hadgraft and Somers, 1965). Drug administration via skin is mainly categorised into two approaches: (1) topical delivery, for local therapeutic effects, e.g. on diseased skin; and (2) transdermal delivery for systemic therapeutic effects. In either case, drug molecules need to be taken up by the skin. The term skin uptake is commonly used to describe the fate of drugs upon their entry into the skin. It is a broad definition that encompasses retention, permeation, metabolism, degradation and binding to skin components, various activities which a drug can undergo upon partitioning into the skin. In case of topical delivery, the objective is to have optimal drug residence in the skin layers i.e. skin retention. Whereas in the case of transdermal delivery, an optimal net transport across the skin (skin permeation) becomes an important criterion in determining the drug efficacy (Behl *et al.*, 1990)

The ability of drugs to permeate the complex, multilayered, heterogenous skin (i.e. skin permeability) varies as a function of individuals, body site, race, gender, age, overall skin condition and the state of the skin, that is, diseased or normal (Behl *et al*., 1990). Flynn (1979) reports that the permeability of skin of the same body site of apparently healthy individuals can differ as much as ten-fold. For example, premature babies have exceptionally permeable skin as opposed to senile skin which is dry, irritable and poorly vascular. The stratum corneum of Caucasian and black skin have essentially equal thickness but the latter contains more cell layers and is more dense. Therefore, the black skin is less permeable than white skin (Flynn, 1979).

Drug delivery via the skin offers several advantages over conventional routes. It avoids the first-pass metabolism by the liver and enzymatic degradation in the gastrointestinal tract. It is a non-invasive method of drug delivery with no trauma or risk of infection that has the potential for sustained and controlled drug release, and may improve patient compliance because its user-friendliness (Denete *et al*., 2004). However, because the skin is a complex organ that serves to protect the body against harmful invasions from the external environment, the transdermal drug delivery systems are faced with barriers and difficulties that will be discussed further in the following section.

2.1.1 Structure of the skin

The skin is the largest and most easily accessible organ of the body (Thomas and Finnin, 2004). It is a complex organ that serves to protect the underlying tissues against external physical, chemical, immunological and pathogenic intrusion as well as ultraviolet (UV) radiation and free radical attacks, while retaining moisture and providing thermal regulation (Ho, 2004). It is the major thermoregulatory organ and contains sensory organs for sensing pressure, pain and temperature. The skin also functions as an endocrine gland synthesising vitamin D by peripheral conversion of prohormones. In addition, it plays a significant role in reproduction in presenting secondary sexual characteristics and pheromone production (Flynn, 1979).

The skin can be divided into three primary regions: the epidermis, the dermis, and the hypodermis (Figure 2.1).

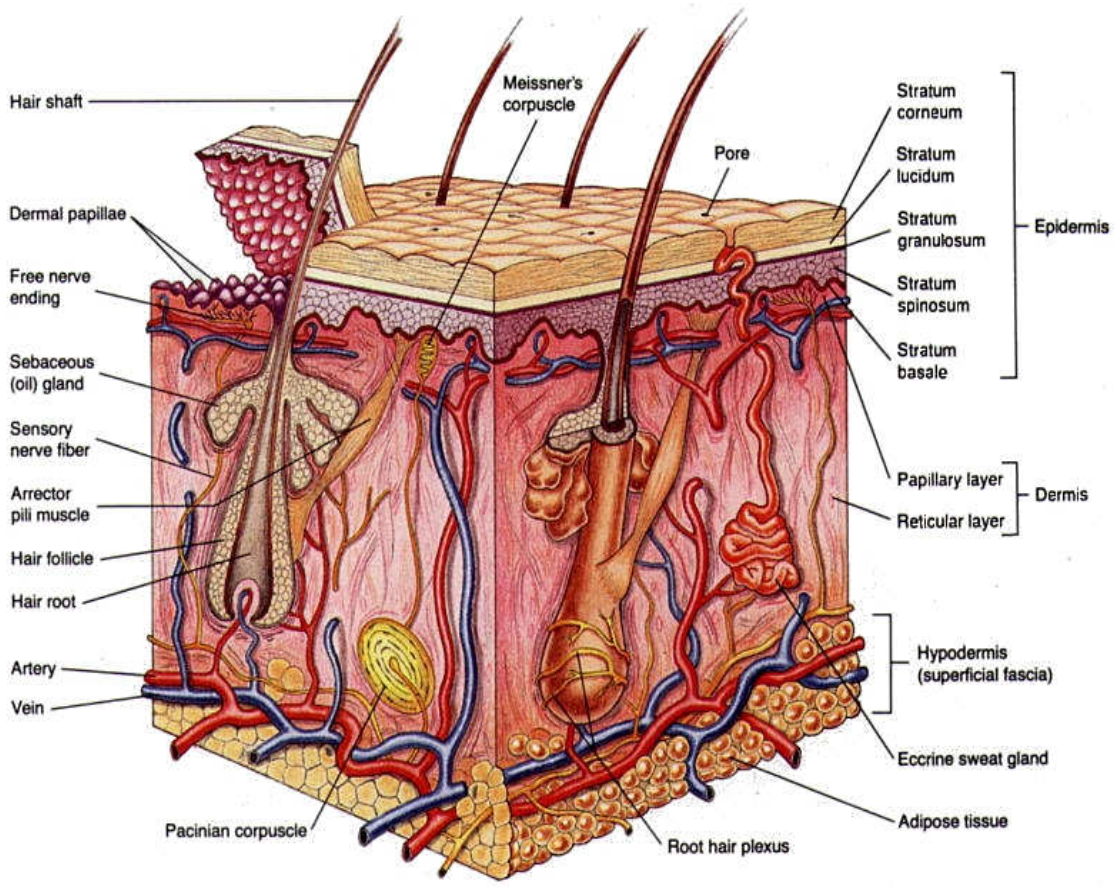


Figure 2.1: Schematic diagram of cross-section of human skin (http://rds.yahoo.com/_ylt=A9G_RtvPXEdE8BcB6pujzbkF;_ylu=X3oDMTA4NDgyNWN0BHNlYwNwcm9m/SIG=12ve841bm/EXP=1145613903/**http://www.anti-aging-skin-care.com/forever-young-how-it-works-diagram.html).

2.1.1.1 Epidermis

The stratified epidermis is the outermost layer of the skin which is in contact with the environment. It can be divided broadly into two layers: the stratum corneum and the viable epidermis. The viable epidermis consists of cells that can be further categorised into three layers that are in continuous differentiation moving outwards to the body surface; the stratum basale, the stratum spinosum, and the stratum granulosum. The epidermis is between 75 to 200 μm thick in most regions and 400 to 600 μm in the palms and soles (Ho,

2004). It is avascular and the cells in this layer are continually shed to the surface of the skin and replaced from the basal layer. The epidermis has a papillose interface with the dermis such that it projects into the dermis like tiny finger bulges. Epidermal cells also extend to subcutaneous regions to form follicular sheaths of hair follicles, which is an epidermal structure. This is important as in the events of skin injury regeneration of a new surface without scarring is possible as long as the tissue damage does not extend to the bulb of the hair (Flynn, 1979).

Since the stratum corneum has been recognised as the rate controlling membrane in transdermal delivery of drugs and chemicals (Behl, 1990 and Hadgraft and Lane, 2005), only this layer of the epidermis will be discussed in further detail.

Stratum corneum

The stratum corneum is the outermost layer of epidermis as well as the primary permeation barrier of most drugs and chemicals. The stratum corneum consists of 20 to 40 % water, 20 % lipid, and 40 % keratinised protein (Ho, 2004). This epidermal layer is roughly 10 to 20 μm (15 – 20 cell layers) thick (Ho, 2004 and Hadgraft, 2004) with individual corneocytes being, on average, approximately 0.3 μm in thickness covering 1 100 to 1 200 μm^2 of the skin (Cevc, 2004). Groups of up to twelve corneocyte columns in the stratum corneum form clusters that characterize the basic skin permeation resistance unit. The junctions between corneocyte clusters correspond to the microscopically detectable surface corrugations that are considered as a “hot spot” for transdermal delivery (Cevc, 2004). More than 90 % of all cells in the stratum corneum are terminally differentiated (dead) keratinised cells (keratinocytes or corneocytes) tightly packed and connected to one another in a planar array by desmosomes (Cevc, 2004). Filling the intercellular spaces are lipid lamellae that tightly seals this region forming a continuous and extremely tortuous

intercellular network (Cevc, 2004 and Ho, 2004). This organisation results in the diffusional path length being much longer than the simple thickness of the stratum corneum through which substances have to traverse and has been estimated as long as 500 μm (Hadgraft, 2004). The compactness of the corneocytes and the densely packed lipid multi-layers is often likened to a brick-and-mortar wall. The aqueous protein phase in the corneocytes is modelled to the bricks and the intercellular lipid phase is modelled as a continuous mortar (Ho, 2004 and Hadgraft and Lane, 2005) acting predominantly as a lipophilic barrier (Hadgraft and Lane 2005), resulting in the already resistant transport pathway even less permeable (Behl, 1990).

The stratum corneum is under continuous formation as fully differentiated cells from beneath replace those that are worn off the surface. The total turnover rate of the stratum corneum is approximated two weeks in normal adults (Flynn, 1979).

2.1.1.2 Dermis and hypodermis

The dermis is a highly vascularised skin layer that embeds the microcirculations that supply the entire skin. Networks of lymphatic and sensory nerves for pressure, temperature and pain are also found in the dermis. Chemicals applied onto the skin must permeate through the epidermis to reach the underlying dermis for uptake into the systemic circulation. The dermis contains moderately dense connective tissue composed of collagen and elastic fibres. Its thickness varies from 1 to 4 mm depending on the location in the body (Ho, 2004).

Skin appendages, the hair follicles and the sweat glands, break the continuity of the epidermal and dermal layers throughout most of the surface of the body. On average, there are approximately 40 to 100 hair follicles and 210 to 220 sweat ducts perforating per

square centimeter of skin, occupying about 0.1 % of the total body surface area (Ho, 2004). The hair follicles root in the dermis where the bases are well vascularised and extend through the epidermis to the skin surface. Sebaceous glands co-exist with hair follicles secreting sebum into the region between the hair and the sheath. The sweat glands consist of tubes extending from the dermis, where the tube is coiled and vascularised to the skin surface where sweat is excreted to provide thermal regulation (Ho, 2004).

2.1.2 Routes of penetration through the skin

Three primary transport pathways through skin have been described: (1) intercellular diffusion through the lipid lamellae; (2) transcellular diffusion through both the corneocytes and the lipid lamellae; and (3) diffusion through skin appendages (hair follicles and sweat ducts). Figure 2.2 illustrates the proposed pathways.

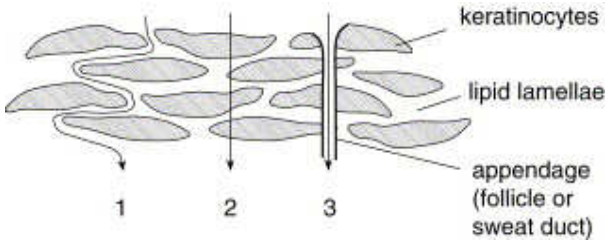


Figure 2.2: Skin permeation routes: (1) intercellular diffusion through the lipid lamellae; (2) transcellular diffusion through both the corneocytes and the lipid lamellae; and (3) diffusion through skin appendages (hair follicles and sweat ducts) (Ho, 2004).

Intercellular diffusion through the lipid lamellae is considered to be the predominant route of transport (Ho, 2004 and Hadgraft, 2004). The intercellular spaces consist of structured lipids and diffusing molecules need to cross a variety of lipophilic and hydrophilic domains of the skin to reach the underlying cell layers (Hadgraft, 2004).

Figure 2.3 is a schematic diagram of the principal steps of penetration. In brief, drug molecules applied onto the skin undergo passive diffusion within their carrier system (vehicle) to the surface of the skin, followed by partitioning into the stratum corneum. After entering the lipophilic stratum corneum and the sweat glands an inward diffusion of the drug takes place and continues into the hydrophilic viable epidermis and dermis (local tissue). This creates a concentration gradient across the skin between the surface of the skin and the microcirculation imbedded in the dermal layer. Once the drug reaches the general circulation it is distributed very rapidly; and due to reasonable rates of systemic metabolism and elimination, generally no appreciable systemic build-up occurs. This phenomenon, maintaining a near-zero concentration of the drug on the plane of the capillaries (dermal layer) is called sink condition and is necessary for the driving force of the diffusion process (Flynn, 1979).

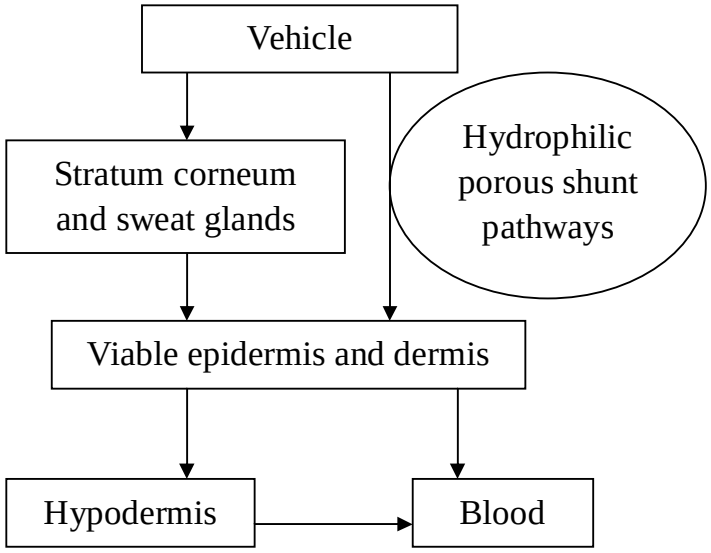


Figure 2.3: Schematic diagram of the principal steps of permeation (modified from Zatz, 1993).

Key factors that control molecular permeation through the stratum corneum of the skin, in

decreasing sequence of importance, are molecular lipophilicity, size, and the ability to interact with other molecules, e.g. via hydrogen bond formation (Cevc, 2004). Consequently, molecules larger than a few hundred Dalton and/or highly polar compounds that cannot efficiently pass through the skin by simple diffusion may alternatively traverse the skin via the hydrophilic porous pathways, i.e. the transport shunts (Cevc, 2004).

2.1.3 Physicochemical parameters influencing transdermal drug delivery

Absorption of drugs and chemicals into or across the skin is influenced by a number of factors: physicochemical properties of the permeant, condition and type of skin, other chemicals (e.g. vehicles or enhancers) present with the permeant, and external conditions (e.g. temperature, humidity, and occlusion) (Smith, 1990). Diffusion through the skin can be described by Fick's law of diffusion. The most basic diffusion equation is Fick's first law:

$$J = KD(c_{app} - c_{rec})/h \quad (1)$$

Where J = steady state flux per unit area (μg/h/cm^2),

K = partition coefficient of the permeant between the applied formulation and skin,

D = diffusion coefficient of permeant,

h = diffusional pathlength,

c_{app} = applied concentration of the permeant in the vehicle,

c_{rec} = concentration of the permeant in the receptor phase.

The diffusivity and the concentration gradient of the drug within the skin influence flux across the skin. The concentration gradient itself is influenced by the ability of the drug to partition into the skin and its ability to partition out of the skin into the underlying tissues.

The octanol/water partition coefficient K_{ow}, as expressed by log P (log K_{ow}), can be used to predict this partitioning behaviour between an aqueous vehicle and skin (Thomas and Finnin, 2004). In most circumstances $c_{rec} << c_{app}$ as a result of sink condition and thus Eq. (1) is often simplified to:

$$\boldsymbol{J = k_p c_{app}} \qquad (2)$$

where $k_p = (KD/h)$ is the permeability coefficient. This parameter (from an aqueous donor phase) may be estimated by an empirical relationship described by Cronin *et al.* (1999) who deduced a correlation between the permeability coefficient k_p, octanol/water partition coefficient (K_{ow}), and molecular weight (MW) of a permeant (Cevc, 2004):

$$\log k_p \equiv \log P - \log (D/d_{sc})$$
$$= 0.77 \log K_{ow} - 0.013\ MW - 2.33 \qquad [n = 107] \qquad (3)$$

This correlation produced higher significance ($r^2 = 0.86$) and similar results to the previous, statistically inferior relationship of Potts and Guy (1992): log k_p = 0.71 log K_{ow} – 0.0061MW – 6.3, n = 93, r^2 = 0.67. Thus, using Eq. (3), transdermal diffusion of large molecules will fall below 1 μg/h/cm^2 when either MW > 328 for log K_{ow} = 1 or else when permeant hydrophilicity exceeds log P = - 1.34 for MW = 50, assuming 1 wt.% drug-in-vehicle solubility limit (Cevc, 2004).

The maximum flux of a molecule is achieved when the applied concentration c_{app} is equal to the solubility of the permeant in the vehicle. From the equations it can be seen that the

important physicochemical parameters are the partition coefficient, diffusion coefficient, and solubility; and increasing MW will decrease the rate of diffusion. Molecules with low log P exhibit low permeability because little partitioning into the stratum corneum occurs. On the other hand, molecules with high log P values also confer low permeability due to their inability to partition out of the stratum corneum (Thomas and Finnin, 2004). In general, molecules must have good solubility in both oils and water and with a log P ~ 1 – 3 for maximum permeation (Hadgraft, 2004).

Many permeants are weak acids or weak bases and therefore, their degree of ionization will influence their solubility in the applied phase as well as the diffusion through the skin. If a permeant is ionisable in quantities dependent on pH, the transport of the ionised species will occur less rapidly than transport of the unionised species due to interactions between the polar head groups of the intercellular lipids with hydrogen-bond-forming functional groups in the permeant structure (Thomas and Finnin, 2004). As a general rule, the number of hydrogen bonding groups in the permeant should not exceed two (Thomas and Finnin, 2004). Higher flux is obtained by maintaining the pH in the vehicle such that the permeant is unionised. However, pH values outside the physiological range of pH 4 – 7 may also change properties of the skin that could affect solubility, partitioning or binding, resulting in changes in transdermal penetration (Smith, 1990 and Hadgraft, 2004).

2.2 Materials and methods

2.2.1 Materials

The powdered extracts of green (unfermented) rooibos (GRE) obtained by aqueous extraction (EURO Ingredients) was provided by Dr. E. Joubert. The aspalathin pure compound was obtained from PROMEC (Tygerberg, South Africa). Two commercial skin care products (cream) containing the green rooibos extracts (quantity unspecified) were

obtained from local pharmacies. HPLC grade acetonitrile (CH_3CN) and 0.1 % acetic acid (CH_3COOH) were obtained from BHD Laboratory Supplies (Poole, UK). Potassium dihydrogen phosphate (KH_2PO_4), disodium hydrogen phosphate dihydrate ($Na_2HPO_4 \cdot 2H_2O$), and sodium chloride (NaCl) were supplied by Merck (Midrand, South Africa) (ISO 9001 certified). n-Octanol (98 %) was obtained from Acros Organics (Edenvale, South Africa). Double distilled water was prepared by a Milli-Q water purification system (Millipore, Milford, USA), which was used throughout the study.

2.2.2 High performance liquid chromatography (HPLC) method for the analysis of aspalathin

2.2.2.1 Apparatus

All analyses were carried out using a HPLC system (Agilent 1100 series, Palo Alto, CA, USA) equipped with a diode array UV detector, gradient pump, autosampler injection device, and Chemstation Rev. A.08.03 data acquisition and analysis software. A Luna C18-2 column (150 x 4.6 mm, 5 µm particle size) from Phenomenex® (Torrance, CA, USA) was used.

2.2.2.2 Chromatographic conditions

All analyses were performed at a flow rate of 1.0 ml/min and the mobile phase consisted of a mixture of HPLC grade acetonitrile (CH_3CN) and 0.1 % acetic acid (CH_3COOH) in HPLC grade water, buffered at pH 7.4 with 0.02 M potassium dihydrogen phosphate (KH_2PO_4). The column temperature was held constant at 25 °C and the effluent was monitored at a wavelength of 287 nm. The retention time for aspalathin was approximately 7.5 ± 0.3 minutes. The injection volume for all the samples was 50 µl. The total time of detection was 20 minutes for all samples and separation was performed by solvent gradient elution as shown in Table 2.1.

Table 2.1: Gradient elution employed for reverse-phase HPLC separation of aspalathin.

Time (min)	Solvent composition (% acetonitrile)
0	5.0
5:00	25.0
12:00	25.0
12:50	80.0
16:00	80.0
16:20	5.0
20:00	5.0

2.2.2.3 Preparation of stock solution

A stock solution with a concentration of 730 µg/ml was prepared by dissolving 3.65 mg aspalathin in 5 ml of HPLC grade water. The stock solution was stored in the dark at -20 °C and was stable for at least 3 months.

2.2.2.4 Validation of HPLC procedure

The method was validated according to ICH guidelines (ICH, 2005).

2.2.2.4.1 Linearity

A calibration curve for aspalathin was established by preparing standard solutions from the stock solution by performing a serial dilution consisting of the following concentrations: 0.6, 2.9, 5.8, 14.6, 29.2, 73.0, 146.0, 365.0, and 730.0 µg/ml. Linear regression analysis from the plot of peak area *versus* concentration of the analyte was performed and the obtained calibration equation was $y = 111.69x + 0.5196$ where the correlation coefficient (R^2) was found to be better than 0.999.

2.2.2.4.2 Accuracy and precision

Accuracy was determined as the relative deviation of the obtained value from the nominal value and was calculated as follows:

$$\textbf{Accuracy (\%)} = \frac{\textbf{analysed conc.}}{\textbf{added conc.}} \textbf{ X } \frac{\textbf{100}}{\textbf{1}}$$

The precision is the determination of the closeness of measurements after multiple sample preparations of the same homogenous sample mixture i.e. the relative standard deviation (% RSD) of the analysed concentration. Accuracy and precision were determined by HPLC analysis of three different concentrations (11.53, 115.3, and 345.9 µg/ml) each in triplicate (n = 9) on the same day. The results are presented in Table 2.2. The values obtained for all three concentration levels were lower than 1.0 % and therefore, the method could be considered as accurate and precise.

.

Table 2.2: Quantification of accuracy and precision of aspalathin recovery from three concentrations.

Added conc. (µg/ml)	Analysed conc. (µg/ml) (mean ± SD) (n=3)	Accuracy (%) (n=3)	Precision (%RSD) (n=3)
11.5	11.63 ± 0.042	100.86	0.362
115.3	115.44 ± 0.142	100.12	0.123
345.9	346.73 ± 1.95	100.24	0.563

SD = standard deviation.

2.2.2.4.3 Sensitivity

The sensitivity of the analytical HPLC method for aspalathin was assessed by determining the lowest limit of quantification, and the limit of detection. The sensitivity of a method can be improved by increasing the sample volume.

The limit of quantification (defined as the lowest concentration of an analyte in a sample that can be determined with acceptable precision and accuracy) is a parameter of quantitative assays for low levels of compounds in sample matrices. It is used in particular for the determination of impurities and/or degradation products. The quantification limits for aspalathin was 0.584 μg/ml.

The limit of detection is the lowest concentration of analyte in a sample that can be detected, but not necessarily quantified. The detection limit for aspalathin was 0.06 μg/ml.

2.2.2.4.4 Selectivity

Selectivity is the capacity of an analytical method to analyse a component in the presence of other components such as degradation products and biological material. Figure 2.4a shows a chromatogram of an aspalathin standard with a single, well separated peak at a retention time of 7.66 min. An aspalathin peak amongst other unidentified flavonoid compounds was elucidated at 7.77 min in the GRE (Figure 2.4b). Figure 2.4c and Figure 2.4d show HPLC chromatograms of a blank skin tissue (epidermis and dermis) sample and a blank tape strip (stratum corneum) sample. Samples of blank skin tissue and blank tape strip were obtained using the method described in section 2.2.6.3 and 1ml of phosphate buffer system (PBS) (pH 5.5) was used on the donor compartment in place of the test formulations. No peaks at the retention time of aspalathin were elucidated indicating that

the skin tissue and tape strip samples had no interference with aspalathin detection.

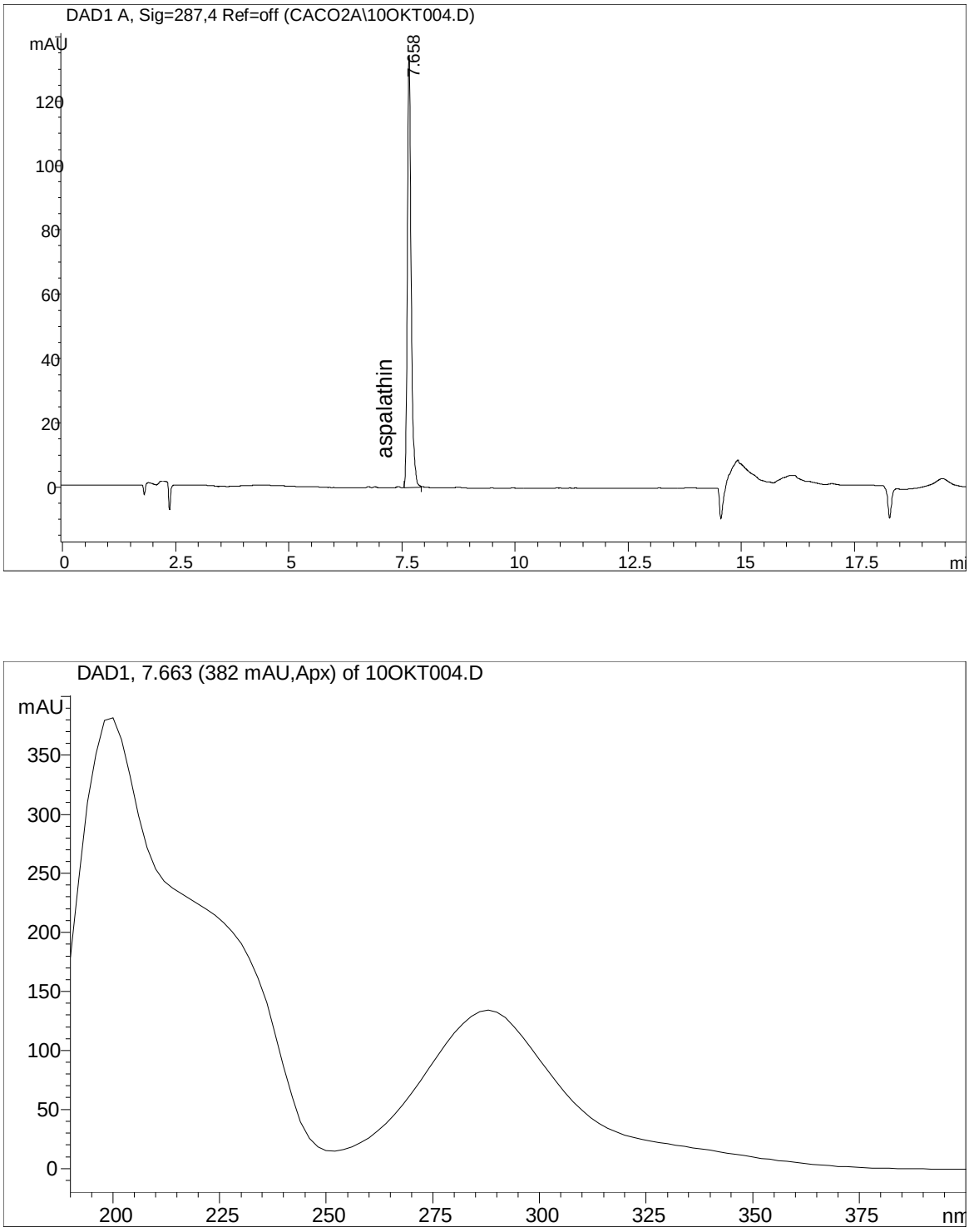


Figure 2.4a: HPLC chromatogram and UV spectrum of aspalathin (7.05 µg/ml), Rt = 7.658 min.

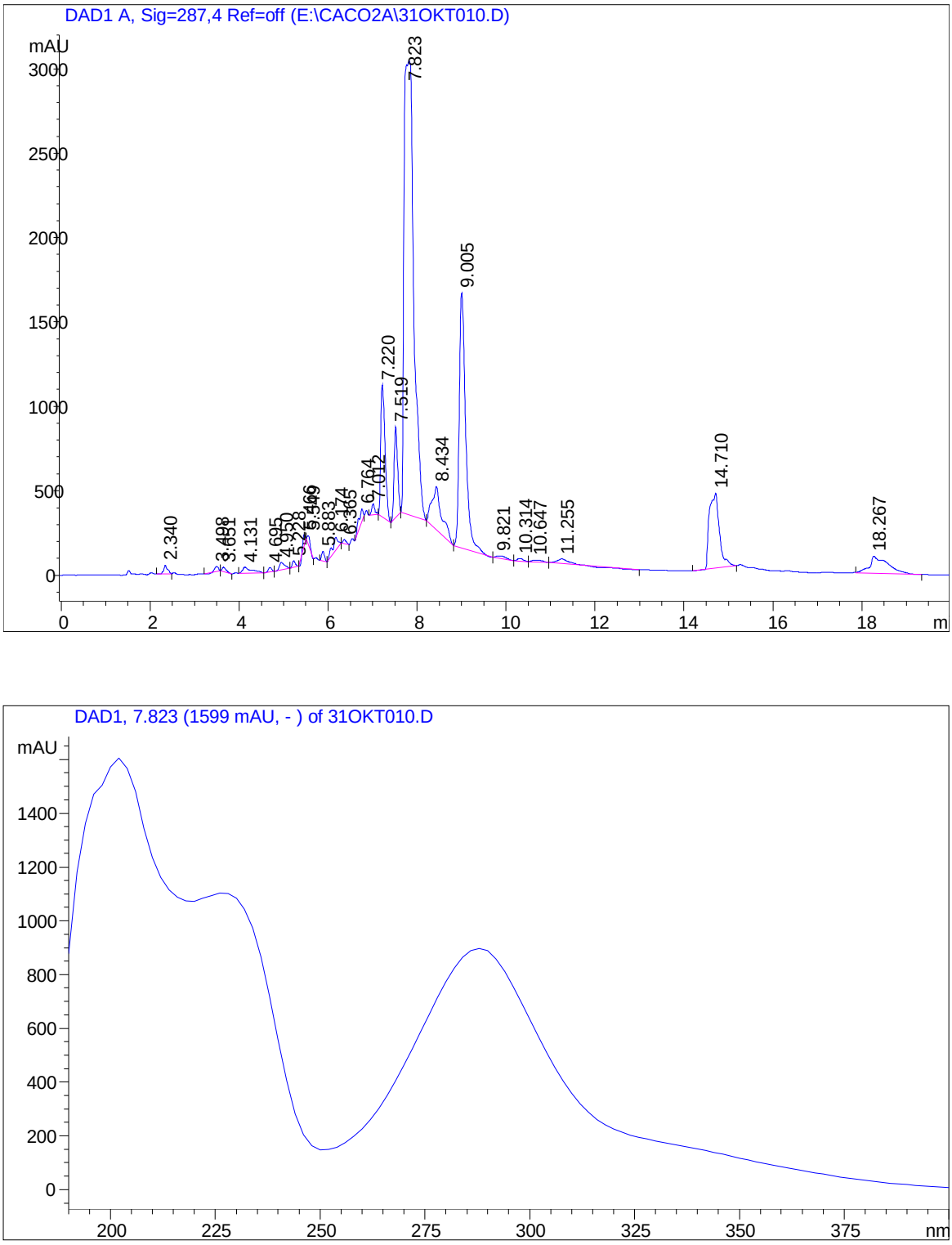


Figure 2.4b: HPLC chromatogram and UV spectrum of green rooibos extracts (5 µg/ml) aspalathin Rt = 7.823.

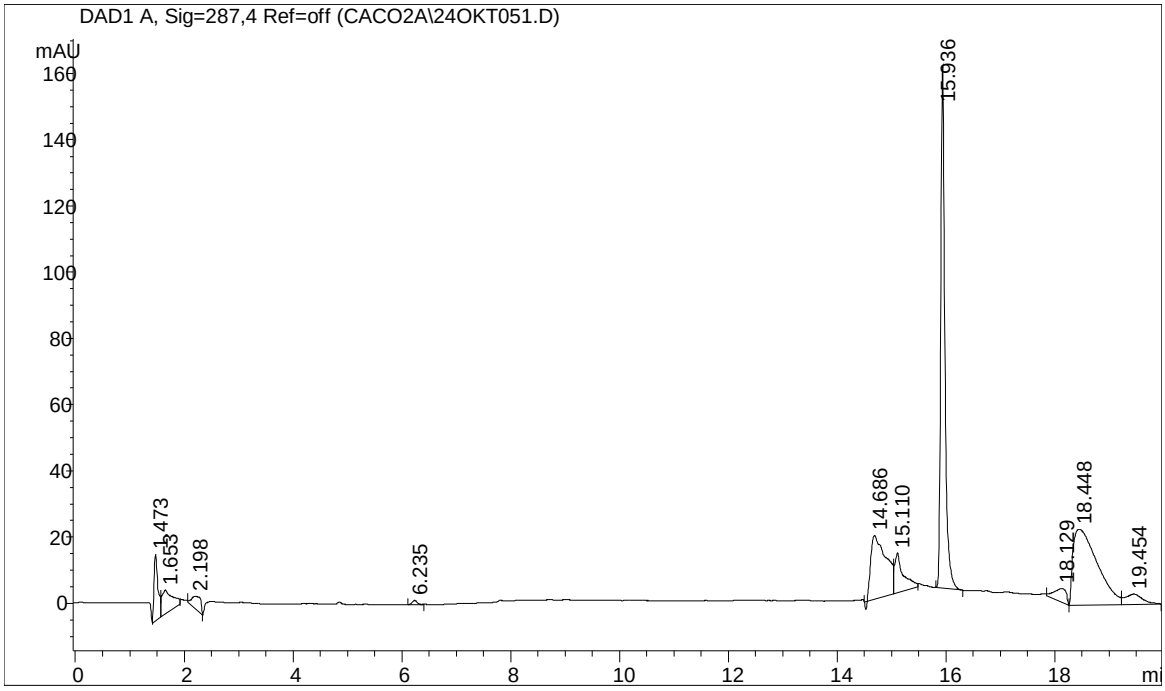


Figure 2.4c: HPLC chromatogram of skin tissue.

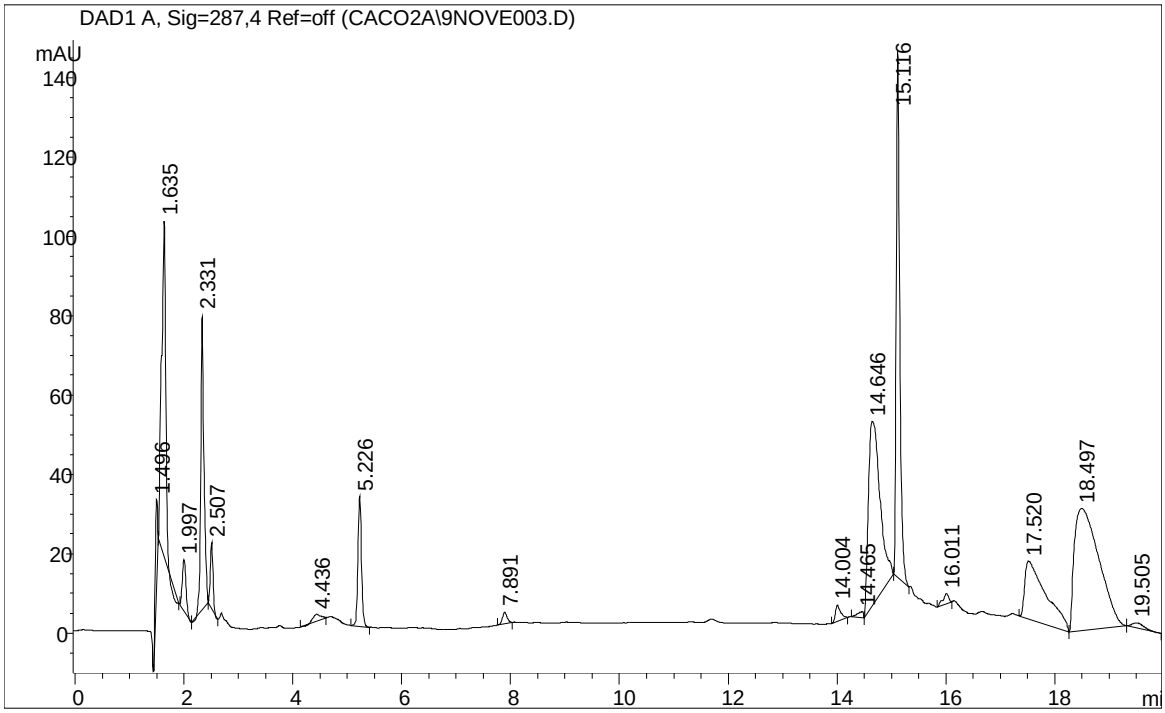


Figure 2.4d: HPLC chromatogram of skin surface sample.

2.2.3 Determination of stability of aspalathin in transport medium

Phosphate buffer systems (PBS) of mixtures of 0.2 M potassium dihydrogen phosphate (KH_2PO_4) solution (27.2 mg/ml) and disodium hydrogen phosphate dihydrate ($Na_2HPO_4 \cdot 2H_2O$) solution (35.6 mg/ml) were prepared according to British Pharmacopoeia (1993) and buffered to pH 5.0, pH 6.0, and pH 7.0, respectively. Samples of 1.4 μg/ml of aspalathin were prepared in PBS of the respective pH values and left on an autosampler tray at room temperature 25 °C for analysis by HPLC at hourly intervals for 14 hours. The percentage of aspalathin from the initial concentration was plotted as a function of time and is shown in Figure 2.7a, depicting the percentage loss of aspalathin over time.

Another stability test was performed to determine at which pH value of the PBS the permeation experiment should be carried out. PBS buffered at pH 5.0 and pH 5.5 were prepared as mentioned above. Samples of 1.4 μg/ml of aspalathin were prepared in PBS of the respective pH values and left on an autosampler tray at room temperature 25 °C for analysis by HPLC for 9 hours. Figures 2.7b is a plot of the percentage of aspalathin from the initial concentration *versus* time.

In addition, samples of GRE and aspalathin solution test formulations were left in the water bath (37 °C) for the duration of the permeation experiment and the concentration of aspalathin from the two test formulations at time zero and at the end of the experiment was compared for monitoring the stability of aspalathin.

2.2.4 Determination of octanol/water partition coefficient (K_{ow})

In section 2.1.1.1 the stratum corneum of the skin was discussed and modelled to "brick-and-mortar", where the structure of stratum corneum consists of a continuous lipid phase surrounding a large number of thin parallel polar protein "plates". When this

structure is intact, permeation occurs either by diffusion through both the lipophilic lipid phase and the hydrophilic protein phases or (for lipophilic permeants) by diffusion via the tortuous pathway solely through the lipid phase (Smith, 1990). Permeation requires good solubility of the permeant in both lipophilic and hydrophilic phases. The principal use of partition coefficient *K* is in predicting relative rates of transport between two liquid phases. The partition coefficient of a compound between the lipid domain and protein domain of the stratum corneum can be related to the partition between octanol and water to allow for experimental validation of the two-domain concept (Rieger, 1993). Since the permeation experiment utilises a phosphate buffer system at pH 5.5 as the donor phase, the water phase in the determination of K_{ow} was replaced with a phosphate buffer system (pH 5.5), but will still be referred to as octanol/water partition coefficient. The K_{ow} of aspalathin was experimentally determined by pre-saturating 250 ml of phosphate buffer system and 250 ml of n-octanol with one another in a separating funnel. Aspalathin solution of 0.1 mg/ml was prepared by dissolving 1 mg aspalathin in 10 ml of the pre-saturated phosphate buffer system (pH 5.5) giving a clear solution of aspalathin (solution not saturated). Approximately 2 ml of the aspalathin solution (n =3) was mixed with 2 ml of n-octanol in a 10 ml screw-cap test tube and tumbled in a water bath at 25 °C for 24 hours. The mixture was then centrifuged for 30 minutes at 3000 rpm (relative centrifuge force (RCF) 377.33 g) and 250 µl of each phase was removed and analysed by HPLC. The phosphate buffer system phase was analysed as is and the n-octanol phase was diluted 1:4 with methanol prior to analysis. The concentration of the aspalathin was calculated with the calibration curve established in 2.2.2.4.1 and K_{ow} was determined by the relationship of the amount dissolved in each phase as follow:

$$K_{ow} = c_o / c_w \qquad (4)$$

Where c_o = concentration in octanol phase,

c_w = concentration in water phase.

2.2.5 Determination of aspalathin in commercial products

Approximately 2 g of each of the commercial products (n = 2) was extracted with 8 ml of: (i) methanol/water 50/50 v/v; and (ii) tetrahydrofuran, respectively, in a 15 ml screw-cap test tube and placed in a water bath at a constant temperature of 60 °C for 5 minutes. The dispersions were allowed to cool down after extraction, made up to 10 ml and centrifuged at 3000 rpm (relative centrifuge force (RCF) 377.33 g). The supernatant was analysed by HPLC.

2.2.6 Aspalathin permeation study

2.2.6.1 Preparation of test formulations

In a preliminary HPLC analysis of the green rooibos aqueous extracts, approximately 1.0 mg/ml (20 %) of aspalathin was found in 5.0 mg/ml of green rooibos aqueous extracts. Thus, the test formulations subject for testing were prepared as follows: 5.0 mg/ml green rooibos extracts and 1.0 mg/ml aspalathin solutions were prepared by dissolving 35.0 mg of GRE and 7.0 mg aspalathin in 7.0 ml of PBS (pH 5.5). The resulting test formulations contained approximately the same concentration of aspalathin.

Sodium chloride (NaCl) saline solution (0.9 %) for the skin integrity test prior to the permeation experiment was prepared by dissolving 900 mg NaCl in 100 ml water.

2.2.6.2 Preparation of skin

Human abdominal skin was used in the permeation study. Full thickness white female abdominal skin was obtained from 2 individual patients who underwent cosmetic surgery

and kept frozen at -20 °C for no longer than 24 hours after removal. The skin was thawed at room temperature, washed with distilled water and dried with paper tissue. Split-thickness skin of approximately 400 μm in thickness, comprising of the stratum corneum, viable epidermis and part of the upper dermis, was dermatomed (Figure 2.5) using a Zimmer® electric dermatome and placed onto Whatman® filter paper. The skin samples prepared were wrapped and sealed in aluminium foil and kept frozen at -20 °C until utilised. Prior to conducting the diffusion study the frozen skin samples were thawed at room temperature, examined for defects, and cut into circles of approximately 15 mm in diameter (n = 6 from skin donor 1 and n = 6 from skin donor 2) for mounting onto the diffusion apparatus. Storage of skin up to 6 months at -20 °C showed no impact on skin integrity (Harrison *et al*., 1984).

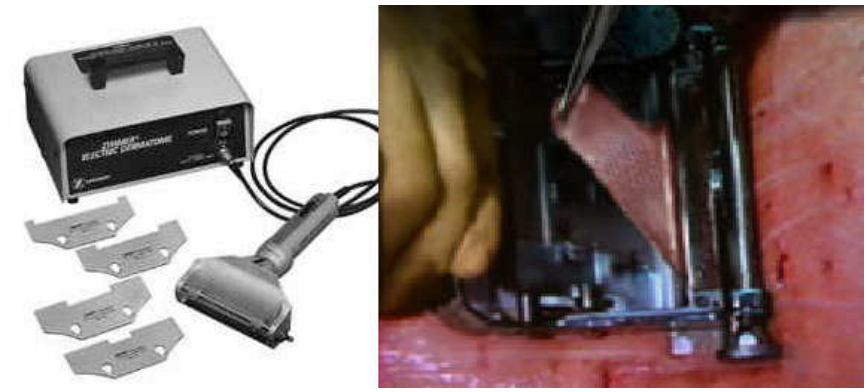


Figure 2.5: Skin dermatome obtaining split-thickness skin using a electric dermatome (http://www.zimmergermany.de and http://www.residentnet.com).

2.2.6.3 Transport of aspalathin across skin

Vertical Franz diffusion cells (Figure 2.6) consisting of an upper donor compartment and lower receptor compartment were used in the permeation study, with a receptor capacity of approximately 2.0 ml and a diffusional area of 1.131 cm^2. A small magnetic stirring bar was placed in each receptor compartment to maintain stirring throughout the entire

experiment. The prepared skin was thawed prior to the experiment and mounted onto the receptor compartment with the stratum corneum facing up in the direction of the donor compartment. The donor compartment was then placed and fastened onto the receptor compartment with a metal clamp, wedging the skin between the two compartments. The donor and receptor compartments were then loaded with 0.9 % NaCl solution and the cells placed into a preheated water bath at 37 °C which results in a skin surface temperature of 32 °C and equilibrated for approximately 30 minutes. After equilibration, the integrity of the skin in each cell system was assessed by measuring the transepidermal electrical resistance (TEER) using a Tinsley LCR Databridge (Model 6401). The reading was conducted at a frequency of 1 kHz with a maximum voltage of 300 mV root mean square in the parallel equivalent circuit mode utilising an alternating current. The experimental set up was according to the study of Fasano *et al.* (2002). Skin discs with TEER values between 14.0 and 25.0 kΩ were selected for use in this study. It was important for a comparison study to select cells with similar resistance values. The 0.9 % NaCl solution in the donor and receptor compartments was removed. The receptor compartments were filled with PBS (pH 5.5) with caution to avoid air bubbles underneath the skin. Therefore, the PBS was degassed in an ultrasonic bath for 15 min prior to the experiments. The donor compartments were loaded with 1 ml of freshly prepared GRE (n = 6) and pure aspalathin solutions (n = 6), respectively, and immediately covered with a cap to prevent any significant evaporation during the permeation experiment. The cell systems were left in the water bath at a constant temperature (37 °C) for 12 hours to allow permeation to take place. The receptor phases sampled after 12 hours of incubation were analysed by HPLC and the skin discs dismounted from each cell system were subjected to tape stripping.

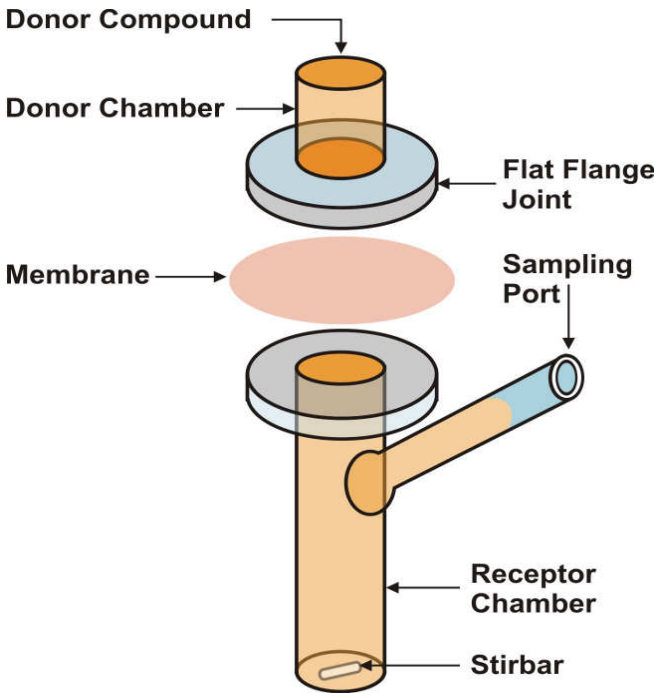


Figure 2.6: Vertical Franz diffusion cell consisting of an upper donor compartment (chamber) and bottom receptor compartment (re-drawn from http://www.permegear.com/franz.htm).

2.2.6.4 Tape stripping the stratum corneum and epidermis

An adhesive tape (3M Scotch® Magic™ Tape) was cut into pieces the size of the skin dismounted from each cell system and placed onto the stratum corneum of the skin. The tape was smoothed out on the skin to ensure even pressure and contact with the skin and then gently peeled off from the skin removing some cells of the stratum corneum. This process was repeated 14 times with each skin disc and a total of 15 tapes for each skin disc were obtained and placed into a vial containing approximately 2 ml of PBS (pH 5.5). The remaining skin (epidermis and dermis) after tape stripping was then cut into smaller pieces to increase surface area for extraction and put into a separate vial containing approximately 1 ml PBS (pH 5.5). All collected samples were kept in a fridge at 4 °C overnight to allow extraction of aspalathin into the PBS. Samples were then filtered and withdrawn from the

tape strip (stratum corneum) solutions and the skin solutions and were subjected to HPLC analysis.

2.2.6.5 Sample analysis

The concentration of each sample was calculated from the analysed peak area using the calibration curve. The amount of aspalathin in each sample could be determined with the volume and dilution factor and were expressed as mass of aspalathin per diffusional area ($\mu g/cm^2$).

2.2.6.6 Statistical analysis

The experiment was conducted with skin obtained from 2 different skin donors. Each donor skin was able to produce three replicates (n = 3) of each of the two test formulations resulting in a total of six replicates (n = 6) for each formulation. Data were expressed as means ± standard deviation (SD). Differences between mean values of the two different tested formulations were analysed by means of one-way analysis of variance (ANOVA). The difference between the two formulations was assessed and P-values < 0.05 were considered to be significantly different.

2.3 RESULTS AND DISCUSSION

2.3.1 Stability in transport medium

The stability of aspalathin in PBS of pH 5.0, 6.0, and 7.0 over 14 hours is depicted in Figure 2.7a. The highest aspalathin degradation occurred at pH 7.0 with a loss of approximately 40 % over 14 hours, followed by pH 6.0, and the least at pH 5.0. Figure 2.7b is a plot of the percentage of aspalathin from approximately 1.4 μg/ml pure aspalathin solution, buffered at pH 5.0 and pH 5.5 *versus* time. Less than 30 % of the aspalathin was lost in the pH 5.5 PBS. Since the physiological pH of the skin is pH 5.5 and less

degradation occurred at this pH range, the permeation experiment in this study was carried out using PBS buffered at pH 5.5.

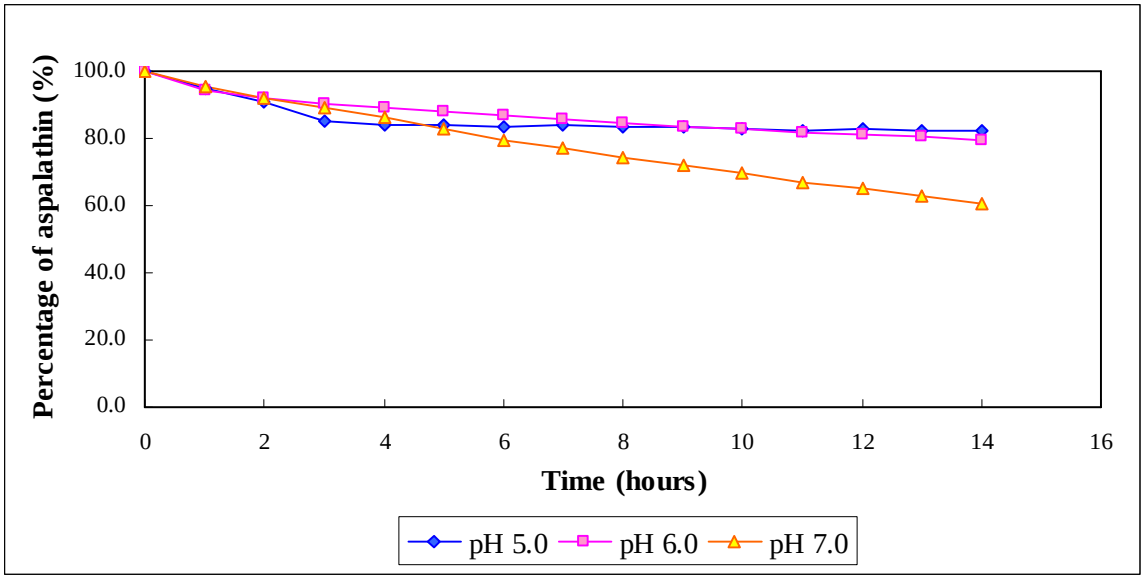


Figure 2.7a: Amount of aspalathin (% of initial concentration) in 1.4 µg/ml of aspalathin solution, buffered at pH 5.0, 6.0, and 7.0, stored for 14 hours at room temperature (25 °C).

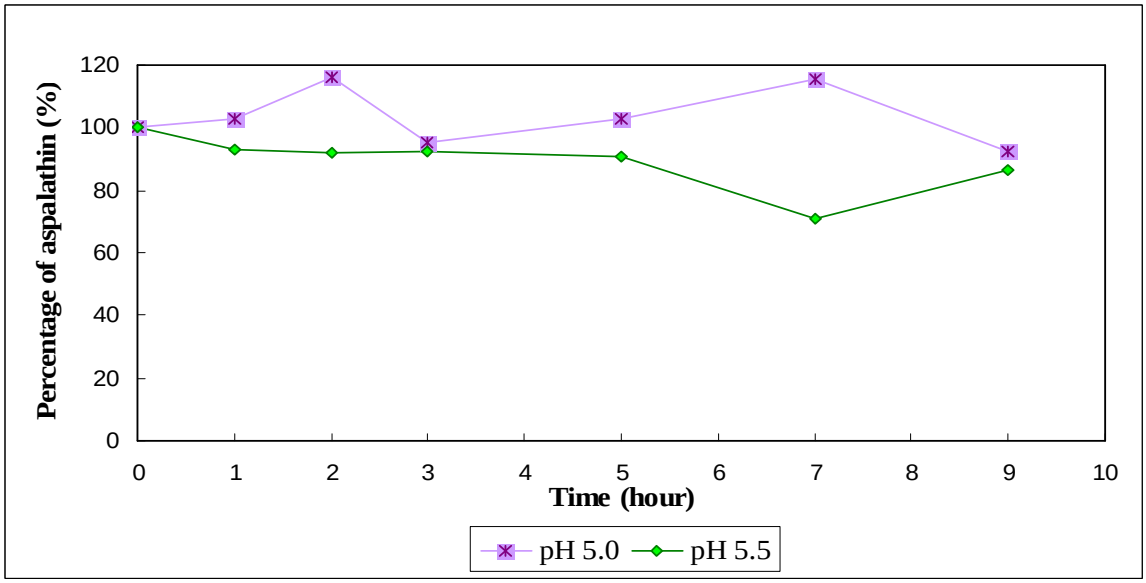


Figure 2.7b: Amount of aspalathin (% of initial concentration) in 1.4 µg/ml pure aspalathin solution, buffered at pH 5.0 and 5.5, at room temperature (25 °C) for 9 hours.

In addition, the applied concentrations of the test formulations were approximately 1.13 mg/ml and 0.93 mg/ml of aspalathin in GRE and in pure aspalathin solutions, respectively. After 12 hours of incubation in water bath approximately 1.3 mg/ml and 1.0 mg/ml of aspalathin elucidated, respectively. This indicates that the aspalathin was stable under the experimental conditions. The difference in concentration between the initial and the end concentration may be a result of error in analysis.

2.3.2 Octanol/water partition coefficient (K_{ow})

For a molecule to permeate well through the skin it must have good solubility in both the water phase and oil phase, and exhibit a log P of ~1 – 3 for optimum partition behaviour (Hadgraft, 2004). However, the K_{ow} (n = 3) of aspalathin was 0.450 and log P equals -0.347 with a RSD of 6.6 %. Drugs displaying log P values close to 2 are generally predicted to be completely absorbed in humans (Artursson *et al*., 2001). Table 2.3 is the experimentally determined K_{ow} and calculated log P value. The permeability coefficient (k_p) of aspalathin was calculated using Eq. 3 and was 1.52 x 10^{-4} cm/h.

$$\log k_p = 0.77 \log K_{ow} - 0.013\,MW - 2.33$$

$$= 0.77 \log 0.450 - (0.013 \times 452.41) - 2.33$$

$$= -3.818$$

$$k_p = 1.52 \times 10^{-4}\ cm/h$$

Due to the low log P it can be expected that the partitioning of aspalathin from the vehicle into the stratum corneum will be very low. Hence, it could be expected that aspalathin would not permeate human skin to an appreciable amount which can be seen from the low k_p value.

Table 2.3: Octanol/water partition coefficient (K_{ow}) of aspalathin and log P value.

	Mean concentration (μg/ml)		K_{ow}	Log P
	PBS	**n-Octanol**		
	57.9	27.9	0.482	-0.317
	56.5	23.9	0.423	-0.374
	56.2	25.1	0.447	-0.350
AV	**56.9**	**25.6**	**0.450**	**-0.347**
SD	0.907	2.053	0.030	0.028
% RSD	1.596	8.008	6.575	-8.191

2.3.3 Determination of aspalathin in commercial products

Cream extraction was performed with two extraction methods (i) water/methanol (1:1) and (ii) tetahydrofuran. Table 2.4 presents the concentration of aspalathin per gram of cream analysed. In cream A, both extraction methods produced aspalathin amounting to approximately 0.871 μg/g and 0.922 μg/g of cream, respectively, composing less than 0.1 % of the cream. The peak areas of aspalathin elucidated by HPLC in cream B were diminutive and below the limit of detection, therefore, the amount of aspalathin in cream B was not detectable. Figure 2.8 shows the chromatogram of cream A with a small peak representing aspalathin elucidating at 7.48 min.

Due to the negligible amount of aspalathin detected in the commercial products and limit of detection of aspalathin by HPLC, the permeation study on the products was considered not feasible and investigation of aspalathin penetration from the creams was not carried out.

Table 2.4: Amount of aspalathin extracted per gram of cream using (i) water/methanol (1:1) and (ii) tetrahydrofuran extraction methods (n = 2).

	Water/methanol (1:1)		Tetrahydrofuran	
	Cream A (µg/g)	**Cream B (µg/g)**	**Cream A (µg/g)**	**Cream B (µg/g)**
	0.938	n/a*	0.728	n/a*
	0.804	n/a*	1.116	n/a*
AV	**0.871**	**n/a***	**0.922**	**n/a***
SD	0.095	n/a*	0.274	n/a*
% RSD	10.879	n/a*	29.757	n/a*

* Amount of aspalathin was below the limit of detection (0.06 µg/ml).

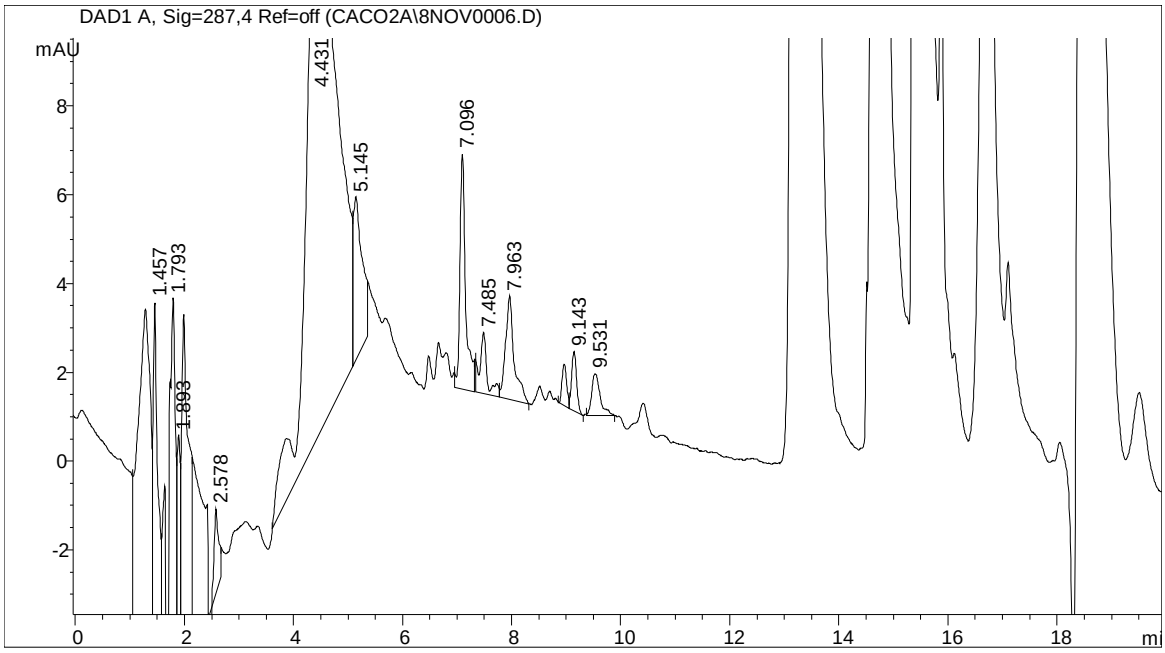


Figure 2.8: Chromatogram of a water/methanol extract of cream A depicting aspalathin at 7.48 min and other flavonoid compounds.

2.3.4 Aspalathin permeation study

This permeation study employed excised human skin that had been frozen for storage, thus the metabolic systems found in viable skin no longer function and permeation of aqueous soluble substances across frozen skin may be greater than that through fresh skin (Brain *et*

al., 2005). The occlusion method employed to prevent water loss from the stratum corneum during the experiment may increase fluidity of the intercellular lipid domains within the stratum corneum and cause a reduction in protein chain interactions and swelling of the corneocytes, and may subsequently increase in hydration to enhance the transdermal flux of the permeant (Nicolazzo *et al.*, 2005). The amounts of aspalathin permeation in aqueous solutions of GRE and pure aspalathin across the human abdominal skin are shown in Table 2.5. Tape stripping was performed to obtain a compartmental distribution of aspalathin in the stratified layers of the skin. After 12 hours of dosing, aspalathin permeated into the stratum corneum (SC), epidermis and dermis (ED), and into the receptor fluid. Approximately 1.13 mg/ml of aspalathin in 5 mg/ml GRE and 0.93 mg/ml pure aspalathin solution were applied onto the skin. A total of 0.08 % and 0.09 % of aspalathin in the applied GRE and pure aspalathin solution permeated the skin, respectively. Figure 2.9 shows that the majority of the aspalathin that permeated the skin remains in the skin (0.07 % and 0.08 % of the applied dose of GRE and pure aspalathin solution, respectively) and was poorly absorbed into the receptor fluid fraction (0.01 % and 0.01 % of the applied dose of GRE and pure aspalathin solution, respectively). Of the 0.07 % of aspalathin in the GRE applied, 0.06 % of aspalathin distributed into SC and 0.01 % distributed into ED. In comparison to GRE, less permeation occurred with the pure aspalathin solution, where 0.05 % and 0.03 % of aspalathin distributed into SC and ED, respectively. No significant difference in the skin distribution of aspalathin between GRE and pure aspalathin solution was observed. However, the amount of aspalathin in GRE permeated into the receptor fluid phase differs statistically from the amount of aspalathin that permeated in the pure aspalathin solution ($P < 0.05$). Batchelder *et al.* (2004) investigated the transdermal delivery of major catechins, epicatechin (EC), epigallocatechin (EGC), epicatechin gallate (ECG), and epigallocatechin gallate (EGCG), in green tea from drug-in-adhesive patches and obtained 0.1 % permeation of

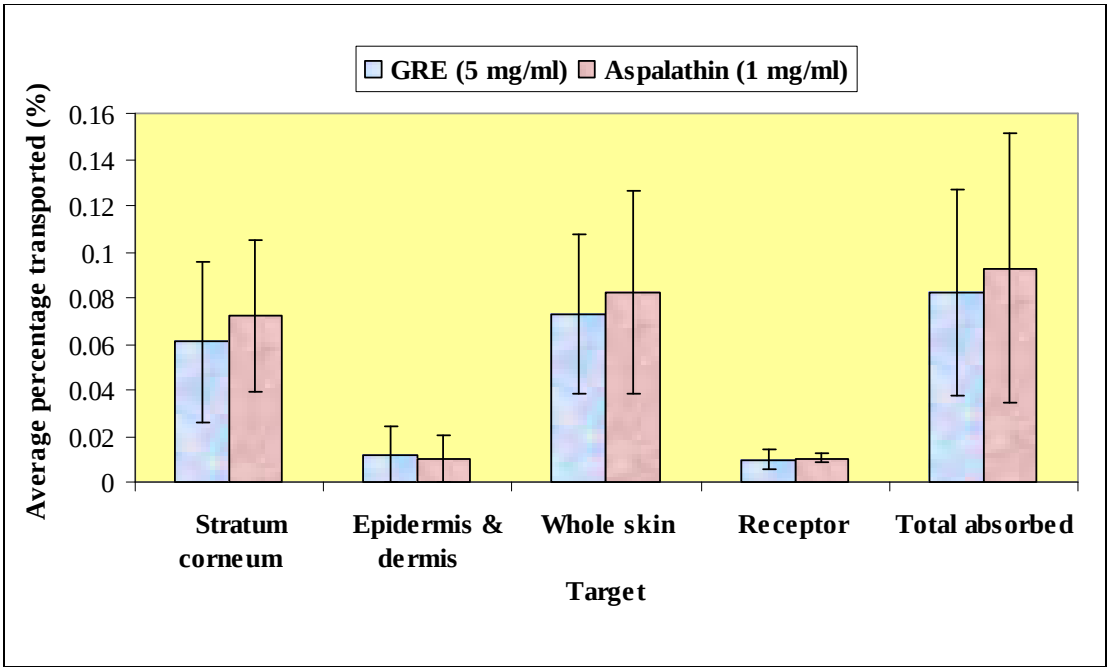


Figure 2.9: The average percentage (%) of aspalathin that permeated the skin in green rooibos extract and aspalathin solution applied. (The outlier has been excluded).

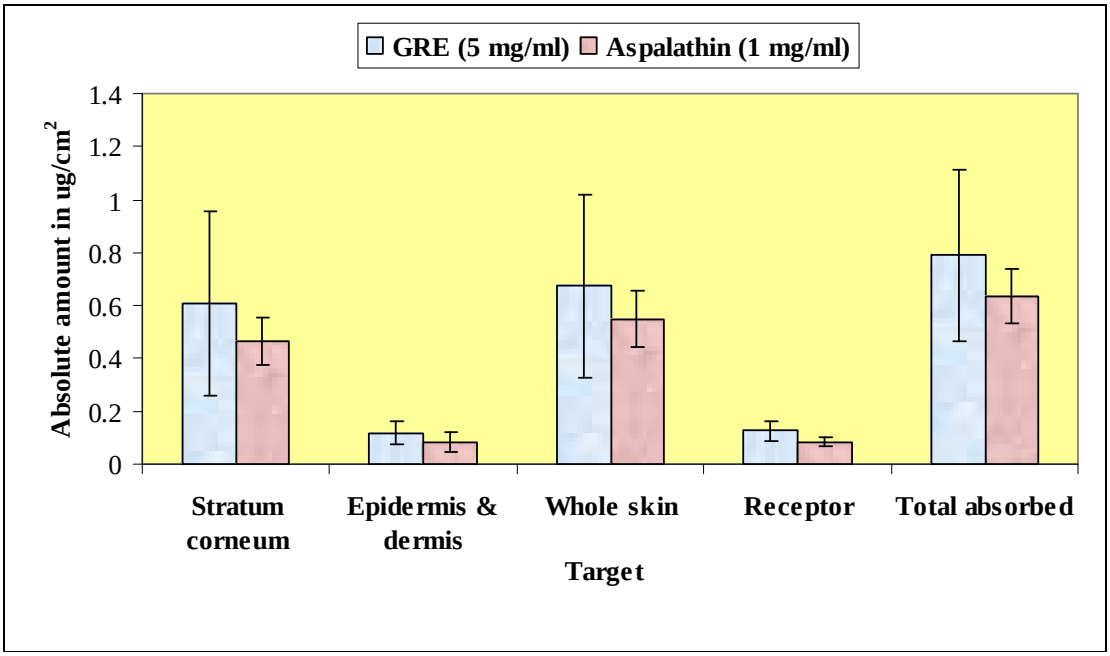


Figure 2.10: Comparison of the absolute amount of aspalathin permeated in green rooibos extracts and aspalathin solutions. (The outlier has been excluded).

Table 2.5: Distribution data of aspalathin in green rooibos extract (GRE) and standard aspalathin (As) solution both at a concentration of approximately 1 mg/ml aspalathin.

	Stratum corneum (μg/cm^2)		Epidermis & dermis (μg/cm^2)		Whole skin (μg/cm^2)		Receptor (μg/cm^2)		Total absorbed (μg/cm^2)	
	GRE	**As**	**GRE**	**As**	**GRE**	**As**	**GRE**	**As**	**GRE**	**As**
Skin donor 1 (n = 3)	0.870 1.094 0.761	0.586 0.483 0.347	1.974* 0.108 0.078	0.074 0.048 0.039	2.844 1.202 0.840	0.660 0.531 0.386	0.183 0.092 0.088	0.062 0.074 0.081	3.027 1.294 0.928	0.722 0.605 0.467
Skin donor 2 (n = 3)	0.337 0.307 0.272	0.530 0.420 0.420	0.134 0.082 0.194	0.130 0.087 0.130	0.471 0.389 0.465	0.661 0.508 0.550	0.150 0.127 0.122	0.099 0.108 0.086	0.621 0.516 0.587	0.759 0.615 0.636
AV	**0.607**	**0.464**[a]	**0.428**	**0.085**[a]	**1.035**	**0.549**	**0.127**[b]	**0.085**[b]	**1.162**	**0.634**
SD	0.348	0.086	0.758	0.039	0.938	0.103	0.036	0.016	0.958	0.103
% RSD	57.326	18.545	177.015	45.996	90.612	18.828	28.125	19.273	82.454	16.186

* Inconsistent value.

[a] The amount of aspalathin distributed into the SC is significantly different to the amount distributed into ED, $P < 0.05$.

[b] The amount of aspalathin that permeated into the receptor phase is significantly different from GRE and standard aspalathin solutions, $P < 0.05$.

the 1.35 mg/cm^2 of green tea extracts applied, which was also equivalent to the percentage absorbed after intragastric administration of green tea extracts in rats. Compared to the findings of Batchelder *et al.* (2004) aspalathin has two-times the skin permeation of green tea catechins. Figure 2.10 is a plot of aspalathin distribution data. The amount of aspalathin in whole skin represents the sum of aspalathin in SC plus ED. The total absorbed is the total amount of aspalathin in total skin plus the receptor fluid fraction. Attention is drawn to the extraordinarily high value produced by GRE at the epidermis and dermis (ED) phase (marked *). Nonetheless, no significant difference in aspalathin permeation was detected between including and excluding this particular value ($P < 0.05$).

Approximately 1 mg/ml of aspalathin was applied onto the skin in this permeation experiment. By substituting k_p determined from Eq. 3 and the applied concentration of aspalathin into Eq. 2 a projected flux of aspalathin from an aqueous solution across the skin may be calculated as follow:

$$\boldsymbol{J = k_p c_{app}}$$

$$\boldsymbol{= 1.52 \times 10^{-4} \text{ cm/h} \times 1\,000 \text{ µg/ml}}$$

$$\boldsymbol{= 0.152 \text{ µg/h/cm}^2}$$

permeation experiment) a theoretical aspalathin steady state flux after 12 hours of approximately 1.823 µg/cm2 is obtained. This predicted value is higher than the value obtained from this experiment. This may be explained by that this estimated flux is obtained by assuming the flux of aspalathin has reached the steady state, yet, the flux of aspalathin might have not reached the steady state in the 12 hours of the diffusion experiment to generate the estimated value. Because aspalathin is a polar compound possessing as many as nine ionisable hydroxyl units available for hydrogen-bond

formation and interaction with cellular components of the skin, its transport across the skin was further hindered and dramatically decreased the diffusion coefficient. In addition, aspalathin may oxidise to the two flavonones dihydro-orientin and dihydro-iso-orientin, which may have occurred during the permeation experiment. Nevertheless, aspalathin is only one of the many flavonoid antioxidants in rooibos tea, permeation of other flavonoid compounds that contribute to the health benefit of rooibos tea were also observed by HPLC.

2.4 Conclusion

Aspalathin is one of the major flavonoid components of rooibos comprising approximately 20 % of the crude extract. Degradation of the compound occured in solution and was found more stable in a phosphate buffer system buffered between pH 5 and pH 6 with less than 30 % loss over 14 hours. Aspalathin is hydrophilic, soluble in water and exhibits an octanol/water partition coefficient (K_{ow}) below the value for optimal partition behaviour. Aspalathin was only detected in one of the two commercial skin care products amounting to less than 0.1 % of 1 g of cream analysed and a permeation experiment on the product was thus not considered feasible. In the permeation experiments of GRE and pure aspalathin solution, aspalathin accumulated mostly in the stratified layers of the skin, rather than permeating into the receptor fluid. Less than 0.1 % of aspalathin from the total dose applied was absorbed transdermally. This is comparible to the percentage permeation of green tea catechins observed by Batchelder *et al.* (2004). Approximately 80 % of the total aspalathin absorbed was distributed in the stratum corneum. Since more hydrolytic activities occur in the deep viable epidermis and less in the stratum corneum (Mavon *et al.*, 2004), aspalathin accumulation in the stratum corneum may be desirable in the topical use of rooibos.

CHAPTER 3. *IN VITRO* INTESTINAL EPITHELIAL TRANSPORT OF ASPALATHIN ACROSS CACO-2 CELL MONOLAYERS

3.1 Introduction

Orally delivered compounds of foods and drugs encounter the gastrointestinal tract as the first barrier to absorption and have to pass across the intestinal epithelium in order to be transferred to the whole body (Carrière *et al.*, 2001). Tea of any sort is a beverage widely consumed throughout the world. There have been studies performed on human subjects indicating that flavonoids, in general, are absorbed to an appreciable amount through rapid absorption process, and remain relatively stable in the luminal fluid (Kuo, 1998). A study performed by Kuo (1998) suggests that flavonoids adopt rapid diffusional transport as their main route of absorption. It has also been suggested that the intestinal cells have the ability to accumulate flavone (Kuo, 1998 and Tammela *et al.*, 2004). In order to determine the required level of flavonoid intake for maximum health-promoting effects, some knowledge of the potential of oral absorption of these compounds is essential. Amongst the *in vitro* systems employed to predict oral drug bioavailability in humans, the most commonly used epithelial cell line is Caco-2 monolayers, which has become regarded as the best model in terms of throughput and reliability (Karlsson *et al.* 1999, Krishna *et al*., 2001, Youdim *et al.*, 2003). Studies have shown that there is a good correlation between permeability across the Caco-2 cell monolayers and the oral absorption in humans (Krishna *et al*., 2001).

3.2 Comparison of *in vivo* and *in vitro* human intestinal epithelia

3.2.1 Anatomy and physiology of the small intestine

The human intestine is estimated 2 – 6 m long and is divided into three sections, namely, the duodenum, the jejunum, and the ileum, comprising 5 %, 50 %, and 45 % of the length, respectively (Balimane and Chong, 2005). The biological and physiological parameters of the

human gastrointestinal tract are listed in Table 3.1 below (Balimane and Chong, 2005). Approximately 90% of all absorption in the gastrointestinal tract occurs over the length of the small intestine (Stoll *et al.*, 2000) as its surface area has various projections that drastically increase the potential surface area for digestion and absorption. The valve-like circular folds encircling the entire intestinal lumen are estimated to increase the surface area of the small intestine threefold (Balimane and Chong, 2005). The presence of villi and microvilli (Figure 3.1) further increase the surface area by 30-fold and 600-fold, respectively (Balimane and Chong, 2005). The uptake of substances occurs mainly in the duodenum and jejunum due to, among others, the decrease in size and the number of circular folds, villi and microvilli in the distal ileum (Stoll *et al.*, 2000).

Table 3.1: Biological and physiological characteristics of the human gastrointestinal tract (Balimane and Chong, 2005).

Gastrointestinal segment	Surface area (m^2)	Segment length (cm)	pH of segment
Stomach	**3.5**	**0.25**	**1.0 – 2.0**
Duodenum	**1.9**	**~35**	**4.0 – 5.5**
Jejunum	**184.0**	**~280**	**5.5 – 7.0**
Ileum	**278.0**	**~420**	**7.0 – 7.5**
Colon and rectum	**1.3**	**~150**	**7.0 – 7.5**

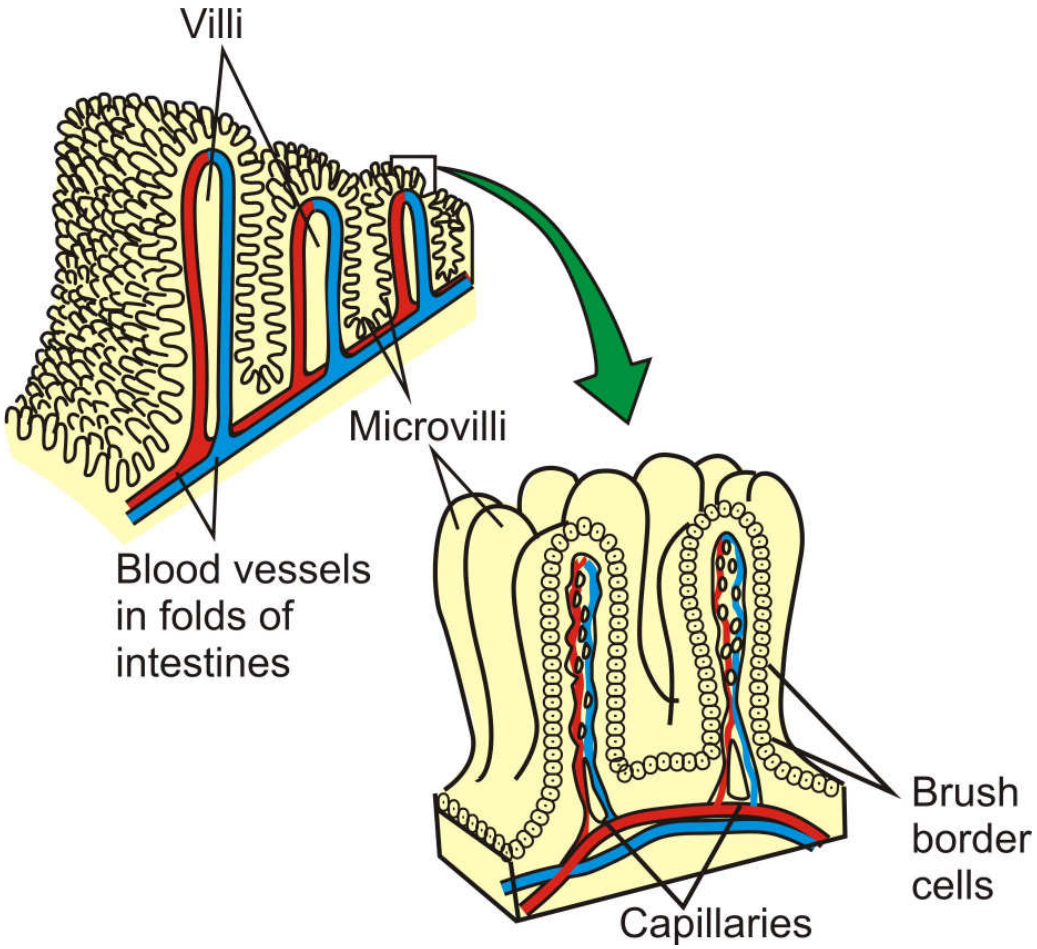


Figure 3.1: Villi and microvilli increase the absorptive surface area of the small intestine (re-drawn from http://www.emc.maricopa.edu/faculty/farabee/BIOBK/BioBookDIGEST.html).

The main functions of the small intestine are the selective absorption of major nutrients and to serve as a barrier to digestive enzymes and ingested foreign substances. The intestinal epithelial cells are heterogenous in nature and include enterocytes or absorptive cells, goblet cells (mucin secreting cells), endocrine cells, paneth cells, M cells, and tuft and cup cells (Shah *et al.*, 2006). Enterocytes are the most abundant epithelial cells that are responsible for the majority of the absorption of nutrients and drugs in the small intestine. These cells are polarized, having distinct apical and basolateral membranes that are linked to each other by tight junctions (Balimane and Chong, 2005).

3.2.2 Pathways of intestinal absorption

Absorption of molecules and substances across the intestinal epithelium occurs mainly by concentration gradient driven passive diffusion via the cell membrane of enterocytes (transcellular) (Figure 3.2A), or via the tight junction between the enterocytes (paracellular), (Figure 3.2B). The passive diffusion transcellular route diffusion is related to lipophilic molecular properties, and the paracellular pathway is mainly size (molecular weight (MW), or volume) and charge-dependent (Ungell, 2004). Lipophilic substances can rapidly and completely partition from the luminal fluid and distribute into the cell membranes of the intestinal epithelium (Artursson *et al*., 2001). Slowly and incompletely passively absorbed hydrophilic drugs and peptides distribute poorly into the cell membranes and are transported through the water-filled pores of the paracellular route (Artursson *et al*., 2001 and Shah *et al*., 2006). However, absorption via this route is generally low as the intercellular tight junctions restrict free transepithelial movement in the intercellular spaces between epithelial cells (Chan *et al*., 2004). Moreover, the surface area of the brush border membrane is >1000-fold larger than the paracellular surface area, thus the larger surface area of the cell membrane may compensate for the differences in partitioning between the cell membranes and the extracellular fluid allowing the hydrophilic substance to be transported in equal amounts by the paracellular and the transcellular routes (Artursson *et al*., 2001). Substances having similar chemical structures as those of certain nutrients and vitamins can be transported across the intestinal epithelium by specific transporters/carriers (Shah *et al*., 2006) (Figure 3.2C). This type of transport is often partly by carrier-mediated and partly by passive routes. Carrier-mediated transport is saturable, thus the contribution of the passive route will increase with increasing dose (Artursson *et al*., 2001 and Shah *et al*., 2006). The plasma membranes of the epithelial cells possess active efflux mechanisms that play a critical role in limiting absorption and accumulation of potentially toxic substances in epithelial cells (Chan *et al*., 2004). Figure 3.2D demonstrates substances being extruded by the efflux transporters,

e.g. the P-glycoprotein (Pgp), multidrug resistance- (MDR) and multidrug resistance-associated protein-type (MRP) transporters, back into the intestinal lumen (Chan *et al.*, 2004 and Hunter and Hirst, 1997). Substances present in high concentrations in the blood may undergo active blood-to-lumen secretion by these plasma membrane efflux transporters (Figure 3.2E). In addition to efflux pumps, the transcellular route of absorption exposes compounds to intracellular metabolic systems. Brush-border enzymes e.g. lactase, sucrase-isomaltase, and dipeptidylpeptidase IV, and cytochrome P450 (CYP)-mediated metabolic systems (phase I metabolism) in the small intestine plus other intracellular metabolic systems, such as phase II conjugation enzymes, may yield metabolites that are substrates for efflux pumps (Figure 3.2F and G) (Hauri, 1996, Suzuki and Sukiyama, 2000 and Chan *et al.*, 2004). Finally but not the least, the vesicular transport (transcytosis) from the apical to the basolateral side of the intestinal epithelium (Figure 3.2H) is considered as a route for highly potent drugs such as peptide antigens. This transport pathway is of limited value due to its low transport capacity and the presence of proteolytic enzymes limit this pathway as a general drug transport route (Artursson *et al.*, 2001 and Shah *et al.*, 2006).

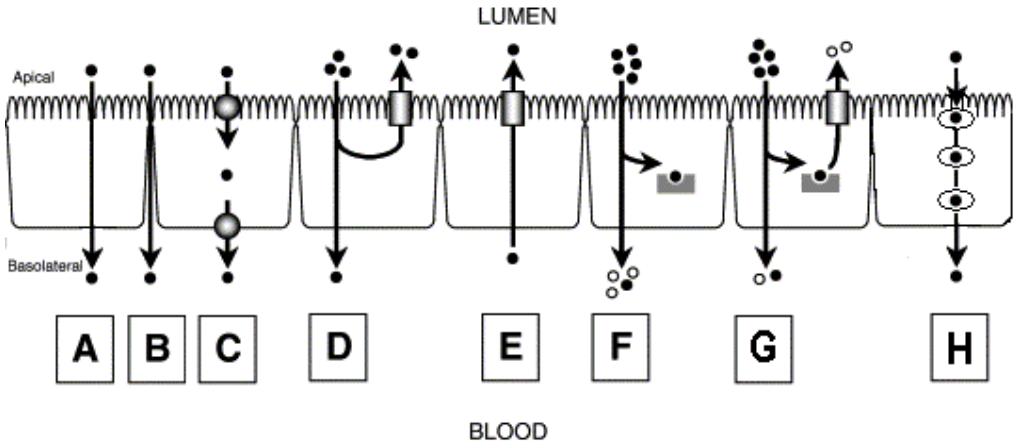


Figure 3.2: Routes of drug transport. (A) Passive transcellular absorption across intestinal epithelium. (B) Paracellular absorption mediated by tight junctions. (C) Carrier-mediated

transcellular transport at the apical and/or basolateral membranes. (D) Efflux transporter at the apical membrane may actively drive compounds back into the intestinal lumen thus restricting their absorption into the blood. (E) Apical efflux transporters that facilitate intestinal clearance of compounds that are already present in blood. (F) Intracellular metabolising enzymes may modify compounds before they enter the blood. (G) Apical efflux transporters and intracellular metabolising enzymes may co-ordinately metabolise and excrete compounds, forming an effective barrier against intestinal absorption. (H) Transcellular vesicular transport (modified from Chan *et al*., 2004; Hunter and Hirst, 1997).

3.2.3 The *in vitro* Caco-2 cell model for transport study

Unlike enterocytes, human tumour cells grow rapidly into confluent monolayers that provide an ideal cell culture model system for the rapid assessment of the intestinal permeability of xenobiotics (Balimane and Chong, 2005). The human adenocarcinoma cell line Caco-2 was originally isolated from a moderately well-differentiated human colon adenocarcinoma by Fogh and co-workers (1997), and has been developed as a model of intestinal epithelium (Gharat *et al.*, 2001 and Isoda *et al.*, 2006). These cells are able to spontaneously polarise and differentiate in long-term cultures *in vitro* to form monolayers that exhibit morphological and functional characteristics of enterocytes (Carrière *et al.*, 2001). When confluent, the cells polarise and join by tight junctions, with well developed and organised microvilli on the apical membrane. The cells start to express several enzymatic activities e.g. brush border enzymes alkaline phosphotase and dipeptidyl peptidase, typical of the small intestine (Carrière *et al.*, 2001; Basson and Hong, 1996). Polarized expression of several transport systems for sugars, amino acids, peptides and P-glycoprotein efflux transporters also follow the differentiation of Caco-2 cells (Yamashita *et al.*, 2000 and Shah *et al.*, 2006). Thus, Caco-2 cells have been used widely to study the effects and metabolism of natural and synthetic compounds at the intestinal level in addition to their transport through the epithelial

barrier. The Caco-2 cell line exhibits both characteristics of the small intestine and that of the colonocytes (Ranaldi *et al.*, 2003 and Tammela *et al.*, 2004). Several permeability characteristics such as the paracellular barrier of the colon present in Caco-2 cell monolayers is much higher than that of the small intestine epithelium, which unfortunately, results in the underestimation of the systemic bioavailability of paracellularly transported compounds (Versantvoort *et al.*, 2002). Nevertheless, Caco-2 monolayers can be used as an absorption model to predict the intestinal absorption of compounds, to investigate their mechanism of transport, and as an *in vitro* model for studying the functionality of the carrier-mediated transport in the small intestine (Versantvoort *et al.*, 2002).

3.2.4 *In vitro*/*in vivo* correlations

When using *in vitro* systems to gain information about drug permeability across the small intestine, the experimental conditions should reflect as closely as possible the real *in vivo* conditions (Youdim *et al.*, 2003). Many drug molecules are ionisable and may coexist in both their charged and uncharged forms in solution. At physiological pH 7.4, these drug molecules are predominantly ionised. The pH hypothesis postulates that the diffusion of a molecule across lipid membranes is through its uncharged form and that the charged form is impermeable. Luminal pH values vary throughout the gastrointestinal tract. Measurement of the "acid microclimate" on the surface of intestinal epithelial cells (intact with mucus layer) in rats reveals that the pH value on the apical side of the cells range from 6-8, whereas the values on the basolateral side was ~7.4 (Figure 3.3) (Said *et al.*, 1986 and Youdim *et al.*, 2003). Yamashita and co-workers (2000) employed gradient-pH conditions i.e. pH 6.0_{apical} – pH $7.4_{basolateral}$ in characterising drug permeability. In comparison to iso-pH condition i.e. pH 7.4_{apical} – pH $7.4_{basolateral}$, weak acids were found more permeable under the gradient-pH condition, whereas weak bases showed no differences in permeability under the two conditions. Nonetheless, for weak acids, both passive diffusion and active transport are

dependent on the concentration of protons in the apical solution. Thus, for an acid neither the presence nor absence of a pH gradient by itself is guiding the interpretation (Ungell, 2004).

In contrast to the extensively folded jejunum the Caco-2 monolayers are flat, representing only a fraction of the anatomical surface area of the intestine, the villi tips (Figure 3.3). This supports the hypothesis that only a fraction of the anatomical surface area of the intestine, i.e. the villi tips, participate in the absorption of drugs that adopt passive transcellular route (Artursson *et al.*, 2001). On the other hand, slowly and incompletely absorbed substances were found to be transported 30- to 80-fold slower in rate in the Caco-2 monolayers than in the human jejunum (Lennernäs *et al.*, 1996). This phenomenon may possibly be a result of differences in the permeability of the paracellular pathway and absorptive surface area between the Caco-2 monolayers and the human jejunum as there are fewer water-filled pores in the tight junctions in the Caco-2 monolayers. *In vivo*, substances with lower permeability will remain in the intestinal lumen longer before they are absorbed. This retention allows diffusion of the substance further down the length of villi as compared to substances having higher permeability which are rapidly and completely absorbed through the villi tips. This diffusion results in an increase in the absorptive area and, in addition, allows a fraction of the substance to be absorbed through the leakier paracellular pathway in the crypt region. Other potential sources of variability may arise from experimental conditions and the specific cell line (Artursson *et al.*, 2001).

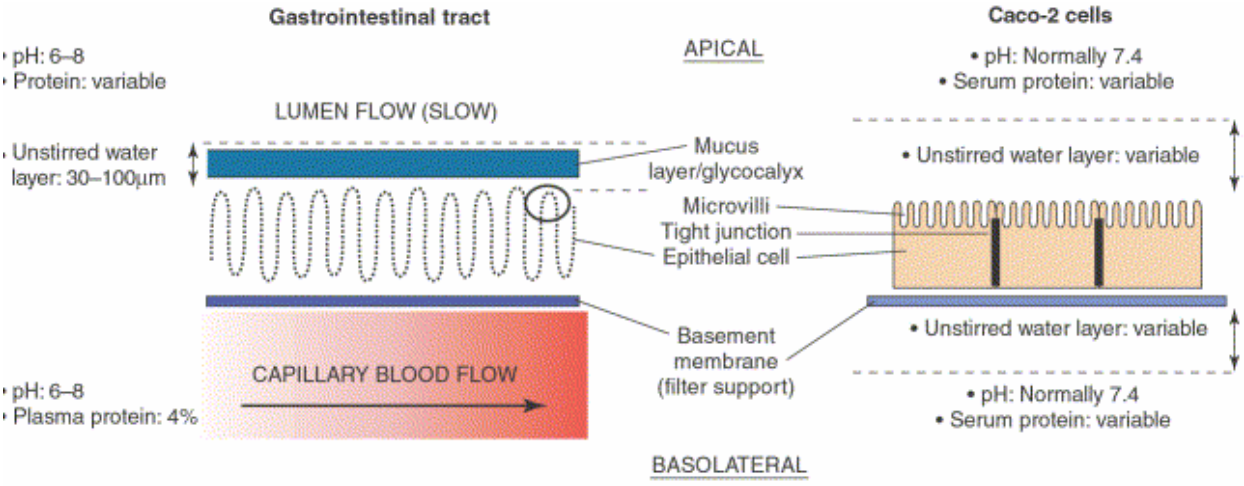


Figure 3.3: A comparison of *in vivo* extensively folded intestinal epithelia and *in vitro* flat Caco-2 cell monolayer, and barriers across which drugs must pass to reach the basolateral phase (Youdim *et al.*, 2003).

3.3 *In vitro* Caco-2 cell monolayer transport study

3.3.1 Caco-2 cell culture and setup for transport studies

Various methods of growing and carrying out transport experiments with Caco-2 monolayers have been described and employed. In general, cells are grown on a porous support, such as polycarbonate filters, for about 15 – 21 days in a cell culture medium containing Delbecco's Modified Eagle Medium supplemented with 20 % foetal bovine serum, 1 % non-essential amino acids and 2mM L-glutamin (pH 7.4 mimicking the physiological pH). The cells are grown at 37 °C in 5 % carbon dioxide at a relative humidity of 95 %. Transport experiments are usually carried out after 21 days of culturing.

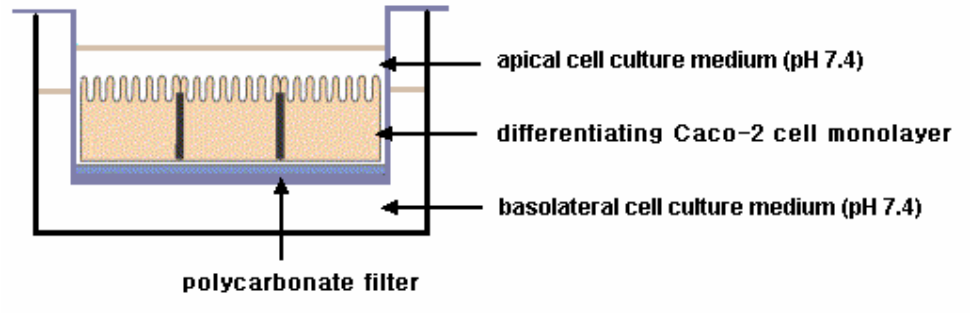


Figure 3.4: The *in vitro* cell culture model (modified from Youdim *et al.*, 2003; During and Harrison, 2005).

3.3.2 Determination of the apparent permeability coefficient (P_{app})

The rate of dissolution and solubility (determining how fast the drug reaches its maximum concentration (C) within the luminal intestinal fluid), and the permeability coefficient (P) (determining the rate at which the drug will cross the intestinal wall to reach the portal blood circulation) are properties that influence the ease with which a drug can be absorbed (Youdim *et al.*, 2003). Together, these factors comprise Fick's first law, describing the rate of transport (flux) (J_{wall}) of a drug across the intestinal wall which can be expressed as follows (Youdim *et al.*, 2003) (cf. Eq. 1, Chapter 2):

$$\mathbf{J_{wall} = P \times C} \qquad (1)$$

When examining drug permeability across *in vitro* cell models, determination of the apparent permeability coefficient (Eq. 2, Artursson, 2001) derived from Fick's first law may be used by taking into account the starting concentration (Ungell, 2004):

$$\mathbf{P_{app} = dQ/dt\ (1/(A.60.C_0))} \qquad (2)$$

Where: P_{app} = apparent permeability coefficient (cm/s),

dQ/dt = permeability rate (amount permeated per minute),

A = diffusion area of the monolayer (cm^2),

C_0 = initial concentration of the marker molecule in the apical compartment.

The apparent permeability coefficient (P_{app}) quantifies the transport of a drug molecule in a two compartmental system (Ekmekcioglu, 2002). The apical-to-basolateral permeability of a substance through the epithelial cell layer is measured as an increase in the concentration of the substance in the basolateral phase over time (Braun *et al.*, 2000)

3.3.3 Measurement of transepithelial electrical resistance (TEER)

Tight junctions play a critical role in epithelial cell biology by forming a selective permeability barrier in the spaces between adjacent epithelial cells and in the maintenance of compositional asymmetry in the cell (Isoda *et al.*, 2006). The tight junctions provide a route of transport of ions across the intestinal epithelial cells. Hydrophilic drugs and peptides, in general, are assumed to adopt this route of transport (passive paracellular pathway) (Artursson *et al*., 2001). Thus, measurement of TEER may reflect the ion permeability of the cell monolayers, where an increase in transport of ions is associated with opening of the tight junctions (increase in diameter) resulting in a decreased TEER. Measurement of TEER also evaluates the integrity of epithelial monolayers and is a sensitive method widely used for screening possible membrane perturbents resulting from cell injury (Isoda *et al.*, 2006).

3.4 Pheroid technology

Various methods have been used to increase the bioavailability of drugs. Some involves the use of specific chemicals to facilitate the absorption of the drug by temporarily increasing the membrane permeability (Ghafourian *et al.*, 2004). Pheroid technology (further referred to as Pheroid or Pheroids, previously known as Emzaloid™ technology) is a patented system that

involves the use of a unique submicron emulsion formulation. A Pheroid is a stable structure within a system that is flexible in terms of morphological, structural, size, and functional manipulation. It is a composite of mainly ethyl esters of plant and essential fatty acids, such as linoleic acid, linolenic acid, and oleic acid, emulsified in water saturated with nitric oxide (NO) (Saunders *et al.*, 1999). Several fatty acid constituents in Pheroids are therapeutically beneficial in maintaining cell membrane integrity, energy homeostasis, and modulating the immune system through leukotrins and prostaglandins (Grobler, 2004). Pheroid technology was first discovered when it was used as a basic formulation which led to the remission of psoriasis (Schlebush, 2002). Three types of Pheroids, namely, (i) lipid bilayer vesicles in both nano- and micrometer size range, (ii) micro-sponges, and (iii) depots or reservoirs that contain pro-Pheroids, have since been formulated in attempt to increase entrapment capabilities, enhance rate of transport, delivery, and stability. The size and shape of vesicles vary depending on the type of formulation, with lipid bilayers of 30 – 80 nm, micro-sponges of 0.5 – 5 μm, and the size of depots varies with the amount of pro-Pheroid contained within (Grobler, 2004). The entrapment of drugs in the three-phased Pheroid system (water, fatty acid, and nitric oxide) proposes to create a safer and more effective formulation in drug delivery (Grobler, 2004).

Pheroid technology is currently being studied for its drug penetration enhancing effect. During the transport experiment of green rooibos extracts and its pure compound aspalathin, this technology was employed as one of the possible mechanisms to enhance intestinal absorption and it was kindly provided by the Department of Pharmaceutics, North-West University (Potchefstroom campus).

3.5 MATERIALS AND METHODS

3.5.1 Materials

The green rooibos extract (GRE) (EURO Ingredients) was provided by Dr. E. Joubert. The aspalathin pure compound was obtained from PROMEC (Tygerberg, South Africa). Pheroids containing green rooibos aqueous extracts were prepared and provided by North-West University. HPLC grade acetonitrile (CH_3CN) and 0.1 % acetic acid (CH_3COOH) were obtained from BHD Laboratory Supplies (Poole, UK). Potassium dihydrophosphate (KH_2PO_4), disodium hydrogen phosphate dihydrate ($Na_2HPO_4 \cdot 2H_2O$), and sodium chloride (NaCl) were supplied by Merck (Midrand, South Africa) (ISO 9001 certified). Cryopreserved Caco-2 cells were obtained from American Type Culture Collection (Virginia, USA). Dulbecco's Modified Eagle's Medium (DMEM), Hank's Balanced Salt Solution (HBSS) (pH 7.4), Dulbecco's Phosphate Buffered Saline (DPBS) with calcium and magnesium (pH 7.4), trypsin-versine solution, 1 % non essential amino-acids (NEAA), and 1 % penicillin/streptomycin mixture (10 000 units penicillin/ml and 10 000 µg streptomycin/ml) were all supplied by Bio Whittaker (Walkersville, Maryland). Foetal bovine serum (10 %) was obtained from Delta Bioproducts, Kempton Park, South Africa. Double distilled water was prepared by Milli-Q water purification system (Millipore, Milford, USA), which was used throughout the study.

3.5.2 High performance liquid chromatography (HPLC) method for the analysis of aspalathin

The method for analysis of aspalathin and validation of HPLC procedure are described in section 2.2.2 of Chapter 2. Pheroid samples were analysed by HPLC as is.

3.5.3 Determination of stability of aspalathin

3.5.3.1 Stability in transport medium

Gastrointestinal assays using Caco-2 cell monolayers is normally carried out with DMEM supplemented with bovine serum albumin (BSA) as the growth medium that provides nutrients for culturing of cells, and as well as the receiver buffer medium in the basolateral phase. The use of BSA is usually recommended to reduce unspecific binding to plastics, filters or accumulation within the lipid bilayer or intracellularly (Ungell, 2004), and may improve permeability by providing a more favourable "sink condition" for partitioning of lipophilic compounds, mimicking the properties of physiological presence of albumin within the capillary lumen (Youdim *et al*., 2003). Phenolic compounds are renowned for their strong affinities for proteins to form both non-covalent and covalent association according to the size of the phenolic compound (Laurent *et al*., 2007). Kuo (1998) observed binding of flavonoids to extracellular proteins and to BSA in the incubation and led to impedance in transport and cellular accumulation of flavone in a dose-dependent fashion. In addition, a preliminary aspalathin transport experiment carried out using BSA supplemented DMEM showed interference in the recovery of aspalathin. Thus, an investigation on the stability of the aspalathin in DMEM is critical to eliminate possible compound-vehicle interaction. Three vehicle systems: (i) double distilled water, (ii) phosphate buffer system (PBS) (pH 7.4) (prepared as described in Chapter 2), and (iii) DMEM were used in determining the stability of aspalathin. Water serves as a control medium as rooibos tea is an aqueous extract of the rooibos plant, and the PBS serves as a possible alternative to DMEM as the receiver buffer medium in the basolateral phase. Solutions of approximately 120 μg/ml of aspalathin were prepared in each of the vehicle systems and left on the autosampler under room temperature 25 °C for analysis by HPLC at hourly intervals. The peak areas of aspalathin at each hour were determined and plotted as a function of time (Figure 3.7).

3.5.4 *In vitro* transport study

3.5.4.1 Preparation of test formulations for the transport study

Three concentrations: 10.0 mg/ml, 5.0 mg/ml, and 1.0 mg/ml, of GRE dissolved in DPBS were prepared in a volume of 10 ml, respectively, to allow experimentation of each concentration done in triplicate. In a preliminary HPLC analysis of the green rooibos aqueous extracts 5.0 mg/ml green rooibos extracts contained approximately 1.0 mg/ml aspalathin (described in Chapter 2). Thus aspalathin solutions were prepared at 2.0 mg/ml, 1.0 mg/ml, and 0.2 mg/ml in 10 ml DPBS, respectively, to equate to the amounts of aspalathin contained in the three solutions of GRE. Pheroids containing GRE made up to 10.0 mg/ml, 5.0 mg/ml, and 1.0 mg/ml concentrations were prepared and provided by North-West University.

3.5.4.2 Preparation of Caco-2 cell monolayers

3.5.4.2.1 Culturing of Caco-2 cells

Cryopreserved Caco-2 cells obtained from American Type Culture Collection were thawed in a water bath at 37 °C for one minute. The cells were then transferred to a 25 cm^3 cell culture flask (Coring Costar Corporation, USA) containing 15 ml culture medium, pre-heated to 37 °C. The cell lines were grown and maintained in culture medium consisting of DMEM containing 25 mM glucose, 3.7 g/L $NaHCO_3$, supplemented with 10 % foetal bovine serum, 1 % NEAA and a 1 % penicillin/streptomycin mixture (10 000 units penicillin/ml and 10 000 µg streptomycin/ml). The cells were incubated in a CO_2 incubator (Forma Scientific Inc., Marietta, Ohio, USA) at 37 °C in 5 % CO_2 and an atmosphere of 95 % humidified air. The medium was initially changed 24 hours after the reconstitution of cells, after which the medium was then changed every second day and trypsinated every week.

3.5.4.2.2 Trypsination of the Caco-2 cells

The culture flasks were macroscopically examined and only flasks with cells that had

reached confluence were used for the trypsination procedure (± every 7 days). HBSS, trypsin-versine solution, and culture medium were heated in a water bath at 37 °C. These selected cell culture flasks and the pre-heated solutions were transferred to a laminar airflow cabinet. The cells in the flask were rinsed twice with HBSS and 0.5 ml of the trypsin-versine solution was poured onto the cells and distributed evenly to cover the cell monolayer. The flask was then incubated for 10 minutes at 37 °C in 5 % CO_2 in an atmosphere of 95 % humidified air. After incubation the flask was transferred to the laminar airflow cabinet and inspected macroscopically whether all the cells were detached, and approximately 2 ml of the warm medium (37 °C) was then added to the down surface of the flask. This cell suspension was diluted by adding it to warm (37 °C) culture medium in a tube and agitated with a Pasteur pipette. The flask was rinsed with 1 ml of warm (37 °C) culture medium to ensure all the cells were removed from the flask. Three 25 ml flasks were transferred to the laminar airflow cabinet and marked with the date and new passage number. An amount of 15 ml of the cell suspension was added to each of the three 25 ml culture flasks and incubated.

This trypsination procedure was repeated every week to prevent overgrowth of the cells in the flasks until they were used in the experiments

3.5.4.2.3 Seeding and culturing of Caco-2 cell monolayers on 6-well filter plates

Caco-2 cells were seeded (Figure 3.5A) on tissue culture treated polycarbonate filters (area = 4.70 cm^2) in Costar Transwell 6-well plates (Corning Costar Corporation, USA). A cell suspension was obtained in the same way as described in the trypsination process (previous section). The cells were counted on a hemacytometer and diluted until a concentration of 1.77 x 10^4 cells/ml was reached. The culture medium consisted of DMEM supplemented with 10 % foetal bovine serum, 1 % NEAA and 1 % penicillin/streptomycin fungizone solution (10 000 units penicillin/ml, 10 000 μg streptomycin/ml and 25 μg fungizone/ml).

The medium was added to both the apical (2.5 ml) and basolateral (2.5 ml) compartments and was changed every second day under aseptic conditions. The cell cultures were kept in an incubator at 37 °C in 5 % CO_2 and an atmosphere of 95 % humidified air. The filters were used for drug transport measurements 21 days after seeding.

3.5.4.2.4 Measurement of TEER

The integrity of the cell monolayers was assessed by the measurement of transepithelial electrical resistance (TEER) (Figure 3.5B). Caco-2 cell monolayers exhibiting a TEER value of more than 160 Ω cm^2 were used within 30 days post-seeding. TEER was measured using a Millicell ERS meter (Millipore, USA) before and after the experiment.

3.5.4.3 Transport of aspalathin across Caco-2 cell monolayers

The growth medium was removed from the basolateral chamber and replaced with 2.5 ml DPBS with calcium and magnesium buffered at pH 7.4 and incubated for another 30 min. After the incubation the growth medium from the apical side was removed and replaced with 2.5 ml of GRE, pure aspalathin solution, and Pheroids containing green rooibos aqueous extract, respectively (Figure 3.5 C and D). Samples of 200 µl were taken at time intervals of 0, 20, 40, 60, 90, and 120 minutes from the basolateral side (Figure 3.5E) after incubation of the test formulations on the apical side of the monolayers. The samples withdrawn from the basolateral side were immediately replaced with an equal volume of DPBS. All experiments were done in triplicate in a humidified atmosphere of 95 % air and 5 % CO_2 at 37 °C.

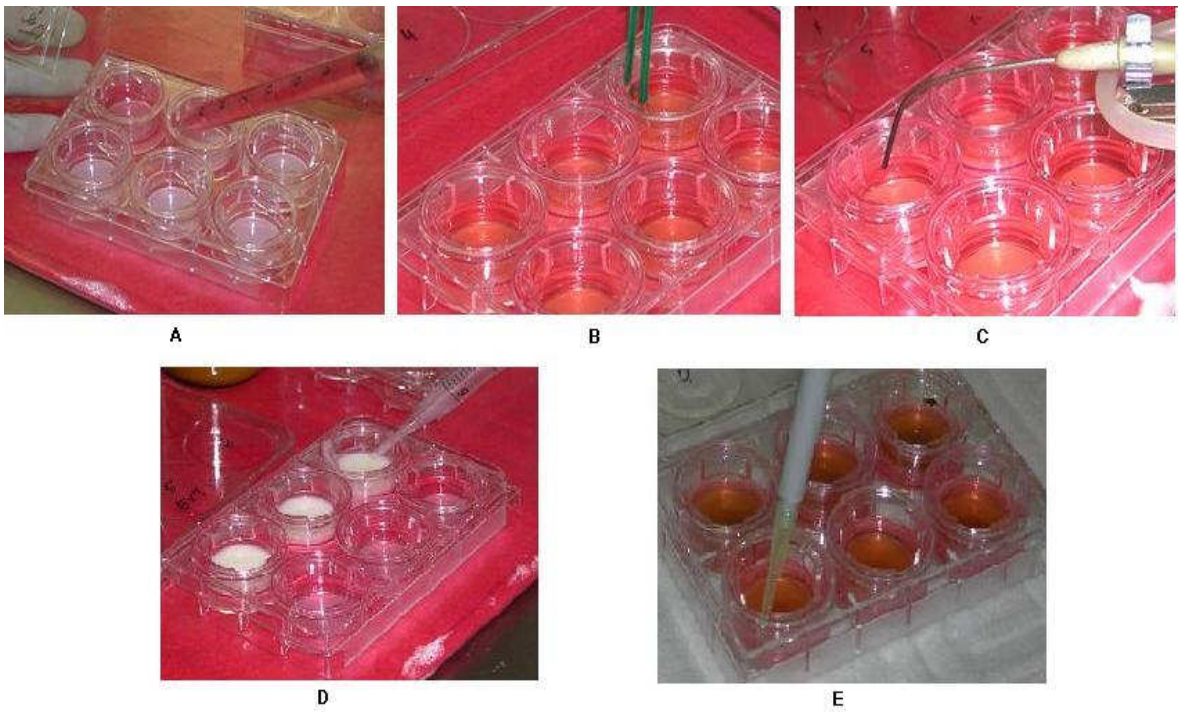


Figure 3.5: Procedures of *in vitro* transport across Caco-2 cell monolayers. (A) Seeding of Caco-2 cells. (B) Measurement of TEER. (C) Removal of growth medium. (D) Loading of test formulation onto Caco-2 cell monolayers. (E) Sampling from the basolateral phase at predetermined time intervals (photos provided by A.M. Viljoen).

3.5.4.4 Sample analysis

Results obtained from HPLC were corrected for dilution and expressed as cumulative transport (% of initial dose) and apparent permeability coefficients (P_{app}) of aspalathin in GRE, pure aspalathin solution, and Pheroids containing green rooibos aqueous extract, respectively, were calculated according to the following equation (detailed previously):

$$\mathbf{P_{app} = (dQ/dt)\ (1\ /\ (A.60.C_0))}$$

3.5.4.5 Statistical analysis

The experiments were done in triplicate and the data expressed as means ± standard deviation. Differences between mean values were analysed by means of one-way analysis of variance

(ANOVA). The difference between the three test formulations was compared and a P-value < 0.05 was considered significantly different.

3.6 RESULTS AND DISCUSSION

3.6.1 Stability of aspalathin in transport medium

Aspalathin solutions prepared in (i) double distilled water (control), (ii) PBS (pH 7.4), and (iii) DMEM were sampled and analysed at room temperature 25 °C at hourly intervals over ten hours by HPLC. Figure 3.6 is a plot of aspalathin peak area over time demonstrating degradation/interference of aspalathin in/with the various vehicles.

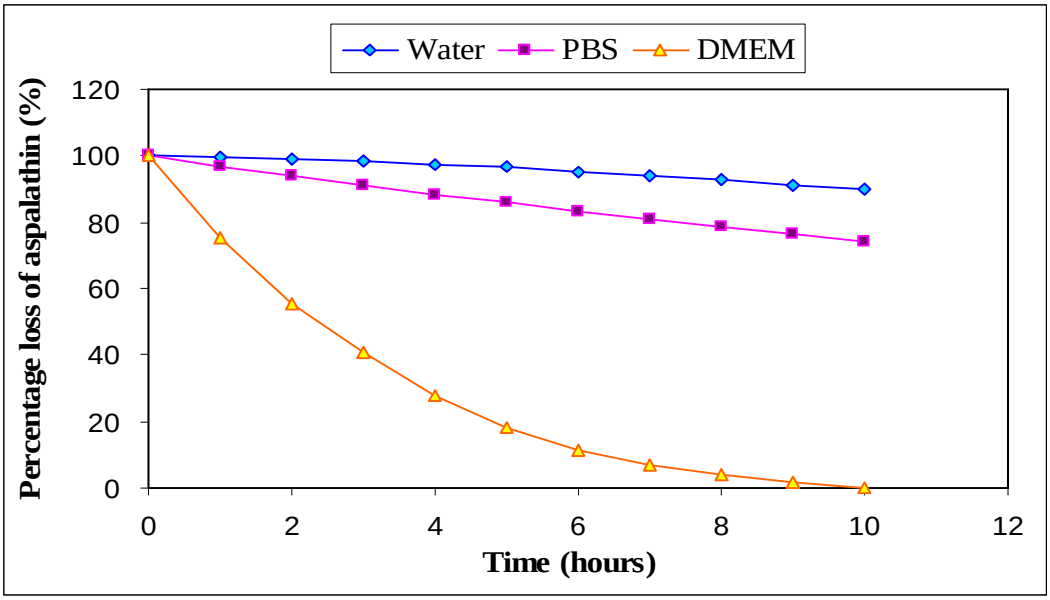


Figure 3.6: Loss of aspalathin over time in vehicles of (i) double distilled water, (ii) phosphate buffer solution (PBS) (pH 7.4), and (iii) Dulbecco's Modified Eagle's Medium (DMEM).

From Figure 3.6 it is noted that there was a general loss of aspalathin in all three of the vehicle systems. The decline in the percentage of aspalathin is highest in DMEM, exhibiting

a rapid logarithmic decline to virtually zero detection of aspalathin at the tenth hour. Approximately 90 % and 74 % of aspalathin in double distilled water and PBS, respectively, remained at the tenth hour. Although aspalathin degradation was less dramatic in the double distilled water and PBS, degradation was still to an appreciable amount accounting for the fact that the decline is a function of time in hours. From these results it can be seen that aspalathin is an unstable compound once in solution. Although Tammela and co-workers (2004) did successfully employ DMEM in their transport study, results from this assay confers the use of PBS as the alternative receiver fluid buffer medium to DMEM for the transport of aspalathin. The aspalathin transport experiment was done over 2 hours where less than 5 % loss of aspalathin could occur (Figure 3.6). To further reduce the rate of degradation, samples of the experiment were stored at -20 °C immediately after collection.

3.6.2 Transport of aspalathin in the green rooibos extracts

The cumulative (% of initial dose) transport of aspalathin in GRE at three different concentrations is shown in Table 3.2. The experiment was carried out over 2 hours and time is expressed in minutes. Each value is expressed as means ± standard deviation (SD) of three experiments (n = 3). The P_{app} is also expressed as means ± SD of the average percentage transport.

Table 3.2: The cumulative (% of initial dose) transport ± SD of aspalathin in green rooibos extract across the Caco-2 cell monolayers.

Time (min)	Average % transport ± SD		
	Extract 1 (10.0 mg/ml)	**Extract 2 (5.0 mg/ml)**	**Extract 3 (1.0 mg/ml)**
0	0.00	0.00	0.00
20	81.24 ± 7.70	9.27 ± 2.14	12.47 ± 1.03
40	94.79 ± 6.99	10.53 ± 3.04	16.27 ± 6.15
60	99.74 ± 9.85	11.65 ± 2.07	16.35 ± 7.78
90	92.80 ± 3.03	12.70 ± 2.05	17.17 ± 0.45
120	96.96 ± 8.95	14.16 ± 1.22	18.13 ± 1.85
P_{app} (cm/sec)	$20.93 \pm 3.61 \times 10^{-06\ a}$	$3.49 \pm 1.45 \times 10^{-06\ b}$	$4.00 \pm 0.42 \times 10^{-06\ b}$

[a,b] P_{app} is statistically significantly different to one another, $P < 0.05$.

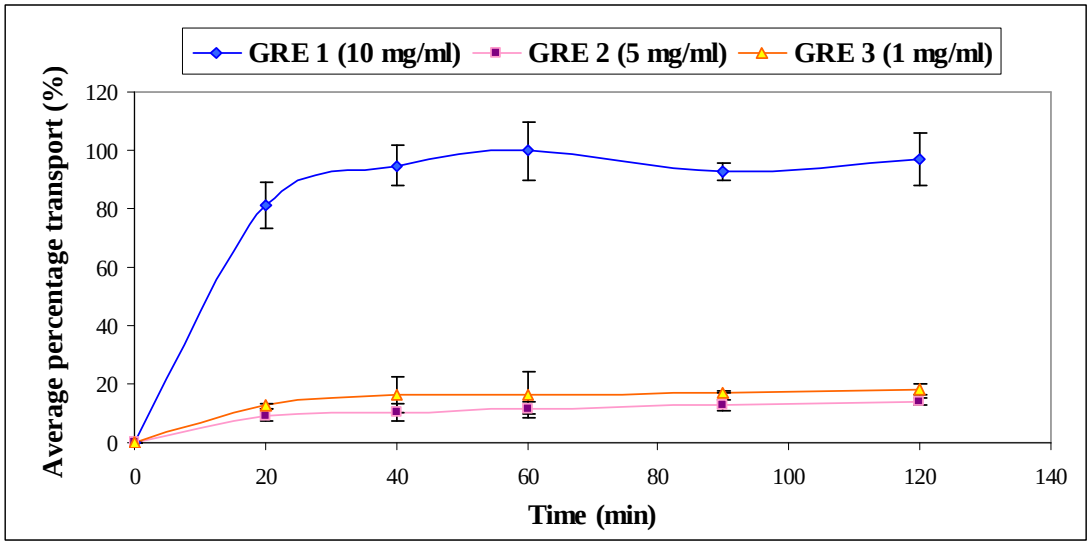


Figure 3.7: Plot of the cumulative transport of aspalathin in green rooibos extracts over time.

Figure 3.7 is a plot of the average percentage transport of aspalathin as a function of time. From the graph it can be seen that transport of aspalathin in GRE 1 (10.0 mg/ml) was rapid and linear at the first 20 minutes, reaching a plateau after 60 min (1 hour). A total of 80 % of aspalathin transported occurred within 20 minutes and reached close to 100 % transport of

aspalathin of the administered dose at 120 minutes (2 hours). The average percentage of aspalathin in GRE 2 (5.0 mg/ml) and GRE 3 (1.0 mg/ml) transported were found considerably less than that in GRE 1. All three extracts showed similar patterns of flux of aspalathin reaching plateau after 60 min but at a higher rate in the case of GRE 1. This may probably be due to a concentration dependent factor in the transport of aspalathin i.e. the higher the concentration the greater the amount transported where the driving force of flux may be greater. Consequently, the P_{app} of aspalathin in GRE 1 ($20.93 \pm 3.61 \times 10^{-06}$ cm/s) is the highest of the three concentrations tested, reflecting a rapid and almost complete apical to basolateral transport. P_{app} of aspalathin in GRE 2 and GRE 3 are similar ($P > 0.05$), which are $3.49 \pm 1.45 \times 10^{-06}$ cm/s and $4.00 \pm 0.42 \times 10^{-06}$ cm/s, respectively, corresponding to a slower rate of transport of aspalathin across the Caco-2 cell monolayers and are statistically significantly different to that of GRE 1 ($P < 0.05$). This difference may be due to that aspalathin transport was rapid in the first 20 min of the experiment in GRE 1.

3.6.3 Transport of aspalathin in pure aspalathin solution

Table 3.3 presents the average percentage (%) transport of aspalathin in pure aspalathin solutions buffered at three concentrations. Each value is expressed as means ± SD of three experiments (n = 3). The P_{app} is also expressed as means ± SD of the average percentage transport.

Table 3.3: The cumulative (% of initial dose) transport ± SD of aspalathin in a pure aspalathin solution across the Caco-2 cell monolayers.

Time (min)	Average % transport ± SD		
	Aspalathin 1 (2.0 mg/ml)	**Aspalathin 2 (1.0 mg/ml)**	**Aspalathin 3 (0.2 mg/ml)**
0	0.00	0.00	0.00
20	68.12 ± 8.20	0.86 ± 0.03	4.02 ± 8.10
40	66.17 ± 6.78	3.19 ± 0.98	2.06 ± 3.75
60	71.59 ± 11.97	4.11 ± 1.01	2.68 ± 3.19
90	67.74 ± 7.01	4.50 ± 0.76	2.76 ± 3.45
120	79.03 ± 0.38	7.54 ± 0.71	4.66 ± 4.70
P_{app}	$15.34 \pm 1.66 \times 10^{-06\ a}$	$2.48 \pm 0.03 \times 10^{-06\ b}$	$0.91 \pm 0.37 \times 10^{-06\ c}$

[a,b,c] P_{app} is statistically significantly different to one another, $P < 0.05$.

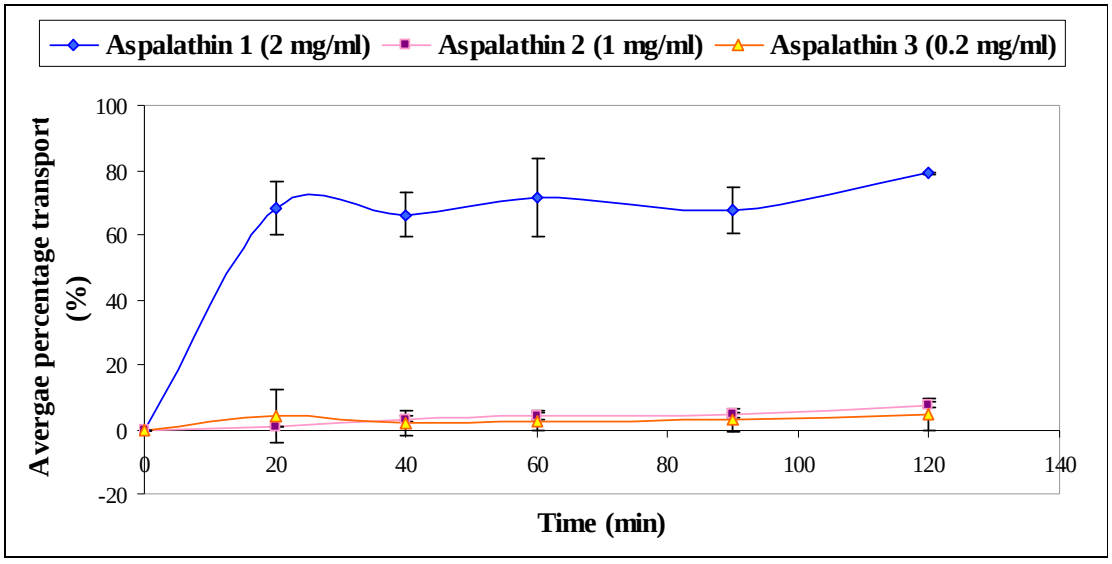


Figure 3.8: Plot of the cumulative transport of aspalathin in a pure aspalathin solution over time.

A plot of the average percentage transport of aspalathin *versus* time of the three pure aspalathin solutions is presented in Figure 3.8. Similar to what is observed in GRE 1 (Figure 3.7) transport of aspalathin at 2 mg/ml (Aspalathin 1) is rapid and linear from 0 (zero) to 20

minutes. Although the aspalathin transport in Aspalathin 1 varied after 20 minutes to 120 minutes, it seems to have reached a steady plateau. Less than 10 % of the administered dose of aspalathin was transported across the cell monolayers in Aspalathin 2 (1 mg/ml) and Aspalathin 3 (0.2 mg/ml). A similar trend in the plot of transport of aspalathin in the GRE and in the pure aspalathin solutions can be seen. A greater amount of aspalathin was transported in formulations at the highest concentrations (GRE 1 and Aspalathin 1), demonstrating once again that the absorption may be concentration dependent. In this experiment, the rate of transport of aspalathin was significantly different ($P < 0.05$) amongst the three solutions, where the P_{app} of aspalathin in Aspalathin 1, 2, and 3 are $15.34 \pm 1.66 \times 10^{-06}$ cm/s, $2.48 \pm 0.03 \times 10^{-06}$ cm/s, and $0.91 \pm 0.37 \times 10^{-06}$ cm/s, respectively.

3.6.4 Transport of aspalathin in Pheroids

Table 3.4 is the average percentage (%) transport ± SD of aspalathin in Pheroids incorporated with GRE over 2 hours. Three concentrations of Pheroids were formulated. Results are expressed as means ± SD and value of P_{app} is expressed as means ± SD of the average percentage transport (n = 3).

Table 3.4: The cumulative (% of initial dose) transport ± SD of aspalathin in Pheroids across the Caco-2 cell monolayers.

Time	Average % transport ± SD		
	Pheroid 1 (10.0 mg/ml)	**Pheroid 2 (5.0 mg/ml)**	**Pheroid 3 (1.0 mg/ml)**
0	0.00	0.00	0.00
20	2.61 ± 1.33	15.46 ± 4.02	2.18 ± 0.97
40	3.94 ± 0.39	32.96 ± 3.03	4.53 ± 0.21
60	5.91 ± 1.19	40.63 ± 4.68	7.93 ± 0.40
90	5.48 ± 0.08	56.24 ± 0.10	12.82 ± 1.04
120	6.04 ± 1.07	61.82 ± 0.71	16.32 ± 1.13
P_{app}	$1.65 \pm 0.12 \times 10^{-06\ a}$	$18.62 \pm 0.23 \times 10^{-06\ b}$	$4.95 \pm 0.27 \times 10^{-06\ c}$

[a,b,c] P_{app} is statistically significantly different to one another, $P < 0.05$.

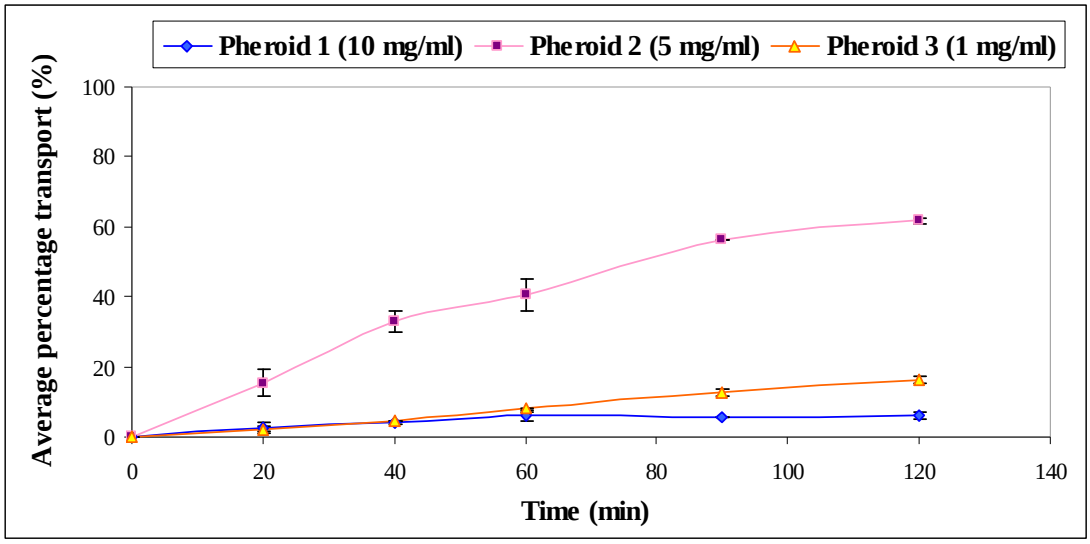


Figure 3.9: Plot of the cumulative transport of aspalathin in Pheroids over time.

Pheroids were developed to act as permeation enhancer in drug delivery across biological membranes. The physicochemical properties of Pheroids have not yet been clearly characterised and its function as permeation enhancer has not completely been elucidated. It can be seen from Figure 3.9 that the pattern in the transport of aspalathin in Pheroids is quite

different to that observed in the GRE and the pure aspalathin solutions ($P < 0.05$). Transport of aspalathin in Pheroids was slow and steady and did not reach a plateau at the end of the experiment. A higher amount of aspalathin was transported in Pheroid 2 than in Pheroids 1 and 3. The P_{app} determined for each concentration differs greatly from one another ($P < 0.05$), where $1.65 \pm 0.12 \times 10^{-06}$ cm/s, $18.62 \pm 0.23 \times 10^{-06}$ cm/s, and $4.95 \pm 0.27 \times 10^{-06}$ cm/s are P_{app} of Pheroid 1, 2, and 3, respectively. Compared to Figure 3.7 and 3.8, Figure 3.9 does not exhibit enhanced transport of aspalathin in the Pheroid technology across the Caco-2 cell monolayers in this experiment.

3.6.5 Comparison of the apparent permeability coefficient (P_{app})

Figure 3.10 presents the $P_{app} \pm$ SD obtained for the transport of aspalathin from the three formulations at three different concentrations. The plot shows that P_{app} of aspalathin is a concentration dependent factor. This may be explained by the higher concentrations result in a greater driving force of diffusion. The P_{app} of aspalathin is higher in the GRE than in the pure aspalathin solutions. This may be explained by GRE being a mixture of numerous flavonoid glycosides and phenolic compounds that may affect the flux of aspalathin by e.g. increasing the driving force of diffusion or facilitating its transport across the Caco-2 cell monolayer. Table 3.5 presents the average $P_{app} \pm$ SD obtained for aspalathin in the various test formulations ($n = 3$).

Table 3.5: The apparent permeability coefficient of (i) GRE, (ii) pure aspalathin solutions, and (iii) Pheroids at three different concentrations.

	Average P_{app} ($x10^{-6}$) (cm/s) ± SD
GRE 1 (10 mg/ml)	20.93 ± 3.61
GRE 2 (5 mg/ml)	3.49 ± 1.45
GRE 3 (1 mg/ml)	4.00 ± 0.42
Aspalathin 1 (2 mg/ml)	15.34 ± 1.66
Aspalathin 2 (1 mg/ml)	2.48 ± 0.03
Aspalathin 3 (0.2 mg/ml)	0.91 ± 0.37
Pheroid 1 (10 mg/ml)	1.65 ± 0.12
Pheroid 2 (5 mg/ml)	18.62 ± 0.23
Pheroid 3 (1 mg/ml)	4.95 ± 0.27

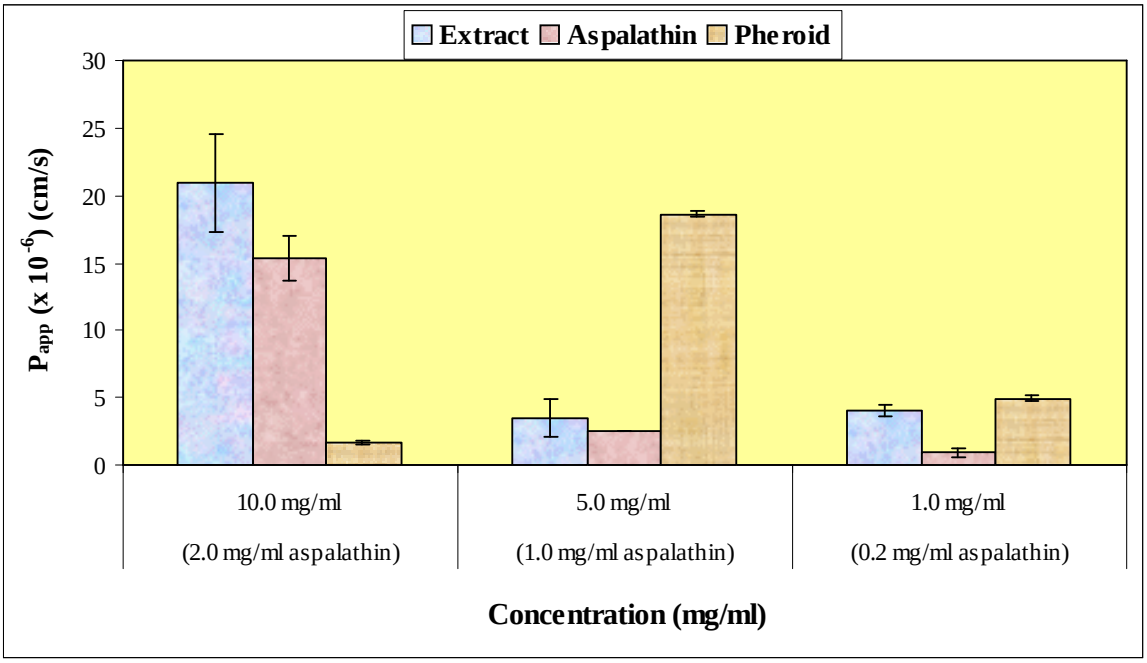


Figure 3.10: Comparison of the apparent permeability coefficient (P_{app}) of: (i) GRE, (ii) aspalathin solution, and (iii) Pheroids at three different concentrations.

In a study conducted by Biganzoli *et al.* (1999), the P_{app} of 13 antibiotics with variable bioavailability in humans were obtained. On the basis of P_{app} they grouped the compounds into : (i) P_{app} values < 0.2 x 10^{-6} cm/s (bioavailability < 1 %); (ii) P_{app} values between 0.2 and

2.0 x 10^{-6} cm/s (bioavailability between 1 % and 90 %); (iii) P_{app} values > 2.0 x 10^{-6} cm/s (bioavailability > 90 %). Artursson *et al.* (2001) also found that completely absorbed drugs have a high permeability coefficient (P_{app} > 1 x 10^{-6} cm/s), whereas incompletely absorbed drugs had a low permeability coefficient (P_{app} < 1 x 10^{-7} cm/s) in the Caco-2 monolayer model. In this study the P_{app} of aspalathin obtained were all greater than 0.2 x 10^{-6} cm/s at the various concentrations and formulations tested suggesting that aspalathin may have a bioavailability up to or greater than 90 % depending on the concentration administered. This correlates with the findings by Kuo (1998) and Tammela *et al.* (2004) in the investigation on the transport of various flavonoids. To compare the amount of aspalathin available for absorption in a cup of rooibos tea (i.e. 3 mg described in Chapter 1 section 1.6.3) to the highest aspalathin concentration (2mg) applied to the Caco-2 cell monolayers for transport study, a greater than 90 % of aspalathin in a cup of rooibos tea is bioavailable. In addition, rooibos tea and green tea have a comparable amount of flavonoid contents and the latter exhibits greater inhibition on lipid peroxidation *in vitro* (described in the section 1.6.4 of Chapter 1). However, Zhang *et al*. (2004) conducted a transport study on the major green tea flavonoids i.e. epicatechin (EC), epigallocatechin (EGC), epicatechin gallate (ECG), and epigallocatechin gallate (EGCG), and found the P_{app} of each of the flavonoids were 1.39 ± 0.082 x 10^{-7} cm/s, 1.49 ± 0.13 x 10^{-7} cm/s, 0.96 ± 0.15 x 10^{-7} cm/s, and 0.83 ± 0.24 x 10^{-7} cm/s, respectively. Although green tea flavonoids exhibit good inhibitory effects on lipid peroxidaiton, their P_{app} would predict a bioavailability of less than 1 %. Thus, aspalathin may exhibit a good bioavailability in humans and that it can be absorbed to an appreciable amount to exhibit biological activities.

3.7 Conclusion

Many flavonoid compounds have been investigated for their *in vitro* transport across intestinal epithelium using Caco-2 cell monolayers. In this study, a chemical interaction was

observed between aspalathin and DMEM (pH 7.4) and almost caused complete degradation of aspalathin within hours. The DPBS may be an alternative to the DMEM for transport studies of flavonoids. Aspalathin has an absorption profile that is concentration dependent where almost 100 % transport of aspalathin was observed in GRE at 10 mg/ml. Better aspalathin absorption occurred in the GRE than in the pure aspalathin solutions and the incorporation of the Pheroid technology did not enhance the transport of aspalathin. The P_{app} of aspalathin in the GRE and in the pure aspalathin solution were all above 0.2×10^{-6} cm/s, a value ten-fold greater than of that of the major green tea catechins obtained by Zhang *et al*. (2004), predicting a greater than 90 % bioavailability *in vivo*.

CHAPTER 4: CONCLUSION AND FUTURE PROSPECTIVE

4.1 Summary and conclusion

The *in vitro* percutaneous permeation and *in vitro* intestinal epithelial transport of aspalathin was investigated. Human female abdominal skin mounted onto vertical Franz diffusion cells and Caco-2 cell monolayers isolated and cultured from human colonic adenocarcinoma cells were used. Extracts of green (unfermented) rooibos and pure aspalathin solutions at various concentrations were put to tested.

- Less than 0.1 % of aspalathin in the applied doses of green rooibos extract and pure aspalathin solution permeated the skin.
- 80 % of the permeated aspalathin was distributed in the stratum corneum.
- Aspalathin was only detected in one of the two rooibos skin care products (cream). Less than 1 mg (0.1 %) of aspalathin was extracted from 1 g of the cream. Permeation study on these skin care products was therefore not considered feasible.
- Transport of aspalathin across Caco-2 cell monolayers exhibited a concentration dependent behaviour.
- Almost 100 % transport was observed at the highest concentration applied.
- Better aspalathin transport was observed with the aqueous green rooibos extracts than with the pure aspalathin solution across the Caco-2 cell monolayers.
- The apparent permeability coefficient (P_{app}) obtained for aspalathin was above 0.2 x 10^{-6} cm/s which may predict a bioavailability of over 90 % *in vivo*.
- The incorporation of the Pheroid technology did not positively enhance the transport of aspalathin across the Caco-2 cell monolayer.
- A greater amount of aspalathin was transported across the Caco-2 cell monolayers than permeated into and through the skin.

4.2 Future prospective

The benefits of rooibos tea and green rooibos, in particular, have only recently been recognised. Unlike the commonly occurring quercetin that has been extensively studied, relatively few studies on aspalathin have been done. Most of the studies have focused on the biological and pharmacological activities of rooibos. The present study is the first to investigate the percutaneous permeation and transport of aspalathin across Caco-2 cell monolayers. Green rooibos extracts contains various antioxidants, which undergo chemical and biological breakdown in the body. Further studies on percutaneous absorption of green rooibos extracts may be carried out to measure the total phenolic content of green rooibos after skin permeation, account for the degradation of the compounds, and evaluate the total antioxidant capacity of the permeants. Various vehicle systems carrying green rooibos extracts may also be investigated to enhance the absorption of rooibos tea.

Many studies on the intestinal absorption of aspalathin can still be done to obtain a more comprehensive absorption profile. In this study, the apical-to-basolateral transport of aspalathin was investigated. The intestinal epithelial cells possess cellular activities such as enzymatic metabolism, carrier systems, and efflux mechanisms that affect absorption of drugs and molecules. By analysing basolateral-to-apical transport, metabolites, and cellular accumulation, the knowledge on the transport of aspalathin may become more complete.

REFERENCES

Afaq F., Adhami V.M., and Mukhtar H. (2005) Photochemoprevention of ultraviolet B signaling and photocarcinogenesis. Mutation Research 571: 153-173.

Artursson P., Palm K. and Luthman K. (2001) Caco-2 monolayers in experimental and theoretical predictions of drug transport. Advanced Drug Delivery Reviews 46: 27-43.

Balimane P.V. and Chong S. (2005) Cell culture-based modules for intestinal permeability: a critique. Drug Discovery Today 10(5): 335-343.

Basson M.D. and Hong F. (1996) Regulation of human Caco-2 intestinal epithelial brush border enzyme activity by cyclic nucleotide. Cancer Letters 99: 155-160.

Batchelder R.J., Calder R.J., Thomas C.P. and Heard C.M. (2004) *In vitro* transdermal delivery of the major catechins and caffeine from extract of *Camllia sinensis.* International Journal of Pharmaceutics 283: 45-51.

Behl C.R., Kumar S., Malick A.W., Patel S.B., Char H. and Piemontese D. Choice of membrane for *in vitro* skin uptake studies and general experimental techniques. (*In* B.W. Kemppainnen & W.G. Reifenrath, eds. Methods for skin absorption. Boca Raton, Fla.: CRC Press, Inc. 1990 pp1-21.

Biganzoli E., Cavenaghi L.A., Rossi R., Brunati M.C. and Nolli M.L. (1999) Use of a Caco-2 cell culture model for the characterization of intestinal absorption of antibiotics. Farmaco 54(9): 594-599.

Bonina F., Lanza M., Montenegro L., Puglisi C., Tomaino A., Trombetta D., Castelli F., and Saija A. (1996) Flavonoids as potential protective agents against photo-oxidative skin damage. International Journal of Pharmaceutics 145: 87-94.

Boone C.M., Olsthoorn M.M.A., Dakora F.D., Spaink H.P., and Thomas-Oates J.E. (1999) Structural characterisatoin of lipo-chiton oligosaccharides isolated from *Bradyrhizobium aspalati*, microsymbionts of commercially important South African legumes. Cabohydrate Reasearch 317: 155-163.

Brain K.R., Walter K.A., Green D.M., Brain S. and Loretz L.J. (2005) Percutaneous permeation of diethanolamine through human skin *in vitro*: application from cosmetic vehicle. Food and Chemical Toxicology 43: 681-690.

Bramati L., Mnoggio M., Gardana C., Simonetti P., Mauri P., and Pietta P. (2002) Quantitative characterization of flavonoid compounds in Rooibos tea (*Aspalathus linearis*) by LC-UV/DAD. Journal of Agricultural and Food Chemistry 50(20): 5513-5519.

Braun A., Hämmerle S., Sauda K., Rothen-Rutishauser B., Günthert M., Krämer S.D. and Wunderli-Allanspach H. (2000) Cell culture as tools in biopharmacy. European Journal Pharmaceutical Science 2: S51-S60.

British Pharmacopoeia. London: HMSO 1993 Vol. II ppA79.

Carrière V., Chambaz J. and Rousset M. (2001) Sesion 4: Xenobiotic and gene expression. Intestinal responses to xenobiotics. Toxicology *in vitro* 15: 373-378.

Cevc G.. (2004) Lipid vesicles and other colloids as drug carriers on the skin. Advanced Drug Delivery Review 56: 675-711.

Cason C. (2004, May). Rooibos tea. TeaMuse monthly newsletter. Retrieved from http://www.teamuse.com/article_040501.html

Chan L.M.S., Lowes S. and Hirst B.H. (2004) The ABCs of drug transport in intestine and liver: efflux proteins and limiting drug absorption and bioavailability. European Journal of Pharmaceutical Sciences 21: 25-51.

Chen C.N. and Pan S.M. (1996) Assay of superoxide dismutase activity by combining electrophoresis and densitrometry. Botanical Bulleton of Academia Sinica 37(2): 107-111.

Cronin M.T.D., Dearden J.C., Moss G.P. and Murray-Dickson G. (1999) Investigation of the mechanism of flux across human skin *in vitro* by quantitative structure- permeability relationships. European Journal of Pharmaceutical Science 7: 325-330.

Dahlgren R. (1963) Studies on *Aspalathus* and some related genera in South Africa. Opera Botanica (Lund) 9(1).

Dahlgren R. (1964) The correct name of the “Rooibos” tea plant. Botaniska Nortieria 117: 188-196.

Dahlgren R. (1968) Revision of the genus *Aspalathus*. II. The species with ericoid and pinoid leaflets. 7. Subgenus *Nortieria*. With remark on rooibos tea cultivation. Botanisika Nortieria 121: 165-208.

Denete A.R., Vanbever R. and Préat V. (2004) Skin electrophoration for transdermal and topical delivery. Advanced Drug Delivery Review 56: 659-674.

During A. and Harrison E.H. (2005) An *in vitro* model to study the intestinal absorption of carotenoids. Food Research International 38:1001-1008.

Ekmekcioglu C. (2002) A physiological approach for preparing and conducting intestinal bioavailability studies using experimental systems. Food Chemistry 76: 225-230.

Erickson L. (2003). Rooibos tea: Research into antioxidant and antimutagenic properties. The Journal of the American Botanical Council. 59: 34-45. Retrieved October 1, 2005, from http://www.herbalgram.org/default.asp

Fasano W.J., Manning L.A. and Greem J.W. (2002) Rapid integrity assessment of rat and human epidermal membranes for *in vitro* dermal regulatory testing: correlation of electrical resistance with tritiated water permeability. Toxicology *in vitro* 16: 731-740.

Flynn G.L. Topical drug absorption and topical pharmaceutical systems. (*In* G.S. Banker & C.T. Rhodes, eds. Modern Pharmaceutics. New York, N.Y.: Marcel Dekker.) 1979 pp263-327.

Fogh J., Wright W.C. and Loveless J.D. (1977) Absence of Hela cell contamination in 169 cell lines derived from human tumours. Journal of the National Cancer Institute 21: 393-408.

Ghafourian T., Zandasrar P., Hamishecker H. and Nokhodchi A. (2004) The effect of

penetration enhancers on drug delivery through skin: a QSAR study. Journal of Controlled Release 99: 113-125.

Gharat L., Taneja R., Weerapreeyakul N., Rege B., Polli J. and Chikhale P.J. (2001) Targeted drug delivery system 6: Intracellular bioreductive activation, uptake and transport of an anticancer drug delivery system across intestinal Caco-2 cell monolayers. International Journal of Pharmaceutics 219: 1-10.

Grobler A.F. (2004) Emzaloid™ Technology. Potchefstroom: NMU.20p (Confidential: Concept document).

Hadgraft J.W. and Somers G.F. (1965) Percutaneous absorption. The Journal of Pharmacy and Pharmacology 8: 625-634.

Hadgraft J. (2004) Skin deep. Europe Journal of Pharmaceutics and Biopharmaceutics 58: 291-299.

Hadgraft J. and Lane M.E. (2005) Skin permeation: The years of enlightenment. International Journals of Pharmaceutics 305: 2-12.

Harrison S.M., Barry B.W. and Dugard P.H. (1984) Effects of freezing on human skin permeability. The Journal of Pharmacy and Pharmacology 36: 261-262.

Hauri H.P. (1996, August 8). Regulation of digestion in cell culture. 3R-Info-Bulletin. 3R Research Foundation. Retrieved February 23, 2006, from http://www.forschung3r.ch/en/publications/bu8_print.htm

Heim K.E., Tagliaferro A.R., and Bobilya D. (2002) Flavonoid antioxidants: chemistry, metabolism and structure-activity relationships. Journal of Nutritional Biochemistry 13: 572-584.

Ho C. K. (2004) Probabilistic modelling of percutaneous absorption for risk-based exposure assessments and transdermal drug delivery. Statistical Methodology 1: 49-69.

Hunter J. and Hirst B.H. (1997) Intestinal secretion of drugs. The role of P-glycoprotein and related drug efflux systems in limiting oral drug absorption. Advanced Drug Delivery Review 25: 129-157.

Inanami O., Asanuma T., Inukai N., Jin T, Shimokawa S., Kasai N., Nakano M., Sato F., and Kuwabara M. (1995) The suppression of age-related accumulation of lipid peroxides in rat brain by administration of rooibos tea (*Aspalathus linearis*). Neuroscience Letter 196(1-2): 85-88.

ICH harmonised tripartite guideline (2005, November).Validation of analytical procedures: text and methodology Q2 (R1). International conference on harmonisation of technical requirements for registration of pharmaceuticals for human use. Retrieved by 23 October 2006 from http://www.ich.org/cache/compo/276-254-1.html

Isoda H., Talorete T.P.N., Han J. and Nakamura K. (2006) Expressions of galectin-3 glutathione S-transferase A2 and peroxiredoxin-1 by nonylphenol-incubated Caco-2 cells and reduction in transepithelial electrical resistance by nonylphenol. Toxicology *in vitro* 20: 63-70.

Joubert E. (1996) HPLC quantification of the dihydrochalcones, aspalathin and nothofagin in rooibos tea (*Aspalathus linearis*) as affected by processing. Food Chemistry 55(4): 403-411.

Joubert E., Winterton P., Britz T. J., and Ferreira D. (2004) Superoxide anion and α,α-diphenyl-β-picrylhydrazyl radical scavenging capacity of rooibos (*Aspalathus linearis*) aqueous extracts, crude phenolic fractions tannin and flavonoids. Food Research International 37: 133-138.

Juliet P.A.R., Joyee A.G., Jayaraman G., Mohankumar M.N., and Panneerselvam C. (2005) Effect of L-canitine on nucleic acid status of aged rat brain. Experimental Neurology 191: 33-40.

Karlsson J., Unfell A.L., Gråsjö J. and Artursson P. (1999) Paracellular drug transport across intestinal epithelia: influence of charge and induced water flux. European Journal of Pharmaceutical Sciences 9: 47-56.

Koeppen B.H. (1963) Isolation and partial characterisation of aspalathin, the principle phenolic constituent of unfermented rooibos tea (*Aspalathus acuminatus*). South African Journal of Laboratory and Clinical Medicine 9: 141-142.

Koeppen B.H. and Roux D.G. (1965a) C-Glycosylflavnonoids. The chemistry of orientin and iso-orientin. Biochemistry Journal 97: 444-448.

Koeppen B.H. and Roux D.G. (1965b) Aspalathin: a novel C-glycosylflavonoid from *Aspalathin linearis*. Tetrahedron Letters 39: 3497-3503.

Koeppen B.H. and Roux D.G. (1966) C-Glycosylflavonoids. The chemistry of aspalathin. Biochemistry Journal 99: 604-609.

Koeppen B.H. (1970) C-glycosyl compounds in rooibos tea. Food Industries of South Africa 49.

Krishna G., Chen K.J., Lin C.C. and Nomeir A.A. (2001) Permeability oflipophilic compounds in drug discovery using *in vitro* human absorption model, Caco-2. International Journal of Pharmaceutics 222: 77-89.

Kuo S.M. (1998) Transepithelial transport and accumulation of flavone in human intestinal Caco-2 cells. Life Sciences 63(26): 2323-2331.

Kunishiro K., Tai A. and Yamamoto I. (2001) Effects of rooibos tea extract on antigen-specific antibody production and cytokine generation *in vitro* and *in vivo*. Bioscience, Biotechnology and Biochemistry 65(10): 2137-2145.

Laurent C., Besançon P. and Caporiccio B. (2007) Flavonoids from a grape seed extract with digestive secretions and intestinal cells as assessed in an *in vitro* digestion/Caco-2 cell culture model. Food Chemistry 100(4) 1704-1712.

Lee L.T., Huang Y.T., Hwang J.J., Lee P.P., Ke F.C., Nair M.P., Knandaswam C. and Lee M.T. (2002) Blockade of the epidermal growth factor receptor tyrosine kinase activity by quercetin and luteolin leads to growth inhibition and apoptosis of pancreatic tumour cells. Anticancer Research 22(3): 1615-1627.

Lennernäs H., Palm K., Fagerholm U. and Artursson P. (1996) Correlation between paracellular and transcellular drug permeability in the human jejunum and Caco-2 monolayers. International Journal of Pharmaceutics 127: 103-107.

Marnewick J.L., Gelderblom W.C.A. and Joubert E. (2000) An investigation on the antimutagenic properties of South African herbal teas. Mutation Research 471: 157-166.

Marnewick J., Joubert E., Joseph S., Swanevelder S., Swart P. and Gelderblom W. (2004) Inhibition of tumour promotion in mouse skin by extracts of rooibos (*Aspalathus linearis*) and honeybush (*Cyclopia intermedia*), unique South African herbal tea. Cancer Letters 224(2) 1193-202.

Mavon A., Raufast V. and Redoulès D. (2004) Skin absorption and metabolism of a new vitamin E prodrug, δ-tocopherol-glucoside: *in vitro* evaluation in human skin model. Journal of Controlled Release 100: 221-231.

Morton J.F. (1983) Rooibos tea, *Aspalathus linearis*, a caffeineless, low-tannin beverage. Economic Botany 37(2): 164-173.

Muscoli C., Cuzzocrea S., Riley D.P., Zweier J.L., Thiemermann C., Wang Z.Q. and Selvemini D. (2003) Review on the selectivity of superoxide dismutase mimetics and its importance in pharmacological studies. British Journal of Pharmacology 40: 445-560.

Nicolazzo J.A., Morgan T.M., Reed B.L. and Finnin B.C. (2005) Synergistic enhancement of testosterone transdermal delivery. Journal of Controlled Release 103: 577-585.

Phytochemicals. (Rooibos *Aspalathus linearis*) Retrieved October 1, 2005, from http://www.phytochemical.info/plants/rooibos.php

Potts R.O. and Guy R.H. (1992) Predicting skin permeability. Pharmaceutical Research 9: 663-669.

Ranaldi G., Consalvo R., Sambuy Y. and Scarino M.L. (2003) Permeability characteristics of parental and colonal human intestinal Caco-2 cell lines differentiated in serum-supplemented and serum-free media. Toxicology *in vitro* 17: 761-767.

Red Bush Tea. Retrieved October 3, 2005, from http://www.redbushtea.com/

Research and Rooibos. Retrieved October 1, 2005, from http://www.kalahariusa.com/tea/ResearchOnRooibos

Rieger M.M. Factors affecting sorption of topicaly applied substances. (*In* J.L. Zatz, ed. Skin permeation fundamentals and application. Allured Pubishing Corporation. 1993 pp33-72.

Rooibos Limited. Retrieved October 1, 2005, from http://www.rooibosltd.co.za/

Said H.M., Blair J.A., Lucas M.L. and Hilburn M.E. (1986) Intestinal surface acid microclimate *in vitro* and *in vivo* in the rat. Journal of Laboratory and Clinical Medicine 107: 420-424.

Sasaki Y.F., Yamada H., Shimoi K., Kator K. and Kinae N. (1993) The

clastogen-suppressing effects of green tea, Po-lei tea and Rooibos tea in CHO cells and mice. Mutatation Research 286(2): 221-32.

Saunders J.C.J., Davis H.J., Coetzee L., Botha S., Kruger A.E. and Grobler A. (1999) A novel skin penetration enhancer: evaluation by membrane diffusion and confocal microscopy. 2(3) 99-107.
(Available on line www.ualberta.ca/~csps/JPPS2(3)/J.Saunders/mircroscopy-saunders.pdf).

Schlebusch J. (2002) A briefing document on the use of the MeyerZall therapeutic system, based on Emzaloid™ technology, to increase the absorption of active ingredients, with special refernce to MeyerZall Laboratories Tuberculosis Medicine Project. (Briefing document as tribute to the colleagues at MeyerZall.) George 139. (Unpublished).

Shah P., Jogani V., Bagchi T. and Misra A.M. (2006) Role of Caco-2 cell monolayers in prediction of intestinal drug absorption. Biotechnology Progress 22: 186-198.

Smith K.L. Penetrant characteristics influencing skin absorption. (*In* B.W. Kemppainnen & W.G. Reifenrath, eds. Methods for skin absorption. Boca Raton, Fla.: CRC Press, Inc.) 1990 pp23-34.

South Africa: rainbows and deserts. History of Rooibos tea. Retrieved October 3, 2005, from http://members.tripod.com/~Meerkat_2/erooibos.html

Stoll B.R., Batycky R.P., Leipold H.R., Milstein S. and Edwards D.A. (2000) A theory of molecular absorption from the small intestine. Chemical Engineering Sciences 55: 473-489.

Suzuki H. and Sugiyama Y. (2000) Mini Review: role of metabolic enzymes and efflux transporters in the absorption of drugs from the small intestine. European Journal of Pharmaceutical Sciences 12: 3-12.

Tammela P., Laitinen L., Galkin A., Wennberg T., Heczko R., Vuorela H., Slotte J.P. and Vuorela P. (2004) Permeability characteristics and membrane affinity of flavonoids and alkyl gallates in Caco-2 cells and in phospholipids vesicles. Archives of Biochemistry and Biophysics 425: 193-199.

The rooibos history. Retrived October 3, 2005, from http://www.dr-nortier.com/history.htm

Thomas B.J. and Finnin B.C. (2004) The transdermal revolution. Drug Discovery Today 9(16): 679-703.

Ulicna O., Greksak M., Vacova O., Zlatos L., Galbavy S., Bozek P. and Nakano M. (2003) Hepatoprotective effect of rooibos tea (*Aspalathus linearis*) on CCl_4-induced liver damage in rats. Physiological Research 52(4): 461-466.

Ungell A.L.B. (2004) Caco-2 replace or refine. Drug Discovery Today: Technologies 1(4): 423-430.

Versantvoort C.H.M., Ondrewater R.C.A., Duizer E., Van de Sandt J.J.M., Gilde A.J. and Grote, J.P. (2002) Monolayers of IEC-18 cells as an in vitro model for screenin the passive transcellular and paracellular transport across the intestinal barrier: comparison of active and passive traspot with the human colon carcinoma Caco-2 cell line. Environmental Toxicology and Pharmacology 11: 335-344.

Von Gadow A., Joubert E. and Hansman C.F. (1997) Comparison of the antioxidant activity of rooibos tea (*Aspalathin linearis*) with green, oolong and black tea. Food Chemistry 60(1): 73-77.

Yamashita S., Furubayashi T., Kataoka M., Sakane T., Sezaki H. and Tokuda H. (2000) Optimized conditions for prediction of intestinal drug permeability using Caco-2 cells. European Journal of Pharmaceutical Sciences 10: 195-204.

Youdim K.A., Avdeef A. and Abbott N.J. (2003) *In vitro* trans-monolayer permeability calculations: often forgotten assumptions. Drug Discovery Today 8(21): 997-1003.

Zatz J.L. Scratching the surface: rationale and approaches to skin permeation. (*In* J.L. Zatz, ed. Skin permeation fundamentals and application. Allured Pubishing Corporation. 1993 pp11-32.

Zhang L., Zheng Y., Chow M.S.S. and Zuo Z. (2004) Investigation of intestinal absorption and disposition of green tea catechins by Caco-2 monolayer model. International Journal of Pharmaceutics 287: 1-12.

Diagram of the cross section of the skin. Retrieved February 23, 2006, from http://rds.yahoo.com/_ylt=A9G_RtvPXEdE8BcB6pujzbkF;_ylu=X3oDMTA4NDgyNWN0BHNlYwNwcm9m/SIG=12ve841bm/EXP=1145613903/**http://www.anti-aging-skin-care.com/forever-young-how-it-works-diagram.html

Diagram of electric dermatome. Retrieved September 14, 2006, from http://www.zimmergermany.de

Diagram of skin dermatome. Retrieved September 14, 2006, from http://www.residentnet.com

Diagram of vertical Franz diffusion cell. Retrieved September 8, 2006, from http://wwwpermegear.com/franz.htm

Large intestine. Retrieved March 1, 2006, from http://www.emc.maricopa.edu/faculty/farabee/BIOBK/BioBookDIGEST.html

ANNEXURE 1

YUNIBESITI YA BOKONE-BOPHIRIMA
NORTH WEST UNIVERSITY
NOORDWES UNIVERSITEIT

Etiekkomitee

Tel (018) 299 2558

Faks (018) 297 5308

E-Pos dnvealr@puk.ac.za

Prof J du Plessis

Bussie 36

Noordwes-Universiteit

(Potchefstroomkampus)

30 Augustus 2004

Geagte prof Du Plessis

GOEDKEURING VIR EKSPERIMENTERING MET DIERE

Hiermee wens ek u in kennis te stel dat u projek getiteld *"In vitro transdermale aflewering van geneesmiddels"* goedgekeur is met nommer 04D08. Let asseblief daarop dat pasiënte vooraf toestemmig moet gee en dat die weefsel nie vir 'n ander doel aangewend mag word as dit waarvoor die pasiënt toestemming gegee het nie.

Gebruik asseblief die nommer genoem in paragraaf 1 in alle korrespondensie rakende bogenoemde projek en let daarop dat daar van projekleiers verwag word om jaarliks in Junie aan die Etiekkomitee verslag te doen insake etiese aspekte van hulle projekte asook van publikasies wat daaruit voortgespruit het. U sal in Mei 2005 die dokumentasie hieroor ontvang.

Goedkeuring van die Etiekkomitee is vir 'n termyn van hoogstens 5 jaar geldig (volgens Senaatsbesluit van 4 November 1992, art 9.13.2). Vir die voortsetting van projekte na verstryking van hierdie tydperk moet opnuut goedkeuring verkry word.

Die Etiekkomitee wens u alle voorspoed met u werk toe.

Vriendelike groete

ESTELLE LE ROUX

NAMENS SEKRETARIAAT